DURBAN UNIVERSITY OF TECHNOLOGY
INYUVESI YASETHEKWINI YEZOBUCHWEPHESHE

PRODUCTION PROCESS IMPROVEMENT AND CHARACTERIZATION OF STARCH NANOCRYSTALS

By

Nkosingiphile Lucky Nzama

N.Dip: Food Technology, B.Tech: Food Technology

Submitted in fulfilment of the academic requirement for the degree Masters of Applied Sciences in Food Science and Technology

Department of Biotechnology and Food Science
Faculty of Applied Sciences
Durban University of Technology, Durban, South Africa

Supervisor: Prof Eric Oscar Amonsou

February, 2023

DECLARATION

I hereby declare that the work reported in this thesis and submitted at the Department of Biotechnology and Food Science at the Durban University of Technology for a Masters Degree is my original work. I confirm that it has not been previously submitted for a degree at any Higher Education Learning Institution.

03/04/2023

Nkosingiphile Lucky Nzama — Date

Student

As the candidate's supervisor I agree to the submission of this thesis

03/04/2023

Prof Eric Amonsou — Date

Supervisor

DEDICATION

To God Almighty, and my family.

ACKNOWLEDGEMENTS

I would like to appreciate:

- My supervisor Prof Eric Amonsou for your guidance, numerous discussions, honest comments, and igniting my passion for science. All of which contributed towards the completion of this project too.
- National Research Foundation (NRF) for seeing the best in me and financially support my studies throughout this program is well appreciated.
- The entire Department of Biotechnology and Food Science for their support, and also created an accommodating environment in which to complete this project.
- The professor at the International school of paper, print media Biomaterials, Alain Dufresne, and the technical team especially Cecile Sillard at Grenoble Institute of Technology for their technical assistance on thermal, XRD, and Microscopy analyses, respectively.
- Mr. Melvin Gao, and Dr. Adarsh Puri for always being at beckon each time I needed to locate anything in the laboratories.
- My colleagues and friends, Sharmista Gajadhar, Moddie Gono, Jessica Shaban, Opeyemi Alabi, Sithembile Shongwe, Abiola Adenike, and Samantha Govender for always being there to listen and encourage me when I was giving up.
- My family for always being a pillar of strength.

Finally, I wish to extend my gratitude to anyone who contributed in any way to the success of this project whom I have not mentioned by name.

ABSTRACT

Starch nanocrystals (SNCs) are promising biomaterials for novel applications in foods, cosmetics, and medicine. In general, acid hydrolysis below the gelatinization temperature of starch is the most common method used for nanocrystals production. Major drawbacks associated with this method are the extended hydrolysis time required (up to 5 days) and the low yield (4–15%) of SNCs. Different methods, including physical and enzymatic pretreatments of starch prior to acid hydrolysis, have been investigated. Among these methods, enzymatic hydrolysis can be regarded as a promising and green strategy for the creation of pores in starch to enhance acid diffusion into the inner regions during SNCs fabrication. Debranching enzymes such as pullulanase are gaining attention in the food industry due to their ability to modify the starch structure and properties through selective hydrolysis of the branched chain of α-1,6-glycosidic bonds. However, pullulanase has not yet been applied as a pretreatment method aiming at starch nanocrystal preparation. Therefore, the pretreatment of starch granules with pullulanase and β-amylase (i.e., to hydrolyze the linear α-1,4-linkages) concurrently could be a novel technique to modify starch surfaces for faster production of SNCs and improved yield.

To improve the efficiency of starch nanocrystals production and properties, pullulanase (15 U/g starch) was used alone or together with β-amylase (50 and 100 U/g starch) to modify the starch before acid hydrolysis. The compound enzyme system of pullulanase:β-amylase (15 : 50 U/g starch) had the most pronounced effect on starch morphology compared to a single enzyme system by creating a dense and more porous structure on starch surfaces as evidenced by microscopy images, a high degree of oil absorption and extent of hydrolysis data. Nanocrystals were produced after 3 days with modified starches instead of 5 days. The yield of SNC was approx. 25 wt.%, which is 3 times greater than that of the conventional SNC preparation method. SNC derived from the modified starches were small in size (less than 50 nm) and appeared mostly as platelet and isolated round particle aggregates. Nanocrystals from modified starches showed the A-type crystalline structure similar to the native starch, but with a significant increase in the degree of crystallinity (from 32.85% to 45.28%.), and the short-range molecular order during the early stage of acid hydrolysis. Starch hydrolysis using compound enzymes consisting of pullulanase and β-amylase hydrolysis seems to be the most effective and green to produce SNC in a shorter time and with increased yield and enhanced properties.

SNCs were incorporated in different concentrations (0, 5, 10, 15, and 20 wt.% starch) together with stearic acid to improve cassava starch-based nanocomposite film properties using a solution casting method. The addition of SNCs from 5 to 15% in combined with stearic acid into starch-based nanocomposite films presented better water resistance, water vapor permeability, and tensile strength than native cassava starch film. Conversely, beyond 15% SNC content, nanocrystals seem to aggregate which impaired the tensile strength of the nanocomposite films. The surfaces of the nanocomposite films were relatively smooth and homogenous after the addition of nanocrystals at up to 15 wt.% concentration compared to native starch film as demonstrated by the atomic force microscopy (AFM). Furthermore, the opaqueness of the nanocomposite films progressively increased with the SNC content, which might be beneficial in the packaging of foods that are easily degraded when exposed to light and high moisture. XRD analysis revealed sharp peaks at approximately 2θ of 13.5° and 20.3°, which are characteristics of typical V-type crystalline pattern in starch films prepared with added steric acid. This further indicates the formation of amylose-lipid complexes in films. The inclusion of SNC in films also enhanced their thermal stability. Therefore, the combined effect of SNC at different concentrations and stearic acid into cassava starch-based films was a successful approach to further improve the mechanical reinforcement and barrier properties of nanocomposite films.

Some part of this research work has been submitted for publication to Journal of *Carbohydrate Polymers* (UNDER REVIEW - CARBPOL-D-23 00681).

PREFACE

This thesis is organized into five chapters and presented. Chapter One is a general introduction to the thesis. Chapter Two presents a critical review of relevant literature. Some areas covered in the literature review include starch structure, various properties of starch, methods of starch nanocrystal production, morphological properties of SNCs and applications of SNCs. Chapter Three focuses on the preparation of SNCs using combined enzymatic pretreatment for enhancement of the nanocrystals production. Chapter Four presents the effect of SNCs on the mechanical and barrier properties of cassava starch-fatty acid composite film. Chapter Five covers the general discussion of the work and highlights the conclusion derived from the research and provides recommendations for future work.

TABLE OF CONTENT

LIST OF FIGURES

LIST OF TABLES

Table 4.1: Effect of SNC concentration on the moisture content (MC), swelling ratio (SR), solubility in water (SW), water vapor permeability (WVP), and opacity of starch-based nanocomposite films. 68
Table 4.2: Thermal properties of starch-based nanocomposite films. 76

ABBREVIATIONS

SNC: Starch nanocrystals.

SEM: Scanning electron microscopy.

TEM: Transmission electron microscopy.

AFM: Atomic force microscopy.

DSC: Differential scanning calorimetry.

TGA: Thermo-gravimetric analysis.

WVP: Water vapor permeability.

TS: Tensile strength.

E (%): Elongation at break.

FTIR: Fourier transform infrared (FT-IR) spectroscopy.

XRD: X-ray Diffraction.

T_g: Glass transition temperature

T_m: Melting temperature.

ΔH_m: Enthalpy of melting.

DTG: Differential thermo-gravimetric.

PUBLICATIONS AND CONFERENCES ATTENDED

Publications

Nkosingiphile L Nzama, Alain Dufresne, and Eric O Amonsoua (2023). Pullulanase, a starch debranching enzyme and β-amylase as pretreatment tools for the enhancement of the starch nanocrystal production process. *Carbohydrate Polymers* (UNDER REVIEW - CARBPOL-D-23 00681).

Conferences attended

Nkosingiphile L Nzama, Alain Dufresne, and Eric O Amonsou. Production process improvement and characterization of starch nanocrystals. International Research Day, Durban University of Technology, South Africa. 14th November 2022

CHAPTER ONE

1.0 Introduction

Nanoscience and nanotechnology have great potential for adding value to the food chain by transforming the entire food chain industry such as food production, processing, analysis and packaging (Aswathanarayan and Vittal 2019). The increasing demand for utilizing natural sources, renewable and biodegradable polymers stimulate the interest in nanotechnology (Kim, Park and Lim 2008; LeCorre, Bras and Dufresne 2011). Starch, an abundant natural polymer, has been considered the most promising renewable naturally biodegradable polymer since it is versatile and can be produced at a low cost (Kim, Park and Lim 2008). The global starch market is estimated to reach 160.3 million metric tons by 2026 (Vilpoux and Santos Silveira Junior 2023). Thus, industrialists and researchers are seeking new properties or high-value applications for starch (Kaur *et al.* 2018).

Starch nanocrystals (SNCs) are novel materials that present unusual chemical properties due to their extremely small size of 100 nm or less and wide surface (Jiang *et al.* 2016). According to Dai *et al.* (2018), starch nanocrystals (SNCs) are the preserved crystalline structure arising from the destruction of amorphous structures of starch granules by acid hydrolysis. SNCs had received considerable attention (Mukurumbira *et al.* 2017; Hao *et al.* 2018b; Javidi, Razavi and Mohammad Amini 2019; Zhou *et al.* 2020). A growing number of research on possible areas of application in the food and material industries have been published in literature. (Haaj *et al.* 2014; Li *et al.* 2015; Costa *et al.* 2017; Dai, Zhang and Cheng 2020b). Promising areas of interest for the application of SNCs are in bioplastic packaging (Diaz-Montes and Castro-Munoz 2021) and Pickering emulsions (Wei *et al.* 2014). Li *et al.* (2015), mitigated several drawbacks exhibited by starch films when compared to plastic polymers, such as their hydrophilic character and poor mechanical properties by introducing starch nanocrystals as reinforcement in pea starch films. Their results showed better mechanical and water vapour barrier properties with enhanced thermal stability of pea starch nanocomposite films compare to pure pea starch films. Furthermore, previous studies revealed that square-like nanocrystals are preferred to be used as nano-reinforcements in bio-composite films (Mukurumbira *et al.* 2017). Although SNCs are promising materials for various applications, their production still presents some challenges, which limit their widespread use. Acid hydrolysis is the most commonly used method to derive SNCs from various sources of starch, including tubers,

cereals, and legumes (Sun *et al.* 2014; Mukurumbira *et al.* 2017; Kaur *et al.* 2018). However, the production of SNCs obtained by the conventional acid hydrolysis method is limited because it is time-consuming (5 days) and results in a low yield of about 4-15 wt.% (Putaux *et al.* 2003; Angellier *et al.* 2004).

To address these challenges of the traditional acid hydrolysis method, different modes of preparations including pretreatment methods such as physical (e.g., ultrasonication and ball milling), or enzymatic (e.g., α-, β-amylases, and glucoamylase,) in combination with acid hydrolysis or separation have been investigated (LeCorre *et al.* 2012; Kim *et al.* 2013a; Dai *et al.* 2018). Dai *et al.* (2018), subjected waxy maize starch to mechanical pretreatment with a planetary ball mill before hydrolyzed with sulfuric acid. Their results revealed that after ball milling, H_2SO_4, hydrolysis was reduced to 3 days and SNCs yield of 19.3 wt.% was obtained. However, after 30 min of ball milling treatment, there was a sharp decline in relative crystallinity due to the destruction of the starch crystalline structure. Another research effort to improve SNCs preparation was reported by Hao *et al.* (2018a), who developed an enzymatic pretreatment of starch with glucoamylase to reduce the acid hydrolysis duration. According to these authors, enzymatic pretreatment of native starch was able to achieve a drastic reduction in the acid hydrolysis time from 5 days to 2 days through accelerated penetration of H_3O^+ into inner regions. Although various approaches have been proposed to generate SNCs, the poor yield of nanocrystals is still regarded as a key limitation for large-scale SNC production (Mukurumbira *et al.* 2017). This makes SNCs currently unable to meet the industrial production scale (Silva *et al.* 2018). Therefore, there is still a need to improve processing methods of starch nanocrystals production.

The creation of pores in starch through enzymatic hydrolysis can be regarded as a promising and green strategy for surface starch modification and deserve further consideration. However, previous studies narrowly reported on single enzymes' use of α-amylase and glucoamylase. Debranching enzyme such as pullulanase is known for its ability to rapidly and efficiently hydrolyze the α-1,6 glycosidic bonds, releasing a mixture of linear chains of glucose units from the parent amylopectin molecule. Pullulanase, has been gaining much interest in starch conversion processes (Hii *et al.* 2012). However, pullulanase has not yet been applied as a pretreatment method aiming at starch nanocrystal preparation. But, as a debranching enzyme, pullulanase may offer new possibilities and could be applied to starch modification alone or in combination with

other enzymes (e.g., β-amylase) to increase the efficiency of the SNC production process. Therefore, this study aimed to improve the production process (e.g., enzymatic pretreatments) of starch nanocrystals from various starch sources (e.g., amadumbe, cassava, and waxy corn) and assess their applications in food.

CHAPTER TWO

2.0 Literature review

2.1. Nanotechnology and its applications in food

Nanotechnology is a key advanced technology, exerting significant impacts on the food industry in areas such as food processing; production; analysis; and packaging (He and Hwang 2016; Singh *et al.* 2017). Nanotechnology in food introduces a novel approach to enhancing food bioavailability; taste; texture; and consistency, through modification of particle size that may cause physical improvement and chemical stability in food products (Samal 2017). Furthermore, the incorporation of nanomaterials has been reported as an innovative approach to improving the physical, mechanical; and barrier properties of biopolymer-based food packaging (Hamad *et al.* 2018).

Nanomaterials often display vastly different physicochemical properties compared with their respective bulk materials (Chellaram *et al.* 2014). Mechanical strength; larger specific surface area; high solubility and chemical reactivity are perceived as novel characteristics which can be used in applications involving encapsulation; stabilization (Albert *et al.* 2019); adsorption; and nanoreinforcement (Samal 2017). For instance, Shao *et al.* (2018) constructed a Pickering emulsion stabilized with taro SNCs and encapsulated tea polyphenols to explore the effectiveness of bioactive substances. The SNCs were irreversibly adsorbed at the oil-in-water interface exhibiting a strong indication as a good source of particle stabilizer and, after 24 h, the retention rate for tea polyphenols was 67%. This proved that taro SNCs have great potential in the application of functional factors for the control release (Shao *et al.* 2018).

Innovative packaging technologies using biopolymer-based composites incorporated with nanoparticles (i.e., bionanocomposites) have become a research hotspot (Jeevahan and Chandrasekaran 2019a). Bio-nanocomposites comprise a biopolymer matrix reinforced with nanoparticles having at least one dimension in the nanometer range (1 to 100 nm) (Han 2014). Inorganic nanoparticles of various shapes, such as layered silicates; spherical SiO_2; or carbon nanotubes have been incorporated into biopolymer films, for example, to enhance their performance (Condés *et al.* 2015). However, the safety concern of inorganic nanoparticles has demanded more interest in using biodegradable; biocompatible; natural sources of nanostructured

materials such as rod-like cellulose and chitin whiskers; and platelet-like starch nanocrystals. In particular, starch nanocrystals have become a suitable alternative nanoreinforcement, due to their low cost and abundance in nature (Dai, Zhang and Cheng 2020b).

2.2. Starch

Starch is an abundant natural polymer that has been considered the most promising renewable naturally biodegradable polymer (Nakamura 2015). Starch is generally divided into four categories: cereal, tubers, legumes, and other starches (Wolff 2018). In general, the physicochemical, functional, and morphological properties of starches vary with their botanical sources, and composition (Li *et al.* 2017).

2.2.1. Starch morphology and composition

Starch granules range in size (from 1 to 100 μm diameter) (Bertoft 2017) and shape (polygonal; spherical; lenticular) (Figure.2.1). They vary regarding with content, structure and organization of amylose and amylopectin molecules; the branching architecture of amylopectin; and the degree of crystallinity (Copeland *et al.* 2009).

Starch molecules are the polymers of anhydrous glucose units, which are typically accumulated in a unique and independent granule (Bertoft 2017). Amylose and amylopectin are the major starch fraction polymers that primarily comprise a starch molecule. These two types of α-glucan (amylose & amylopectin) represent approximately 98-99% of the dry weight (Schirmer *et al.* 2013). Amylose and amylopectin are anhydroglucose polymers comprising α-D-glucopyranose units (Bertoft 2017).

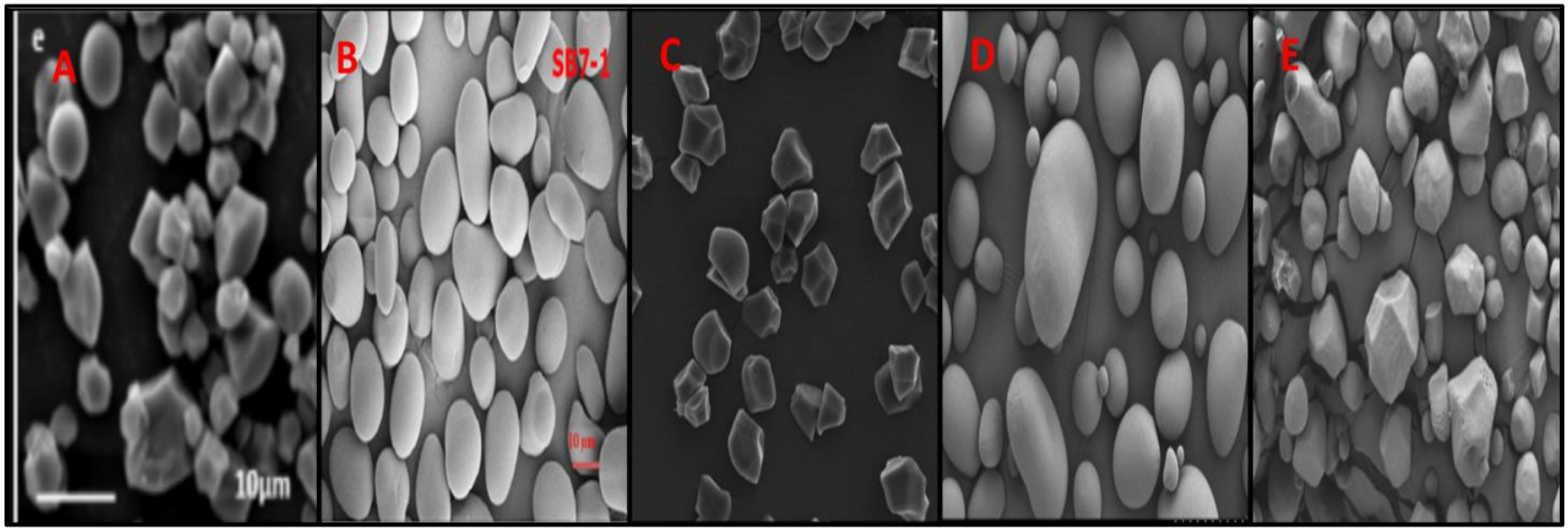

Figure 2. 1: Scanning electron micrograph of different morphologies of starch granules from various botanical sources: A-amadumbe; B-bambara groundnut; C-finger millet; D-potato starch; and E-corn starch. Adapted from [A]Mukurumbira *et al.* (2017), [B]Kaptso et al. (2015), [C]Abdalla et al. (2009), [D]Noda et al. (2005), and [E]Singh and Singh (2003).

Amylose exists as a long linear chain α-glucan containing approximately 99% of α(1→4) glycosidic bonds (Figure.2.2) (Tester, Karkalas and Qi 2004b). Amylose has a molecular weight range of approximately 10^5–10^6 Da, corresponding to polymerization (DP) of 1000–10000 glucose units. Less than 0.5% of glucose in amylose are in α(1→6) linkages, resulting in low branching, and a structure with 3–11 chains of approximately 200–700 glucose residues per molecule (Pérez and Bertoft 2010). Amylose is predominantly found in the low-density layers of the growth rings. However, depending on the botanical source, and environmental growth factors, the size and structure of amylose have been observed to differ considerably, as previously discussed. Furthermore, some amylose molecules are considered to be interspersed between amylopectin in the crystalline layers, disrupting the crystal packing of amylopectin (Lindeboom, Chang and Tyler 2004; Copeland *et al.* 2009).

The amylose content, molecular size, shape, structure and polydispersity of the molecules vary with botanical origin (Tester, Karkalas and Qi 2004b). In general, waxy starches comprise less than 15% amylose, normal-maize (20 – 35%) and high-amylose starches of more than 40% (Schirmer *et al.* 2013). In high-amylose starches, amylose helices may contribute to the crystallinity of granules (Copeland *et al.* 2009).

Amylopectin is an extensively branched portion of the starch molecules and formed through chains of α-D-glucopyranose residues joined primarily by α-(1→4) glycosidic bonds with α-(1→6) linkages at branch points (Tester, Karkalas and Qi 2004b; LeCorre, Bras and Dufresne 2011). Amylopectin has approximately 5% of its glucose in α-(1→6) linkages, giving it a highly branched, tree-like structure and a complex molecular architecture that can vary substantially between starches concerning percentages and length of branches (Pérez and Bertoft 2010). The amylopectin branches may be classified according to their pattern of substitution: A-chains are defined as unsubstituted, B-chains are substituted by other chains, and there is a single C-chain that carries the reducing glucose (LeCorre, Bras and Dufresne 2012; Schirmer *et al.* 2013; Bertoft 2017).

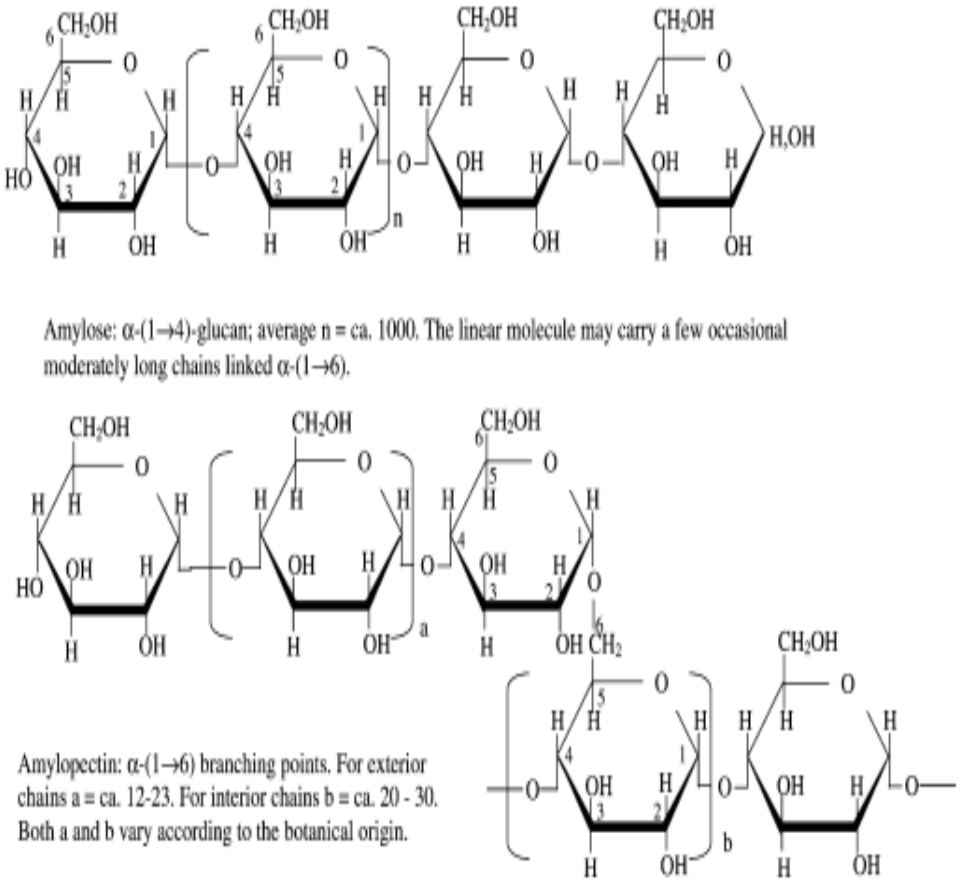

Figure 2. 2: Amylose and amylopectin chains Adapted from Kaur et al. (2018).

For the structure of amylopectin (Figure 2.3), the A-chains of amylopectin are (1→6)-α linked by B-chains which in turn can be linked to other B-chains or the 'backbone' of the amylopectin molecule, the single C-chain (Tester, Karkalas and Qi 2004b). Further classification could be based on variations to the degree of hydration and packing arrangements of the double helices of A-and B-type crystalline forms. The packing with the A-type polymorph is fairly compact with minimal water content whilst the B-type is characterized by a more open structure containing a hydrated helical core (Figure 2.4) (Tester, Karkalas and Qi 2004a; Copeland *et al.* 2009).

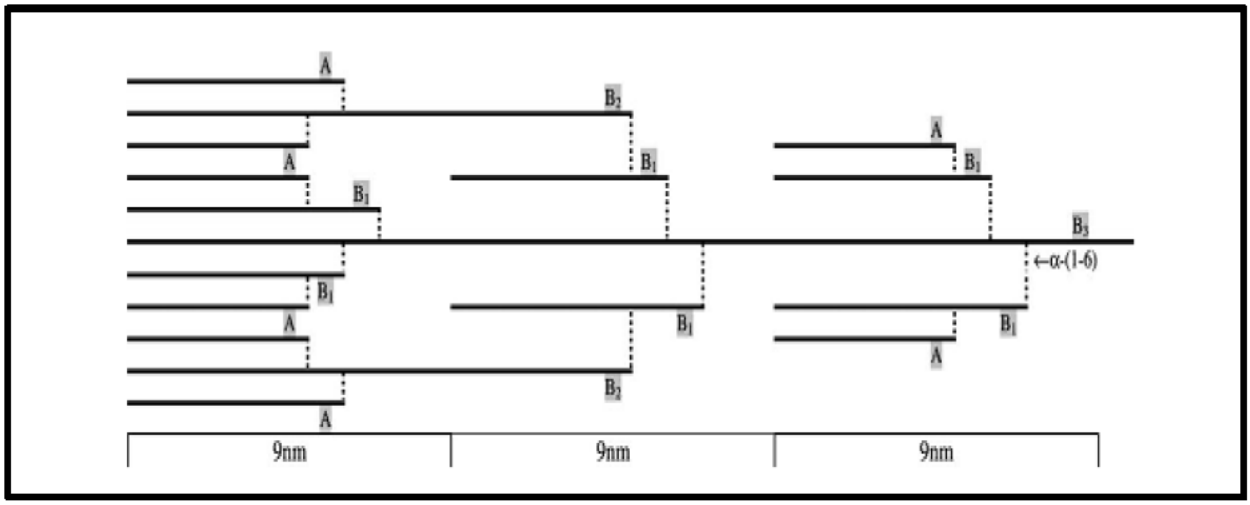

Figure 2. 3: Diagrammatic representation of a part demonstrating the branching patterns of unit chains A, B and C. Adapted from Perez and Imberty (2002).

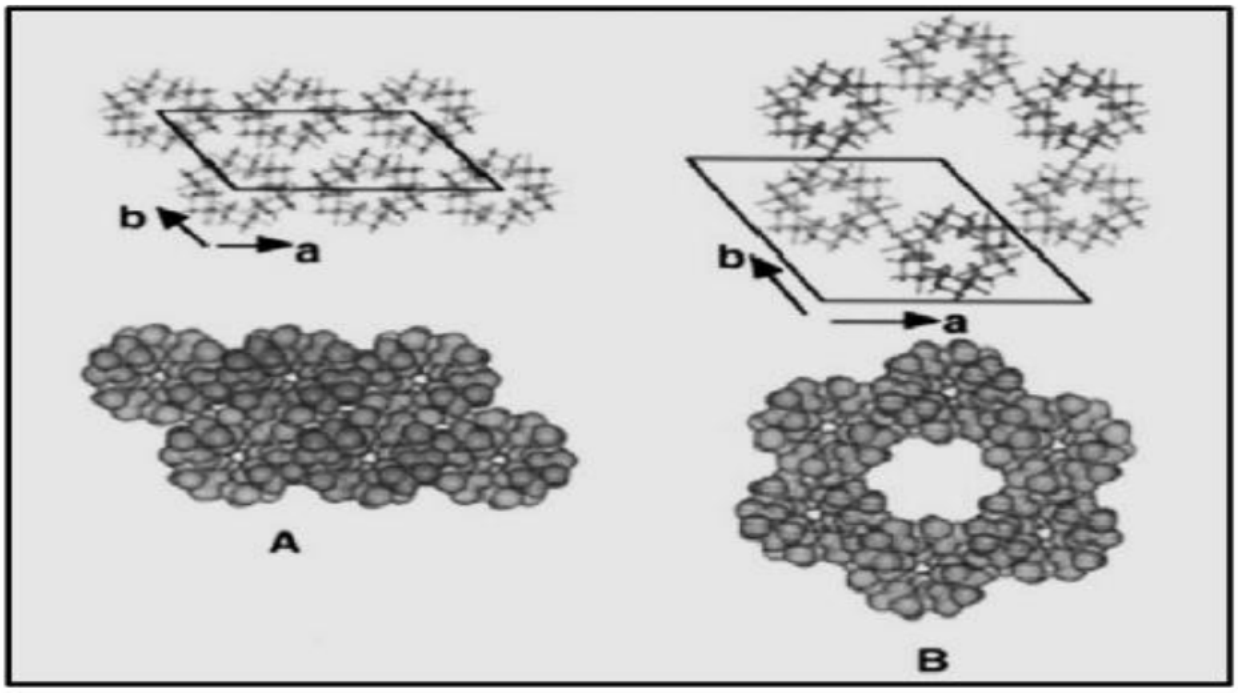

Figure 2. 4: Double helixes packing configuration according to a crystalline type. Adapted from LeCorre, Bras and Dufresne (2011).

2.2.2. Starch granule organization

Native starch granules are widely regarded to be composed of a multiscale structured biopolymer which ranges from nanometer to micrometer in scale, i.e., amylose and amylopectin chains (~nm); crystalline and amorphous lamellar structure (9-10 nm); alternating amorphous and semi-crystalline growth rings (100-400 nm) and starch granule (< 1-100 μm) (Figure 2.5). Preferential acid hydrolysis of the amorphous regions can isolate the crystalline region of starch granules to produce starch nanocrystals (LeCorre, Bras and Dufresne 2011; Santana and Meireles 2014; Li *et al.* 2016).

The amorphous regions of starch primarily contain amylose, whilst amylopectin is located in the crystalline regions (Copeland *et al.* 2009). Depending on the botanic origin of starch, amylose is preferably found in the amorphous region (e.g., wheat starch), interspersed among amylopectin clusters in both the amorphous and crystalline regions (e.g., normal maize starch), bundles between amylopectin clusters, or co-crystallized with amylopectin (e.g., potato starch) (LeCorre, Bras and Dufresne 2011). The amorphous regions are more susceptible to hydrolysis (LeCorre *et al.* 2012; Mukurumbira *et al.* 2017).

Amylose and amylopectin in the starch granule form a semi-crystalline structure, comprising the crystalline lamella and amorphous lamella (Cornejo-Ramírez *et al.* 2018). The crystalline lamella comprises parallel glucan chains, ordered and closely packed, whereas the amorphous lamella consists predominantly of less ordered branching regions (Oates 1997). Several factors affect the crystallinity of starch granules, such as amylose content, amylopectin chain length, lipid content, amylose-lipid complexes and starch granule size (Cornejo-Ramírez *et al.* 2018).

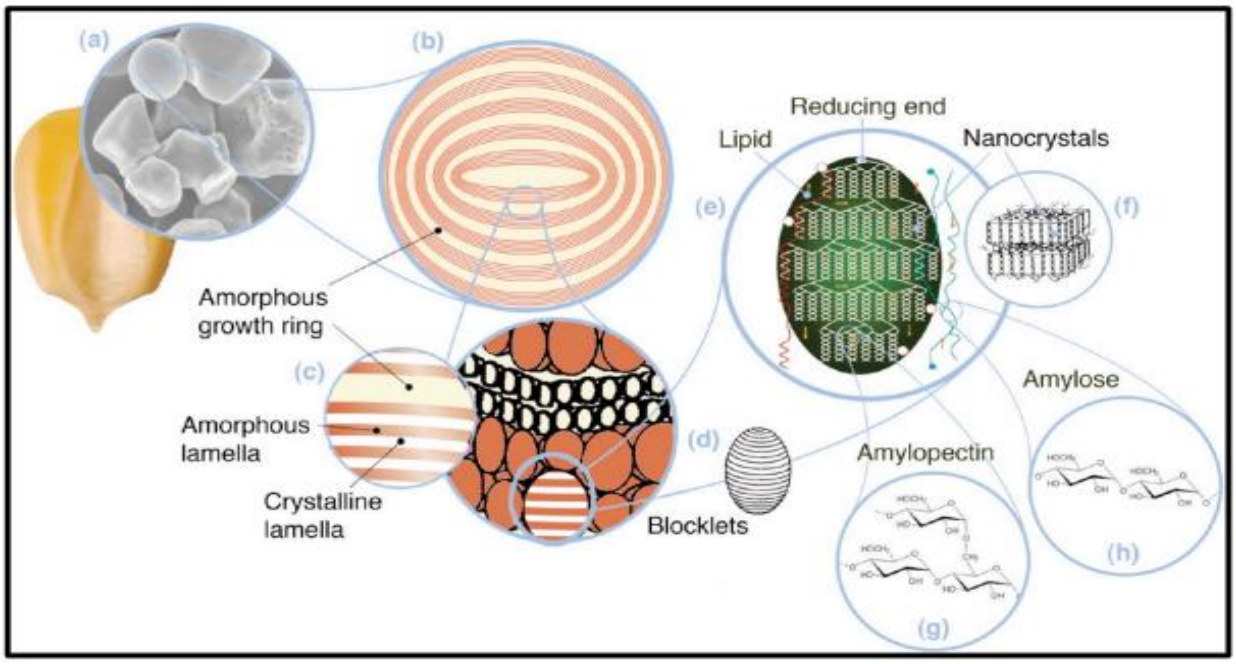

Figure 2. 5: Overview of starch granule multi-scale structure. Adapted from Le Corre et al. (2011).

2.3. Starch nanocrystals

The disruption of the semi-crystalline structure of starch granules by the acidic and/or enzymatic treatment causes the selective hydrolysis of the amorphous region, resulting in crystalline residue in nanoscale size, with platelet morphology known as nanocrystals (Kim *et al.* 2013a; Le Corre-Bordes and Angellier-Coussy 2014; Mukurumbira *et al.* 2017). Starch crystallites, starch nanocrystals, microcrystalline starch and hydrolyzed starch are all referred to as the crystalline part of starch. But Le Corre-Bordes and Angellier-Coussy (2014) distinguish from each other based on the extent of hydrolysis they underwent (from the most to the least). The ones that may contain amorphous matrices are referred to as starch nanoparticles.

The preparation of nanomaterials has been classified into top-down and bottom-up approaches. In the "bottom-up" process, nanostructures may be prepared from a build-up of atoms or molecules in a controlled manner that is regarded by thermodynamic means such as self-assembly (Kim, Park and Lim 2015; Kaur et al. 2018). The "top-down" approach is commonly used and involves the breakdown of larger particles into nanoparticles produced from the structure and size reduction of

bulk materials using various techniques (Zheng et al. 2009; Lin et al. 2011). The preparation of starch nanocrystals by the top-down approach includes acid hydrolysis, enzymatic treatment, and physical treatment (Le Corre-Bordes and Angellier-Coussy 2014; Mukurumbira *et al.* 2017).

2.4. Production methods for starch nanocrystals

2.4.1. Acid hydrolysis

Acid hydrolysis is the most commonly used approach to derive starch nanoparticles (Kim, Park and Lim 2015). The most used acids for nanocrystal production are hydrochloric acid (HCl) and sulphuric acid (H_2SO_4) (Putaux *et al.* 2003; LeCorre, Bras and Dufresne 2011). The crystalline regions in starch granules are more resistant to acid hydrolysis than the amorphous regions and thus crystalline moieties can be isolated by mild acid hydrolysis (Kim *et al.* 2013a). All starches, when exposed to these acids, exhibit two-stage hydrolysis kinetics. The initial fast hydrolysis step is presumable due to the hydrolysis of the amorphous regions of starch granules which are highly susceptible to acid. The second slow step of hydrolysis is assumed to be hydrolyzing the more densely packed crystalline regions which do not allow readily the penetration of H_3O^+ (Le Corre-Bordes and Angellier-Coussy 2014; Kaur *et al.* 2018). Another hypothesis that has been put forward to explain the slow rate of hydrolysis in the crystalline region is that the hydrolysis of the glycosidic bond requires a change in conformation from chair to half-chair to allow hydrolysis of the glycosidic bonds in the crystalline regions (LeCorre, Bras and Dufresne 2011; Kim, Park and Lim 2015).

Starch characteristics (granule size, amylose content, granule surface porosity); starch source; and hydrolysis conditions (time, acid type and concentration and temperature) influence the hydrolysis of starch concerning the final properties and yield of nanocrystals produced (LeCorre, Bras and Dufresne 2011; Kim, Park and Lim 2015; Mukurumbira *et al.* 2017; Zhou *et al.* 2020). LeCorre, Bras and Dufresne (2011), studied the influence of some botanic origin, amylose content and crystalline type of native starch on the features and properties of SNCs under mild acid hydrolysis. The authors reported amylose content and crystalline type could be more of an influence on the size and shape, respectively. They claimed that as the amylose content increases, the particle size becomes bigger since amylose is believed to jam the pathways for hydrolysis (LeCorre, Bras and Dufresne 2011).

Although SNCs produced by acid hydrolysis present high crystallinity, the lengthy duration of acid treatment and low yield make this method inappropriate for practical applications. Furthermore, due to its long processing time, this treatment can lead to total degradation of the already formed nanocrystals. Thus, other various processes such as enzymatic (Sun *et al.* 2014) and physical treatment (Bel Haaj *et al.* 2013a; Ahmad *et al.* 2020; Hedayati, Niakousari and Mohsenpour 2020) applied alone or in combination with chemical processes have been proposed (Figure 2.6).

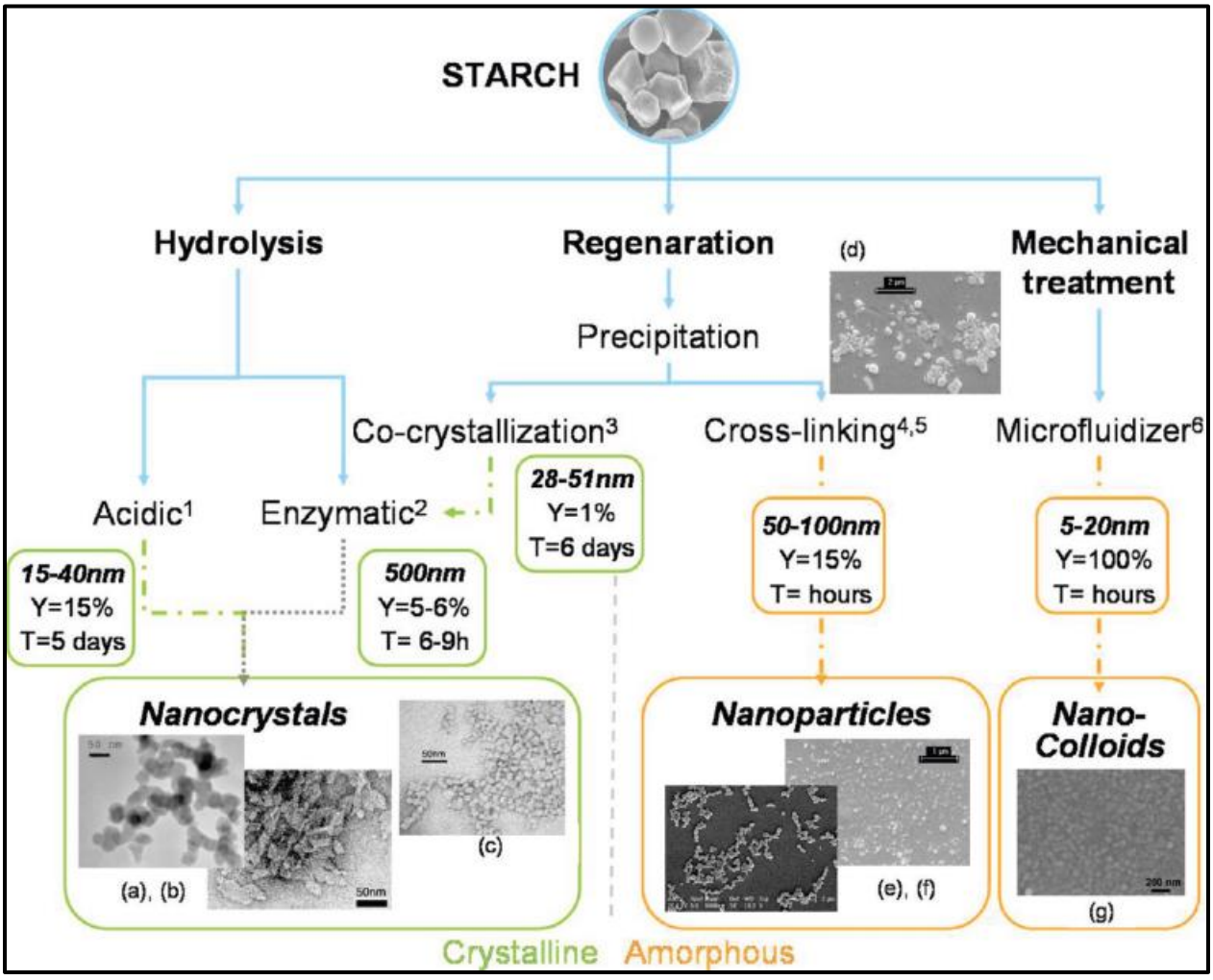

Figure 2. 6: Different methods of producing nanocrystals and nanoparticles. Adapted from LeCorre, Bras and Dufresne (2011).

2.5. Impact of starch pre-treatment methods on nanocrystals production

2.5.1. Physical pretreatment

Physical treatments used in the production of nanocrystals include high-pressure homogenization, ultrasonication, reactive extrusion and gamma radiation (Bel Haaj *et al.* 2013a; Kim *et al.* 2013b; Ahmad *et al.* 2020). However, such physical treatment methods have been unsuitable for the starch nanocrystals preparation due to partial or complete disintegration of the starch crystalline structure, which appeared to lead to nanoparticles that had a low crystallinity or an amorphous structure (Kim *et al.* 2013a; Kim, Park and Lim 2015). Thus, a combination of physical pretreatment and acid hydrolysis has been employed to produce nanocrystals (Bel Haaj *et al.* 2013b; Kim *et al.* 2013a; Dai *et al.* 2018). For example, Kim, Park and Lim (2015), reported the preparation of starch nanoparticles from waxy maize starch by a combined process of acid hydrolysis (2 days at 40°C) and subsequently ultrasonic treatment (60% vibration amplitude, 3 minutes) applied to the re-dispersed suspension of the large microparticles of starch hydrolysates which had been recovered by mild centrifugation.

2.5.2. Enzymatic pretreatment

Nanocrystals have rarely been prepared by enzymatic treatment alone, but a combination of enzyme pretreatment and acid hydrolysis has been used (Silva *et al.* 2018). LeCorre *et al.* (2012) investigated an enzymatic pre-treatment of waxy maize starch to reduce preparation duration and increase the yield of subsequent acid hydrolysis during the production of nanocrystals. The authors reported that the extent of acid hydrolysis, which normally required 5 days, was obtained after only 45 h with a yield of ∼15% (LeCorre *et al.* 2012). Another study was reported by Hao *et al.* (2018b), on the pretreatment of starch with a starch hydrolyzing enzyme such as glucoamylase. According to their findings, glucoamylase treatment resulted in the creation of pores on the granules' surface, which accelerated the penetration of H_3O^+ into inner regions and decrease the acid hydrolysis time from 5 days to 2 days. Thus, the creation of pores in starch through enzymatic hydrolysis can be regarded as a promising and green strategy for surface starch modification and deserve further consideration. Although various amylolytic enzymes (e.g., α-amylase; glucoamylase; and β-amylase) have been utilized for starch surface modification during SNC production, these studies are limited only to a single enzyme used. Different enzymes hydrolyze starch granules at specific binding sites (Bertoldo and Antranikian 2002b). Hence, combining more

than one enzyme with different substrate specificity as a pretreatment method could further improve these manifestations.

2.6. Starch modification enzymes

Native starches are modified to overcome shortcomings, including retrogradation, syneresis, and low water-holding potential, which limit their industrial applications (Punia Bangar *et al.* 2022). Various enzymatic modification techniques have been attempted to alter starch characteristics for its novel application in the food industry (Park *et al.* 2018). However, the most common enzymes utilized for starch modification include α-amylase, β-amylase, glucoamylase, pullulanase, and isoamylase (Dura, Blaszczak and Rosell 2014b). In this section, the mechanism actions of these amylolytic (e.g., α-amylase, β-amylase, glucoamylase) and debranching (e.g., pullulanase, and isoamylase) enzymes on starch modification into food ingredient is described.

Amylases are starch-transforming enzymes that hydrolyze glycosidic bonds (LeCorre *et al.* 2012). These enzymes are often divided into three groups: endo-amylases, which cleave internal α-(1→4) bonds resulting in α-anomeric products; *exo*-amylases which cleave α-(1→4) and α-(1→6) from non-reducing end resulting in α- or β-anomeric products; and debranching enzymes which include isoamylase and pullulanase which hydrolyze exclusively α-(1→6) bonds leaving long linear polysaccharides (Hii *et al.* 2012; Park *et al.* 2018). The process of enzymatic starch conversion is displayed in Figure 2.7.

Endo- and exoamylases

Endo-acting enzymes or endoamylases mainly hydrolyze α-1,4 linkages present in the inner part (endo-) of the amylose or amylopectin (Hii *et al.* 2012). α-Amylase (EC 3.2.1.1) produced by a wide variety of microorganisms, belonging to *Bacteria* and *Archaea* are well-known as endoamylases. They can attack any point in the interior part of the starch polymer, which leads to the formation of linear or branched oligosaccharides or α-limit dextrins (LeCorre *et al.* 2012).

Exoamylases such as barley β-amylase (EC 3.2.1.2) exclusively hydrolyze α-1,4 glycosidic bonds on the external glucose residues of amylose and amylopectin from the non-reducing end and thus produce maltose and β-limit dextrin (Hii *et al.* 2012). β-amylolysis contributed to thinning effect to the soluble starch particles and increased DP (2 – 5 chains). A plant-derived β-amylase has a

substantial technological value in the starch processing sector due to its safety and high specificity (Punia Bangar *et al.* 2022).

Debranching enzymes

Debranching enzymes selectively hydrolyze α-1,6-glycosidic bonds in amylopectin, leading to the formation of linear short chain molecules of low molecular weights (Liu *et al.* 2017). These enzymes may be divided into three major groups according to their substrate specificity: microbial pullulanases; isoamylases; and amylo-1,6-glucosidases (Hii *et al.* 2012). Microbial pullulanase attracts more interest because of its specification on α-1,6 linkages in pullulan or branched polysaccharides. During starch saccharification processes, pullulanase is generally used in combination with other amylolytic enzymes such as β-amylase. Whereas, the simultaneous action of β-amylase and isoamylase inhibits the activity of isoamylases (Hii *et al.* 2012). Therefore, further promoting the combined action of enzymes in starch modification for the creation of pores would be beneficial for starch nanocrystals production.

2.7. Application of starch hydrolytic enzymes to modify starch granule surfaces

Starches obtained from various botanical origins vary in granule morphology, crystalline organization, and molecular structure, thereby, their susceptibility to the enzyme and/or acid hydrolysis is restricted by low surface area and pore volume (Li *et al.* 2017; Zhao *et al.* 2018). Therefore, modification of starch granule surface can increase the efficiency of native starch hydrolysis (Chen *et al.* 2011). In food and non-food industries, the application of porous starches has been considered to be an attractive material for use as a bioadsorbant (Lacerda, Leite and da Silveira 2019). Porous starches are modified starch granules that contain abundant pores from the surface to the interior part of the granule, which increases the specific surface area, acting as an excellent natural absorbent (Benavent-Gil and Rosell 2017a; Yang *et al.* 2019).

The degree of porosity could be controlled by using different enzymes or a combination of enzymes that produce a synergistic effect in altering the granular surfaces and generating inner channels in various patterns (Dura, Blaszczak and Rosell 2014b). Many research studies have reported that by controlling either the type or level of the amylolytic enzyme, a porous starch with varying numbers and sizes of pores could be obtained (Benavent-Gil and Rosell 2017b, 2017c). In addition, Benavent-Gil and Rosell (2017b) confirmed that diverse pore size distribution depended

on the enzyme type and starch source. Four native starches (i.e., wheat, rice, potato, and cassava) were hydrolysed with amyloglucosidase, α-amylase, and cyclodextrin-glycosyltransferase to study the action of different amylolytic enzymes on the microstructure of porous starch. Scanning electron microscopy (SEM) demonstrated porous structures with a diverse pore size distribution, which was dependent on the enzyme type and starch botanical source (Benavent-Gil and Rosell 2017b). Therefore, the enzyme type and native starch source have a substantial impact on the properties of the obtained porous starches.

The efficiency of acid hydrolysis at the granule level could be influenced by the porosity of the starch granule (Chen *et al.* 2017; Li *et al.* 2020). Thus, the creation of random distribution of pores, using enzymes pre-treatment, could result in the high susceptibility of starch granules to be attacked by sulfuric acid (Keeratiburana *et al.* 2020). Moreover, for starches with pores, an inside-out pattern hydrolysis is reported whereas, for starches with smooth surfaces, the hydrolysis can only start from the surface (Zan *et al.* 2021). Hence, such differences in the granule structure substantially affect the rate of acid hydrolysis in starch. Although various amylolytic enzymes (e.g., α-amylase; glucoamylase; and β-amylase) have been utilized for the creation of a starch porous structure. Limited research studies are reported on applying pullulanase enzymes as an enzymatic pre-treatment alone or in combination with other amylolytic enzymes (i.e., β-amylase). The starch-debranching enzymes, pullulanase and isoamylase can specifically hydrolyse the α-(1→6) linkages existing at the branching points (Chen *et al.* 2020). Thus, the combined pre-treatment of a starch-debranching enzyme (i.e., pullulanase) with β-amylase, and other controlled physical treatment methods could be a novel technique to produce porous starch with abundant pores without destroying the structure of the starch granule. Moreover, porous starches might offer an attractive alternative to develop an efficient method to produce SNCs.

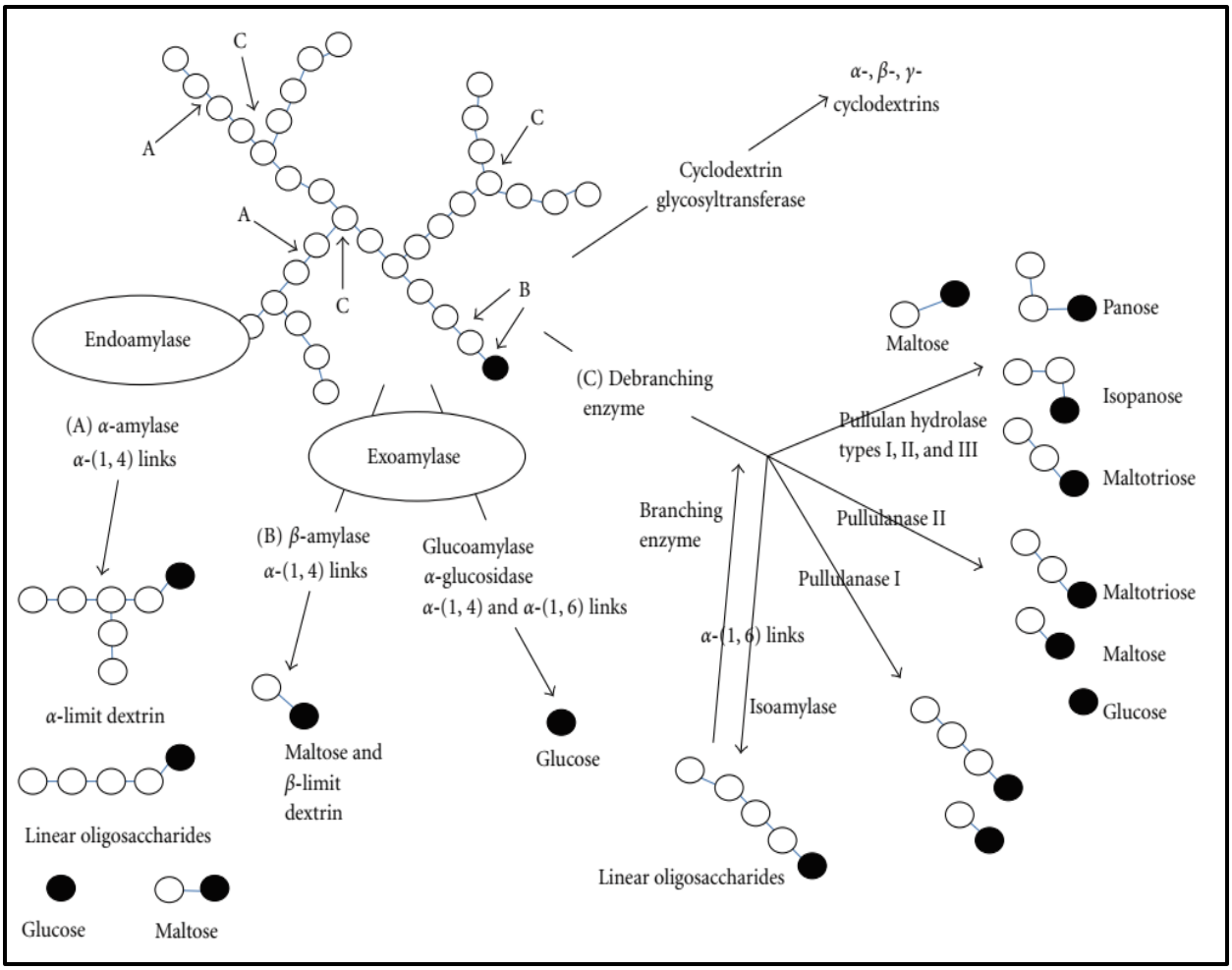

Figure 2. 7: Schematic presentation of the action of amylolytic and pullulytic enzymes. Pullulanase type I also attacks α-1,6-glycosidic linkages in oligosaccharides and polysaccharides. Pullulanase type II also attacks α-1,4-linkages in various oligosaccharides and polysaccharides. Black circles indicate reducing sugars. Adapted from Bertoldo and Antranikian (2002a).

2.8. Impact of pre-treatment methods on characteristics of starch nanocrystals

2.8.1. Morphology

The square-like or round shape platelets are the most observed SNCs (Figure 2.8). Initially, morphological characteristics of SNCs were regarded to be primarily determined by the botanical origin and the preparation method utilized (LeCorre, Bras and Dufresne 2011). However, many scientists have shown that the botanical source has a limited effect on the morphology of SNCs but is influenced by the amylose content; crystalline pattern and the physical and chemical parameters used for the preparation (Le Corre-Bordes and Angellier-Coussy 2014; Ahmad *et al.* 2020; Velasquez-Castillo *et al.* 2020a).

Previous studies suggested that the differences in the arrangement of amylopectin double helices in crystalline lattice might induce the formation of different nanoparticles (Angellier-Coussy *et al.* 2009; LeCorre, Bras and Dufresne 2011; Li *et al.* 2020). Thus, round platelets have been observed for B-type starches such as potato, whilst square-like platelets were reported for A-type corn starches (Figure 2.9). Overall, according to these scientists, the nanocrystals produced from A-type starches (e.g., waxy maize, normal maize, wheat starch) rendered square-like particles, whereas those obtained from B-type starches (e.g., high amylose maize, potato) produced round shape particles. Moreover, Mukurumbira, Mellem and Amonsou (2017a) similarly observed the square-like morphology in amadumbe SNCs (Table 2.1). This was expected since the amadumbe starch displayed the A-type crystallinity pattern (Mukurumbira, Mellem and Amonsou 2017a). However, the morphology and size might not be the same as that in starch granules because those could be changed according to physical and chemical parameters used for the preparation (Kim, Park and Lim 2015; Velasquez-Castillo *et al.* 2020a).

Although there are some differences in the morphology of SNPs, the fact that SNPs obtained from hydrolysis of starch granules tend to self-aggregate, forming microscale agglomerates still limits their further application. The aggregation of SNCs has been attributed to hydrogen bond formation resulting from the interaction of hydroxyl groups on the surface of starch nanocrystals (Kim, Park and Lim 2015). Therefore, a combination of enzymatic pre-treatment and acid hydrolysis could be an attractive approach for SNCs preparation with preferable dispersity.

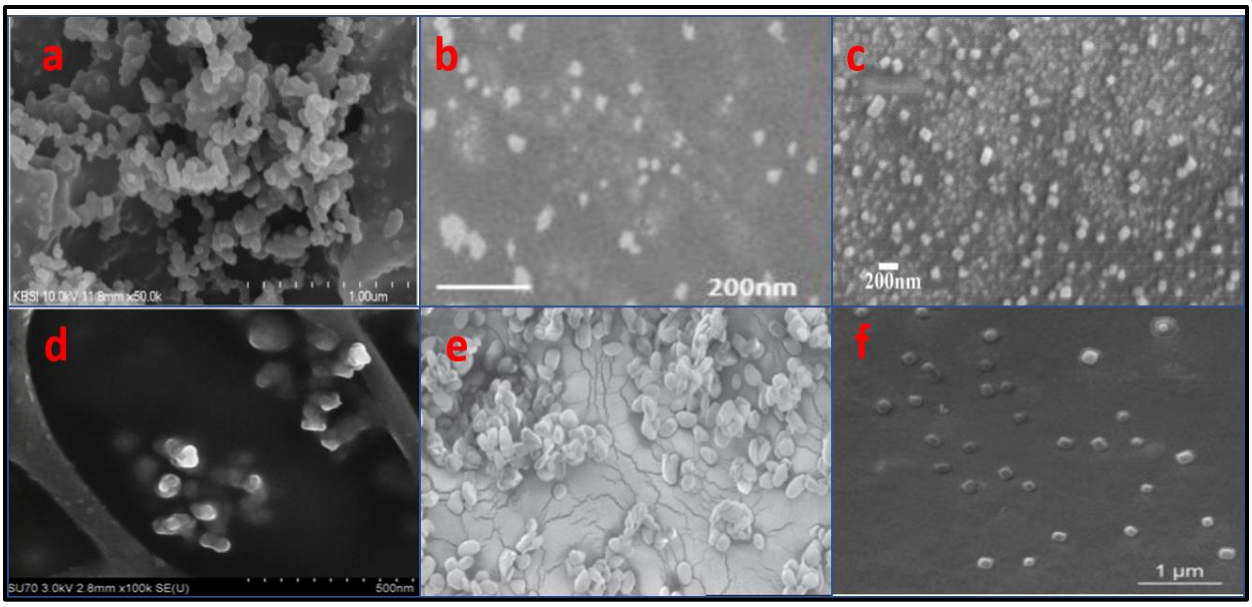

Figure 2. 8: Morphology of SNCs from different starch sources obtained by various preparation methods. (a), SEM micrograph of waxy maize SNCs obtained acid hydrolysis followed by ultrasonication; (c), SEM micrograph of waxy potato SNCs obtained by enzymatic pre-treatment followed by acid hydrolysis (Hao *et al.* 2018b); (d), SEM micrograph for barley SNCs obtained by acid hydrolysis (Xu et al. 2014); (e), SEM micrograph of water chestnut SNCs obtained by planetary ball milling (Ahmad et al. 2020); (f), SEM micrograph of waxy rice SNCs obtained by acid hydrolysis (Xiong et al. 2021).

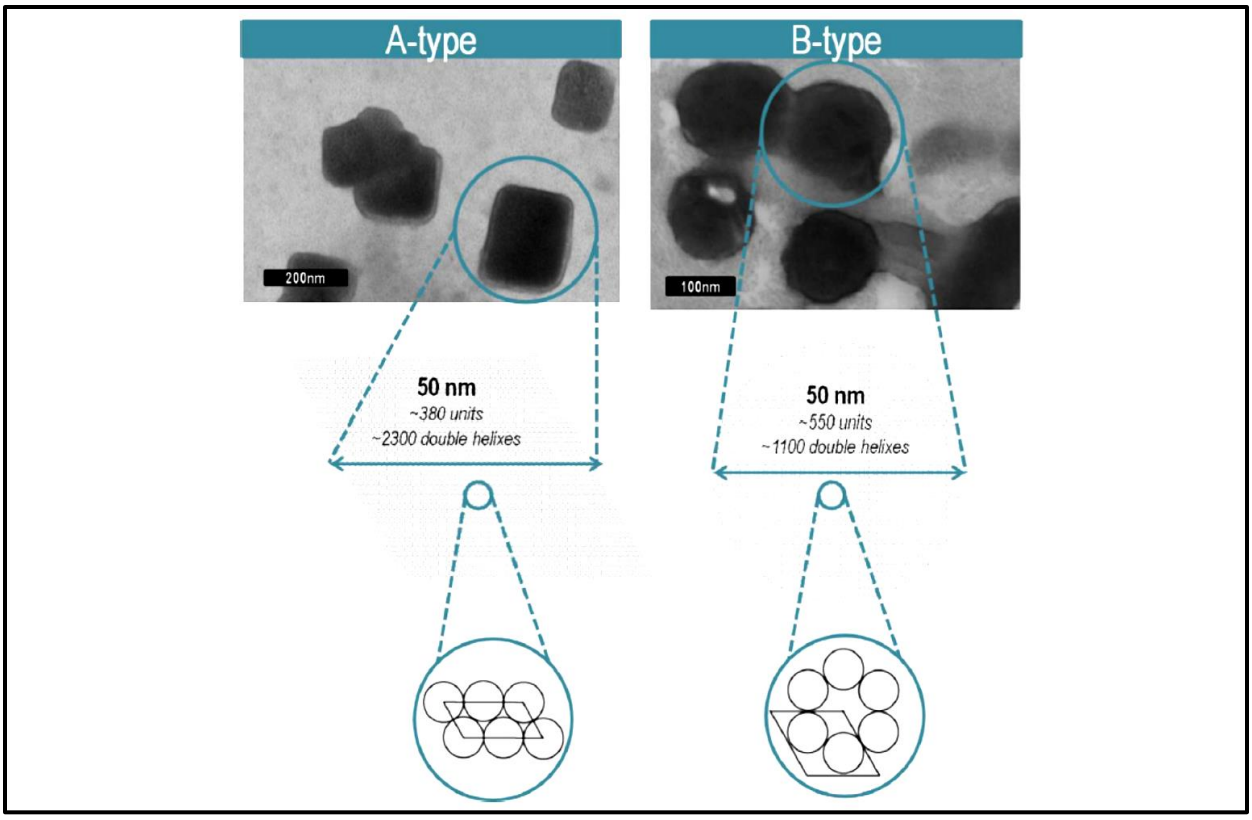

Figure 2. 9: Starch nanocrystals derived from a) high amylose (B- crystalline type) b) wheat (A-crystalline type). Adapted from Dufresne et al. (2013).

2.8.2. Crystallinity properties

Studies on SNCs focused mostly on the changes in the crystalline structure of starch during the production of SNCs. In general, X-ray diffraction (XRD) demonstrated no changes in the crystalline type of starch after acid hydrolysis of starch nanocrystals produced (Kim, Park and Lim 2015; Chen *et al.* 2020; Xiong *et al.* 2021). However, compared to the native starches, the relative crystallinity (RC) of starch nanocrystals is higher (Figure 2.10). This is due to selective hydrolysis of the amorphous layer, making the crystalline more distinct (Le Corre-Bordes and Angellier-Coussy 2014).

Another study, which was conducted by LeCorre, Bras and Dufresne (2011), demonstrated that the most important parameter in determining the crystallinity of SNPs was amylopectin content. These authors reported in comparison amongst the maize starches containing different amounts of amylose, the RC of the SNPs from maize starches increased as the amylose content decreased

(35% and 48% for high amylose maize and waxy maize starch, respectively) (LeCorre, Bras and Dufresne 2011). Moreover, numerous scientists have devoted themselves to improving the preparation methods of SNCs focusing on the production of SNCs in alternative processes such as physical treatment alone or in combination with acid hydrolysis (Table 2.1). However, as compared to acid hydrolysis, difficulties in controlling the physical parameters to minimize the destruction of starch crystallinity are reported. Therefore, the possibility of developing a processing method that could reduce hydrolysis duration without destroying starch semi-crystallinity would be of great significance.

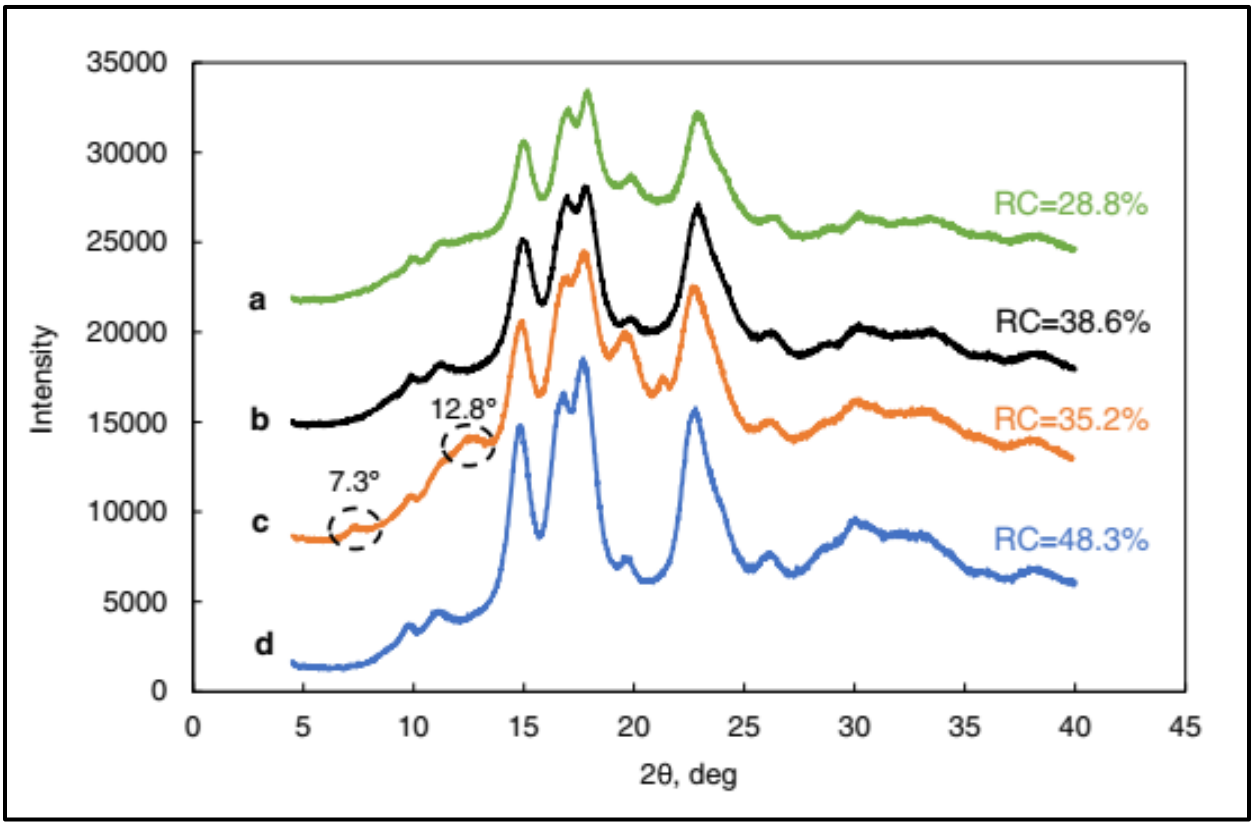

Figure 2. 10: X-ray diffractogram and (relative crystallinity (RC)) of rice starches. (a) native rice starch; (b) waxy rice starch; (c) native rice SNCs; and (d) waxy rice SNCs. Adapted from Xiong et al. (2021).

Table 2.1: Impact of various treatment methods on yield, process duration, morphological and crystallinity characteristics of SNCs from different starch sources.

Starch source	Method	Process time	Yield (%)	Morphological characteristics			Crystallinity characteristics		References
				Microscopy	Particle size (nm)	Shape	Polymorph type	Crystallinity (%)	
Sage	AH[1]	5 days	25.0	FE-SEM	25-100	Round with polygonal structure.	C	45.67	(Azfaralariff *et al.* 2020)
Waxy potato	ENZ[2]→AH	5 days	16.15	SEM and TEM	50-100	Square-like platelet.	A	50.8	(Hao *et al.* 2018b)
Waxy maize	BM[3]→AH	3 days	15.8-19.3	SEM and AFM	598-862	Irregular.	A	46.5	(Dai *et al.* 2018)
Amadumbe	AH	5 days	25.0	FEG-SEM	50-100	Aggregate and square-like platelet.	A	43.2-44.0	(Mukurumbira *et al.* 2017)
Waxy amaranth	AH	3,5, and 10 days	3.6-17.3	TEM	374-484	Parallelepiped and square-like.	A	~35.0	(Sanchez de la Concha *et al.* 2018)
Waxy maize	AH	3,5, and 10 days	7.5-26.0	TEM	322-577	Parallelepiped and densely agglomerated.	A	~37.0	
Corn	AH	5 days	14.1	FE-SEM	47.0[a]	Spherical.	A	44.0	(Xu *et al.* 2014)
Barley	AH	5 days	18.2	FE-SEM	54.0[a]	Spherical.	A	39.0	
Tapioca	AH	5 days	15.1	FE-SEM	25.5[a]	Spherical.	A	51.1	
Potato	AH	5 days	8.8	FE-SEM	117.1[a]	Spherical.	B	32.0	
Native rice	AH	5 days	9.69	SEM	203.2[a]	Square-like platelet.	A	38.6	(Xiong *et al.* 2021)
Waxy rice	AH	5 days	10.01	SEM	296.7[a]	Square-like platelet.	A	48.3	

FE-SEM, field emission scanning electron microscopy; TEM, transmission electron microscopy; SEM, scanning electron microscopy; FEG-SEM, field emission gas scanning electron microscopy and AFM, atomic force microscopy.

[1] AH, acid hydrolysis (sulfuric acid).

[2] ENZ, enzymatic pre-treatment (using glucoamylase).

[3] BM, ball milling pre-treatment.

[a] Average size measured values.

2.8.3. Thermal properties

The thermal behavior of starch and starch nanocrystals can be studied in both dry conditions and in excess water. Thermo-gravimetric analysis can determine their thermal decomposition properties whilst the thermal transitions and enthalpy change are determined by DSC (LeCorre, Bras and Dufresne 2012). Differential scanning calorimetry (DSC) detects changes in heat flow associated with first-order transitions (melting) and second-order transitions (glass transition) of polymers (Le Corre-Bordes and Angellier-Coussy 2014).

Native starches both in excess water and in a dry state have been found to exhibit endothermic peaks while the thermal properties of SNCs from different sources by DSC revealed two thermal transitions, contrary to native starches which indicate only one transition (Le Corre-Bordes and Angellier-Coussy 2014). Generally, the endothermal transition can be attributed to crystallite melting in nanoparticles (Le Corre and Dufresne 2013). Typical responses are presented in (Figure 2.11a) in excess water and (Figure 2.11b) in a dry state by (LeCorre, Bras and Dufresne 2011). In excess water, the first peak was attributed to the first stage of crystallite melting (unpacking of the double helixes) and the second transition to the second stage of crystallite melting (unwinding of helixes). The peaks observed in the dry state for SNCs were attributed to the crystallites melting, with a direct transition from packed helixes to unwinded helixes; and two peaks were attributed to heterogeneity on crystallites quality (LeCorre, Bras and Dufresne 2011).

The higher transition temperatures and enthalpy change for SNCs compared to native starches have been reported by several authors (LeCorre, Bras and Dufresne 2012; Wei *et al.* 2014; Velasquez-Castillo *et al.* 2020a). During acid hydrolysis of starch, the amorphous regions of starch predominately containing amylose are selectively removed. Amylose is regarded as a plasticizer in starch, hence its removal results in higher thermal transition (LeCorre, Bras and Dufresne 2012). The removal of the amorphous regions also results in greater crystallinity of starch nanocrystals compared to their corresponding native starches thus, resulting in higher melting temperature (LeCorre, Bras and Dufresne 2012).

LeCorre, Bras and Dufresne (2012) working with normal corn, waxy maize, potato, and wheat starches, reported that the thermal stability of the starch nanocrystals from B-type starches (e.g., high amylose maize, demonstrated slightly higher melting temperatures, compared to those of A-type starch nanocrystals. However, Mukurumbira *et al.* (2017) observed lower peak melting

temperatures in amadumbe starch nanocrystals as compared with their counterpart native starch. This was possibly explained by the selective removal of the amorphous region resulting in the remaining crystalline portion of starch consisting of amylopectin. The amylopectin is a highly branched α-(1→6) glycosidic linkage it has been suggested that the presence of α-(1→6) linkages increase the free volume and chain mobility, thus resulting in low energy input to initiate phase transition and ultimately resulting in lower melting temperature. Furthermore, other scholars have suggested that the minor differences in preparation and analysis processes might cause such differences in the melting behavior (Kim, Park and Lim 2015; Mukurumbira *et al.* 2017; Zhou *et al.* 2020). Therefore, any modifications (e.g., pre-treatment or duration of starch hydrolysis) on processing parameters for SNCs may induce structural alterations that affect the endothermal transition enthalpy and peak melting temperature for nanoparticles produced. The thermal transition characteristics of the SNCs are important in the application of the SNCs. When the SNCs are applied as nano-reinforcement fillers, thermal resistance in the polymeric blends against the composite preparation conditions is required (Kim, Park and Lim 2015). By changing the physical parameters and starch sources for the SNCs preparation, the thermal characteristics, and resistance of the SNCs might somewhat be controlled (LeCorre, Bras and Dufresne 2012).

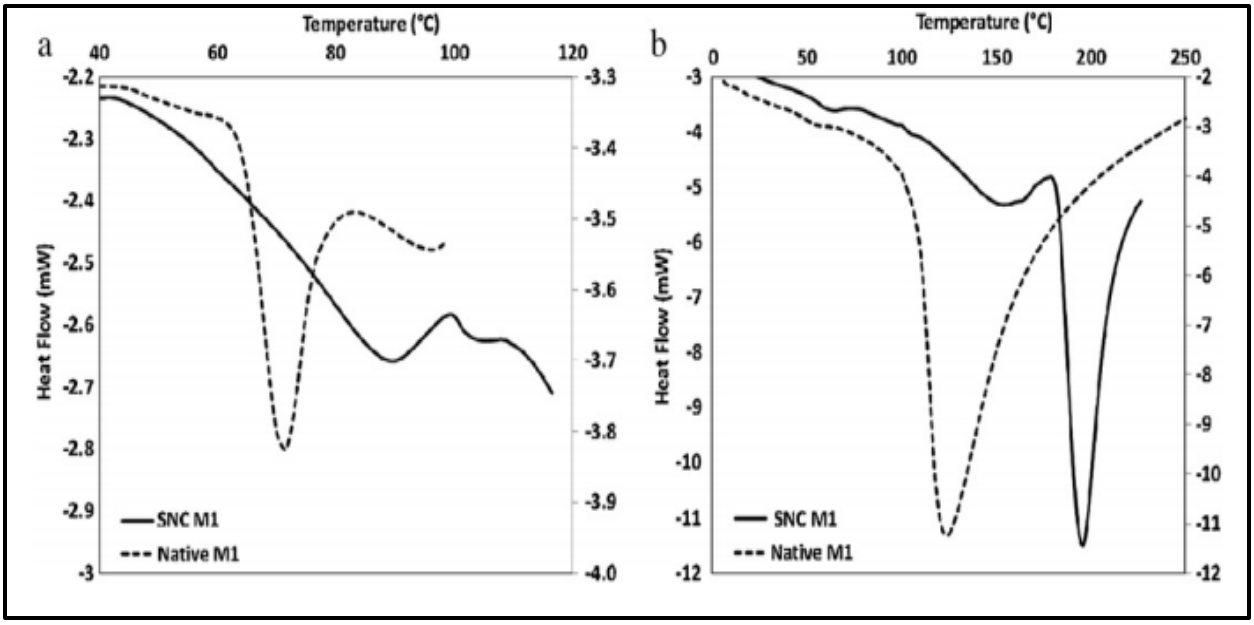

Figure 2. 11: DSC thermogram for native and SNC from waxy maize (M1). (a) in excess water and (b) in dry state (0% water content; 50% relative humidity condition). Adapted from LeCorre, Bras and Dufresne (2012).

2.9. Starch nanocrystals as a promising bionanomaterial in a food packaging application

Limitations for the application of inorganic nanoparticles (i.e., such as inedible and poor compatibility) in food packaging have gradually attracted attention to the use of bionanomaterials as reinforcing agents (Dai, Zhang and Cheng 2020b). Commonly used natural nanostructured objects include rod-like cellulose or chitin whiskers; and platelet-like starch nanocrystals (Condés *et al.* 2015; Zambrano-Zaragoza *et al.* 2018; Liu, Zhang and Bhandari 2020). According to a relevant literature report, the platelet shape of the SNCs is more conducive to the formation of tortuous pathways, which makes the mechanical and barrier properties of SNCs-based nanocomposite films superior to those of CNCs-based nanocomposite films (Espino-Pérez *et al.* 2016). Additionally, the size shape; crystallinity; and thermal properties of SNCs may greatly affect the structure-functional properties of edible coatings or films (Galus and Kadzińska 2015; Dai, Zhang and Cheng 2020b). Therefore, the application of SNCs in edible coatings and films represents an important research area in food packaging applications.

2.9.1. Edible coatings and films for food packaging

An edible coating or film could be defined as primary packaging made from edible components. A thin layer of edible material can be directly coated on food or formed into a film and be used as a food wrap without changing the original ingredient or processing method (Galus and Kadzińska 2015). Edible coatings and films are produced from biopolymers which are categorized into polysaccharides; proteins; and lipids (Figure 2.12). Edible films and coatings have been particularly considered in food preservation, because of their ability to improve global food quality (Jeevahan and Chandrasekaran 2019a). Additionally, they are eco-friendly, and can be used to increase the organoleptic; nutritional properties; and protection against microbiological spoilage of food products (Diaz-Montes and Castro-Munoz 2021). However, their inherent poor mechanical and barrier properties have prompted research on novel techniques, such as incorporating SNCs as reinforcement to improve the mechanical, thermal, and barrier properties of edible coatings and films.

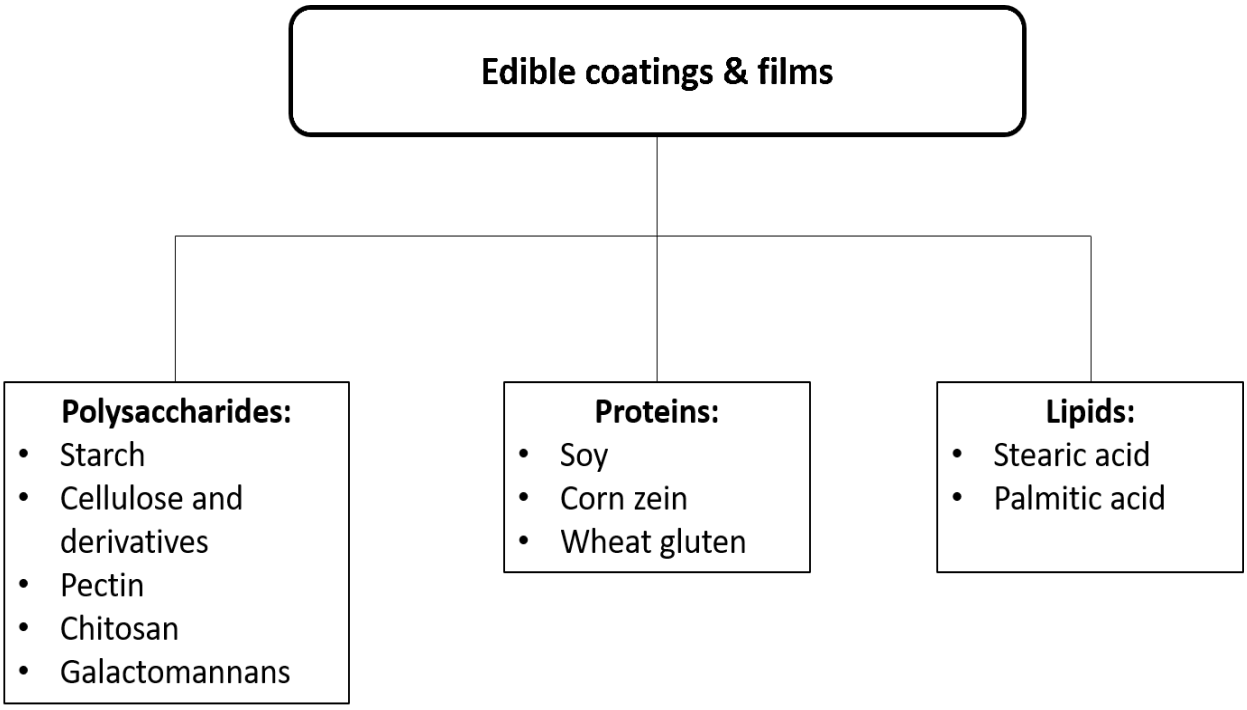

Figure 2. 12: Classification of edible materials.

2.9.2. Types and properties of edible coatings or films

This section will focus on the different types of biopolymers used for edible coatings and films that can be reinforced with starch nanocrystals and the resulting bionanocomposites.

Starch-based composite films

The development of starch-based edible films has become research of interest since starch as a biodegradable and edible product can form edible films for food packaging (Ahmed *et al.* 2018; Abral *et al.* 2019). Additionally, starch has numerous advantages, such as low-cost and wide sources (Dai, Zhang and Cheng 2020b). Starch can form films mainly because the amylopectin in the starch granules is in the crystalline form, due to the large number of hydrogen bonds existing between the hydroxyl groups (Jiménez *et al.* 2012).

Starch films to improve the shelf-life of food must have good transparency; sufficient strength and low moisture absorption (Abral *et al.* 2019). However, their inherent hydrophilic makes the starch-based films have limited use in food packaging. Moreover, once the starch absorbs water (i.e., in

the condition of elevated relative humidity), it will increase the risk of mildew and lead to a further significant decrease in mechanical properties (Dai, Zhang and Cheng 2020b).

Attempts by previous studies to induce the desired functionality of starch-based bioplastics using different hydrophobic components, and reinforcement (e.g., fatty acids, and starch nanocrystals, respectively) in the polymer matrix have been reported (Schmidt *et al.* 2013; Liu *et al.* 2015; Teodoro *et al.* 2015). Fatty acids have been studied widely as hydrophobic agents to improve moisture resistant to hydrophilic films (Fakhouri *et al.* 2009). According to Schmidt *et al.* (2013) the addition of stearic acid enhances the moisture barrier properties of a cassava starch-based film as compared with the control film. Furthermore, previous studies observed that reinforcing starch-based films with a combination of fatty acids and cellulose nanocrystals resulted in films which showed better mechanical and moisture properties (Liu *et al.* 2021c). However, few investigations have been reported on the combined effect of fatty acids and starch nanocrystals in terms of the physicochemical properties and thermal stability of the cassava starch-based film. In view of these findings, it is hypothesized that dispersion of SNC in film-forming suspension with a hydrophobic component before casting may improve the compatibility of the components by generating a homogenous distribution of the nanofillers into the polymer matrix.

Protein-based films

Proteins have received enormous research in short-lived products such as food packaging because of their excellent film-forming properties (Chen *et al.* 2019). Among proteins, those from soybeans have been extensively studied to develop biodegradable films (Echeverría, Eisenberg and Mauri 2014). Most of the soy protein films are based on soy protein isolate (SPI). Moreover, SPI contains more than 90% protein and is obtained by aqueous or mild alkali extraction followed by isoelectric precipitation (Park *et al.* 2002). Most of the soybean protein (i.e., globulins) can be fractionated into 2S; 7S; 11S; and 15S based on their sedimentation coefficients (Wittaya 2012).

Soy film formation involves the development of hydrophobic; disulfide; and hydrogen bonds between proteins polymer chains (Wittaya 2012). The heating of the film-forming solution is the crucial step to disrupt the protein structure; cleave native disulfide bonds, and expose sulfhydryl groups and hydrophobic groups, and then form new bonds between protein chains during film drying (Park *et al.* 2002). Thus, the successful formation of these films is characterized by their excellent barrier properties to oxygen; lipids and flavourings (Condés *et al.* 2015).

Although these materials can form films, many polar amino acids provide hydrophilicity. This property is reflected in film fragility in wet states; poor water vapour barrier and insufficient mechanical properties (González *et al.* 2019a). Thus, the addition of nanoreinforcement to the formulation of soy films is another strategy to improve their functionality, especially the mechanical and barrier properties (González *et al.* 2019b).

Corn zein films

Zein is the alcohol-soluble (prolamin) protein found in corn endosperm (Tihminlioglu, Atik and Özen 2010). Zein has outstanding film-forming ability. This property has been evidenced by the high number of the nonpolar amino acids; leucine, alanine, and prolamine, which make zein water-insoluble (Wittaya 2012). The hydrophobic interaction played an important role in the formation of zein films, and disulfide bonding might be responsible for the structural stability of the zein protein molecule (Cho, Lee and Rhee 2010).

Zein possesses suitable gas barrier properties and good heat sealability (Tihminlioglu, Atik and Özen 2010). Thus, this makes zein protein a great candidate to be a major edible film-forming biopolymer in food packaging (Arcan, Boyacı and Yemenicioğlu 2017). However, there are some limitations to the application of zein protein-based film for food packaging due to their lower oxygen permeability values compared to synthetic polymer films, such as polythene and polyvinyl chloride. Therefore, the properties of zein film can be improved by reinforcement with nanofillers to enhance the permeability properties of zein.

2.9.3. Improvement in properties of bionanocomposite films with starch nanocrystals

Composites are materials that consist of two components: the matrix, which is the continuous phase whose function is to support; protect the filler materials; transmit and distribute the applied load to them and fillers (dispersed phase), which are the stronger and stiffer components reinforcing the matrix (Arora and Padua 2010). Thus, bionanocomposites can be produced by dispersing natural nanostructured objects such as rod-like cellulose or chitin whiskers; and platelet-like starch nanocrystals into a biopolymer matrix (Condés *et al.* 2015). In particular, starch nanocrystals have become a suitable alternative to nanofillers due to their low cost and wide abundance (Mukurumbira, Mellem and Amonsou 2017a).

The successful incorporation of SNCs as reinforcement in biopolymer films has been reported by different authors (Mukurumbira, Mellem and Amonsou 2017a; Silva *et al.* 2019; Liu, Zhang and

Bhandari 2020). The efficient dispersion and distribution of nanocrystals in a biopolymer film significantly strengthen the mechanical and improves barrier properties of the final bionanocomposites film (Condés *et al.* 2015; Dai, Zhang and Cheng 2020b). Furthermore, another promising result of functional bionanocomposites in food packaging is a shelf-life extension of foods (Liu, Zhang and Bhandari 2020; Trajkovska Petkoska *et al.* 2021). Therefore, this section will focus on the effect of the incorporation of SNCs as a nanoreinforcement on the mechanical, permeability, and thermal properties of the final produced bionanocomposites film.

Mechanical properties

For mechanical properties, parameters such as tensile strength (TS), elongation at break (EAB), and elastic/Young's modulus (E/YM) are important for bionanocomposites which use them for a wide range of applications (Ahmed 2020). Moreover, these parameters are influenced by several factors, including the various structures of matrices; the network among nanofillers and the interfacial morphology; and the surface functionality of the crystals (Song *et al.* 2011). González and Alvarez Igarzabal (2015) working on soy protein films reinforced with waxy corn starch nanocrystals noted an increase in tensile strength and Youngs' modulus with the addition of nanocrystals up to 20% and thereafter, further increase resulted in the reduction in TS and E (Table 2.2). The influence of the reinforcing effect produced by the addition of SNCs was attributed to the efficient dispersion and distribution of nanocrystals in protein films, significantly strengthening their mechanical properties (González and Alvarez Igarzabal 2015). The decrease in TS and YM with an increase in starch nanocrystals beyond 20% was attributed to the tendency of nanocrystals to self-aggregate. The aggregation of SNCs reduces their active surface area for interacting with the matrix, which in turn weakens their adhesion on the composite matrix interface (Mukurumbira, Mellem and Amonsou 2017a). Similar behaviour has been reported by other authors (Dai, Zhang and Cheng 2020a; Martins, Latorres and Martins 2022), that at certain exceeded concentration content of SNCs, the mechanical properties of the nanocomposite film were degraded.

Table 2.2 also revealed an interesting relationship between TS and EAB, whereby an inverse relation for TS and EAB of nanocomposite film was observed by many scientists. Elongation at break (EAB) indicates the film's flexibility or stretch-ability (extensibility). This is determined at the point when the film breaks under tensile testing and is expressed as the percentage of stretching or extending from the original length of the film (Piyada, Waranyou and Thawien 2013). Most

studies in literature have reported a significant reduction in EAB percentage as the SNCs content of bionanocomposite film increases (Li *et al.* 2015; Condés *et al.* 2018; Dai, Zhang and Cheng 2020b). However, at a certain high concentration of SNCs, a reduction in TS and E values was reported while values for EAB were noticed to increase (Table 2.2). Other authors, such as Dai *et al.* (2015) suggested that for high concentrations of SNCs, nanocrystals self-aggregated which decreases the surface for interaction with the matrix, thus destroying the ordered structure and leading to lower TS.

Permeability properties

The packaging material should have recommended level of permeability to gases and water vapour to maintain an equilibrium atmosphere and thus prolong the shelf-life of the product (Mangaraj *et al.* 2018). Permeability is defined as the quantification of permeate transition; gas; or vapour through a resisting material (Siracusa 2012). Oxygen; CO_2; and water vapour are the main parameters studied in packaging applications (Swain *et al.* 2018). For instance, the lower the value of oxygen, the higher will be the barrier performance (Rhim and Kim 2014). The permeability of polymers to oxygen or moisture depends upon multiple interrelated factors and these include polarity and structural characteristics of polymeric side chains; hydrogen bonding characteristics; molecular weight; size; shape and polydispersity of the permeability molecule; degree of branching or cross-linking; processing methods and degree of crystallinity of the polymer (Duncan 2011; Siracusa 2012).

However, biodegradable films generally have a low permeability performance in comparison to synthetic (Abreu *et al.* 2017). By inclusion of nanofillers in a composite film, forces the diffusing gas or liquid to take a tortuous pathway, which reduces the film permeability and thereby, improving their barrier properties (Jeevahan and Chandrasekaran 2019a; Liu, Zhang and Bhandari 2020). Moreover, the size distribution or polydispersity index of the incorporated nanofillers plays a significant role in the path length of the created tortuous structure in a composite film (Figure 2.13). The longer the diffusive pathway of the penetrant, the lower the permeability (Mukurumbira, Mellem and Amonsou 2017a). Therefore, to produce a true bionanocomposite suitable for application in food packaging, both nanofiller and composite materials should be biodegradable; environmental-friendly; and edible with food products (Abreu *et al.* 2017; Grumezescu 2017).

Starch nanocrystals are promising nanofillers for biocomposite films because they can reduce porosity; increase crystallinity; and improve the hydrophobicity of the resulting nanocomposite film (Jeevahan and Chandrasekaran 2019a). In addition, their larger aspect ratio allows only a small additional amount to be required to form a strong interfacial interaction with the biopolymer (Liu, Zhang and Bhandari 2020). Dai, Zhang and Cheng (2020b) investigated the effect of the addition of SNCs between 2 and 8% concentration on the water vapour permeability (WVP) of cross-linked cassava starch-based nanocomposite films (Table 2.2). These authors observed a decrease in WVP with an increase in SNCs concentration. However, when the amount of SNCs added exceeded 6%, the WVP of the film rose (Dai, Zhang and Cheng 2020b). In the first stage, the gradual decrease in the WVP of the nanocomposite film was attributed to good dispersion of SNCs at low concentrations (Mukurumbira, Mellem and Amonsou 2017a), thereby creating a long path (tortuosity) through the film. In the second stage, the characteristics of aggregation tendency when the content of SNCs is high, resulting in a heterogeneous distribution of SNCs, which led to an increase in the WVP (Dai, Zhang and Cheng 2020b).

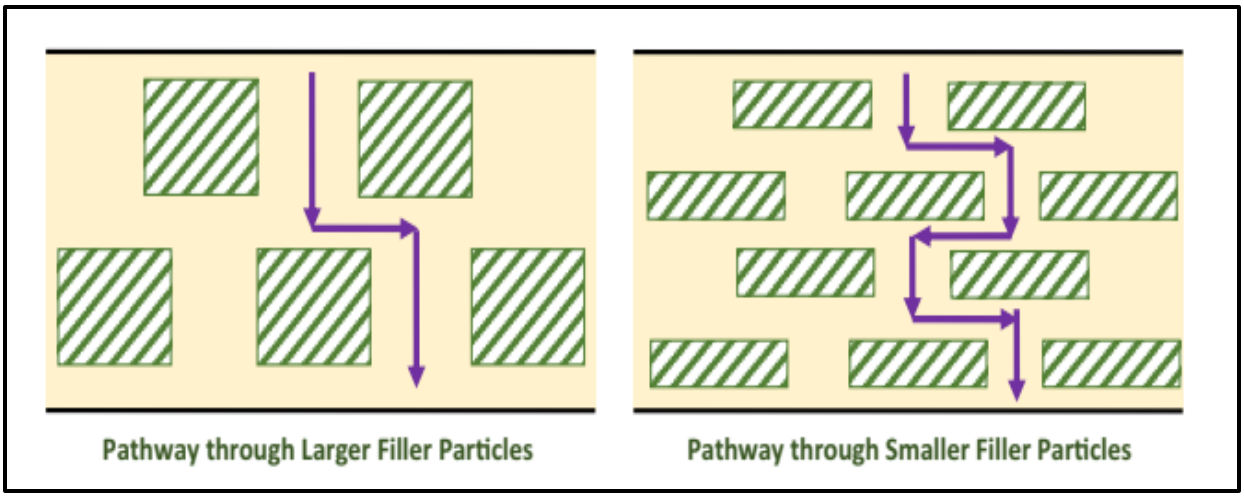

Figure 2. 13: Size effect on the barrire properties. Adapted from Jeevahan and Chandrasekaran (2019a).

Thermal properties

Thermal analysis techniques measure thermal transitions; chemical reactions and decomposition of viscoelastic properties; and thermal conductivity as a function of temperature; heat rate; deformation; and atmosphere (Yadav and Chiu 2019). Further, the specific properties of polymer material and product can be used to determine the composition and to gain information regarding their processing conditions and their end-use (Mukurumbira, Mellem and Amonsou 2017a; Yadav and Chiu 2019). More importantly, to extend shelf-life, the thermal properties of nanocomposites are of critical concern during post-processing treatments such as the pasteurization of fresh fruits and vegetables (Liu, Zhang and Bhandari 2020).

In general, the glass transition temperature (T_g), thermal decomposition (T_d), melting temperature (T_m), and melting enthalpy (ΔH_m) are the most reported thermal properties for bionanocomposites (Condés *et al.* 2015; Mukurumbira, Mellem and Amonsou 2017a; Mujtaba *et al.* 2019). The glass transition temperature is critical at which the material changes behaviour from glassy (hard and brittle) to rubbery (elastic and flexible) and can be determined using DSC and DMA (Dufresne 2013). As seen in Table 2.2, most literature studies have reported a successively increase in the T_g of nanocomposite films with the addition of SNCs (Condés *et al.* 2015; Mukurumbira, Mellem and Amonsou 2017a; Silva *et al.* 2019). According to Dufresne (2013), such an increase in T_g is attributed to strong interfacial interaction between polymer chains and nanocrystal surfaces, which results in the creation of trapped entanglements of matrix polymer chains. For instant, Mukurumbira, Mellem and Amonsou (2017a) working with amadumbe and potato starch films observed that the T_g temperature shifted towards higher temperatures with an increasing amount of SNCs (Table 2.2). These authors attributed the findings to the presence of SNCs restricting the molecular mobility of amylopectin. The restriction in molecular mobility could be ascribed to strong interactions through the formation of hydrogen bonds between the amorphous polymer matrix and the SNCs (Mukurumbira, Mellem and Amonsou 2017a). Condés *et al.* (2015) working with amaranth protein films observed a similar trend with varying concentrations of SNCs. According to these authors, a restriction of protein chains was attributed to strong interaction through hydrogen bonding both between SNCs and also between the filler and the matrix (Condés *et al.* 2015).

The melting temperature (T_m) value for nanocomposite films was reported to increase with the addition of SNCs (Table 2.2). According to some literature reports, such an increase in T_m was attributed to the strong absorption of polymer chains to nanocrystals surfaces, which increases the crystallinity of the film which could result in higher energy needed to melt the composite film (Li *et al.* 2015; Mukurumbira, Mellem and Amonsou 2017a).

Table 2.2: Performance effects with starch nanocrystals concentration on the responsible properties of starch nanocrystals-reinforced bionanocomposite films.

Film type	SNCs concentration (%)	Mechanical properties			Permeability	Thermal properties		References
		Tensile strength (TS)	Elastic/Young's modulus (E)	Elongation at break (EAB)	WVP	T_g(°C)	T_m (°C)	
Pea starch film with waxy maize starch nanocrystals.	1-5	↑ TS maximum of 9.96 MPa.	↑ E maximum of 85.72 MPa.	↓ EAB minimum of 12.58%	↓ by 38%	ND	189.56-193.93	(Li *et al.* 2015)
	>5	↓ TS	↓ E	↑ EAB		ND	189.66-190.10	
Amadumbe and potato starch films with amadumbe starch nanocrystals.	2.5 and 10	↑ TS maximum of 8.11 and 3.86 MPa for amadumbe and potato starch films, respectively.	ND	ND	↓ by 10%	74-94	88.59-105.52	(Mukurumbira, Mellem and Amonsou 2017a)
	5-10							
Cross-linked cassava starch film with starch nanocrystals	2-6	↑ TS maximum of 9.17 MPa.	↑ E maximum of 12.96 MPa.	↓ EAB	↓ by 6-8%	ND	ND	(Dai, Zhang and Cheng 2020b)
Corn starch-based film with taro starch nanocrystals.	>6	↓ TS	↓ E		↓ by 15%			
	0.5-10	↑ TS maximum of 2.87 MPa.	ND	↓ EAB		ND	218.10-223.19	(Dai *et al.* 2015)

T_g, glass transition temperature; T_m, melting temperature; ΔH_m, melting enthalpy; ND, not detected; ↑ increased; and ↓ decreased.

2.10. Conclusions

Although the SNCs exhibit great potential in several applications, e.g., Pickering stabilizers; or as fillers to reinforce biodegradable films, these applications are limited due to the low yield and time-consuming preparation of SNCs. However, contributing to the ongoing research efforts on the process, improvement of SNCs will keep growing and expanding their potential applications in food (i.e., in areas such as food-grade Pickering emulsions; and edible coatings and films). Moreover, the morphology and functionality of SNCs vary with the botanical origin and the preparation process. Therefore, key considerations for the proper selection of a good candidate source of SNCs production include the high yield of starch; low amylose content; and small granule size. Thus, waxy corn, amadumbe and cassava starches are promising candidates that possess such attributes.

2.11. Aim, hypotheses, and objectives

2.11.1. Aim

The study aims to investigate the effect of pullulanase and β-amylase enzymes as a pretreatment tool on starch nanocrystals production process and assess the functional properties of biocomposite films produced with the incorporation of SNC combined with fatty acids to cassava starch.

2.11.2. Hypotheses

1. The pretreatment of starch with a compound enzyme of pullulanase and β-amylase before sulfuric acid hydrolysis will produce starch nanocrystals (SNCs) in a shorter time (less than 5 days) with increased yield. The presence of numerous pores on the starch microstructure created through enzyme treatment will allow quick penetration of the acid solution in the inner region of amorphous starch chains resulting in rapid fragmentation of starch which likely affect the hydrolysis rate and the yield of SNCs (Liu *et al.* 2021b).
2. The addition of SNCs combined with fatty acids to cassava starch during film production will further improve the mechanical and barrier properties of starch-based nanocomposite films. These improvements may be attributed to combined effects of SNCs and fatty acids through enhanced crystallinity, hydrophobicity, and compactness of polymer matrix (Mukurumbira, Mellem and Amonsou 2017a; Kang *et al.* 2020).

2.11.3. Objectives

1. To determine the effect of compound enzymatic pretreatment of starch on starch nanocrystals (SNCs) processing time and the physicochemical properties of the resulting SNCs using dynamic light scattering (DLS); transmission electron microscopy (TEM); differential scanning calorimetry (DSC); X-ray diffraction (XRD); and Fourier transform infrared spectroscopy (FTIR).
2. To determine effect of adding SNCs in cassava starch films incorporated with stearic acid on the microstructure, physicochemical, and mechanical properties of the resulting nanocomposite films.

CHAPTER THREE

3.0 Effect of compound enzymatic pretreatment on starch nanocrystals production process and physicochemical properties

Abstract

There is a growing interest in starch nanocrystals (SNCs) as biodegradable and promising nanostructured materials for various applications. However, the preparation process remains challenging for the industry because it is characterized by a long duration of acid hydrolysis, low yield, and reduced SNC properties. Hence, to improve the efficiency of starch nanocrystals production and properties, pullulanase (15 U/g starch) was used alone or together with β-amylase (50 and 100 U/g starch) to modify the starch before acid hydrolysis. The compound enzyme system of pullulanase:β-amylase (15:50 U/g starch) had the most pronounced effect on starch morphology compared to a single enzyme system by creating a dense and more porous structure on starch surfaces as evidenced by microscopy images, a high degree of oil absorption and extent of hydrolysis data. Increasing the activity of β-amylase to 100 U/g starch in the compound enzyme system did not have any effect on the starch morphology. The duration of acid hydrolysis was significantly reduced from 5 to 3 days with compound enzymes compared to the conventional process (5 days) and single enzyme. The yield of SNC was approx. 25 wt.%, which is 3 times greater than that of the conventional starch. SNC derived from the modified starches were small in size (less than 50 nm) and appeared mostly as platelets and isolated round particle aggregates. Nanocrystals from modified starches showed an A-type crystalline structure similar to the native starch, but with an increased degree of crystallinity from 32.85% to 45.28%. Starch hydrolysis using compound enzymes consisting of pullulanase and β-amylase hydrolysis seems to be the most effective and green to produce SNC in a shorter time and with increased yield and enhanced properties.

Keywords; waxy corn starch, starch nanocrystals, pullulanase, β-amylase, acid hydrolysis, yield.

3.1. Introduction

Starch nanocrystals (SNCs) are crystalline platelet material (size < 100 nm) obtained by preferential acid hydrolysis of the amorphous region of starch granules (Angellier et al. 2004; Sanchez de la Concha et al. 2018). SNCs are promising biomaterials for novel application in foods (Mukurumbira, Mellem and Amonsou 2017b; Choi *et al.* 2020), cosmetics (Tao et al. 2021), and medicine (Odeniyi et al. 2018). The unique platelet shape of SNCs significantly contributes to the enhancement of mechanical and barrier properties of nanocomposite films (Condés *et al.* 2015; Dai, Zhang and Cheng 2020b). Although SNCs are promising materials for various applications, their production still presents some challenges, which limit their widespread use. In general, acid hydrolysis below the gelatinization temperature of starch is the most common method used for nanocrystals production (Putaux et al. 2003; Angellier et al. 2004). Major drawbacks associated with this method are the extended hydrolysis time required (up to 5 days) and the low yield (4–15%) of SNCs (Putaux *et al.* 2003; Liu *et al.* 2021b). Hence, further research is needed to contribute to the ongoing efforts on SNCs production process improvement.

Different methods, including physical and enzymatic pretreatments of the starch prior to acid hydrolysis have been investigated (LeCorre, Bras and Dufresne 2012; Ahmad *et al.* 2020). Dai *et al.* (2018) subjected the starch granules to ball milling before acid hydrolysis. Although these authors successfully reduced the duration of acid hydrolysis from 5 to 3 days, milling induced severe damage to the structural characteristics of SNCs produced due to partial or complete disintegration of a starch semi-crystalline structure. Consequently, the resulting nanocrystals appeared less crystalline. Another study was reported by Hao *et al.* (2018b), on the pretreatment of starch with a starch hydrolyzing enzyme such as glucoamylase. According to their findings, glucoamylase treatment resulted in the creation of pores on the granules' surface, which accelerated the penetration of H_3O^+ into inner regions and decrease the acid hydrolysis time from 5 days to 2 days. Thus, the creation of pores in starch through enzymatic hydrolysis can be regarded as a promising and green strategy for surface starch modification and deserves further consideration.

Various amylolytic enzymes (e.g., α-amylase; glucoamylase; and β-amylase) have been utilized to generate porous starches (Dura, Blaszczak and Rosell 2014b; Benavent-Gil and Rosell 2017b). Among these enzymes, α-amylase and glucoamylase have been broadly adopted to create porous starch via the hydrolysis of α-1,4- and α-1,6-glycosidic linkages. Different enzymes hydrolyze

starch granules at specific binding sites (Bertoldo and Antranikian 2002b). Hence, the combined effect of glucoamylase and α-amylase on the formation of pores on granular starch with the increased specific surface area has been proposed from previous studies (Dura, Blaszczak and Rosell 2014b; Guo *et al.* 2020). However, previous studies narrowly reported on single enzymes' use of α-amylase and glucoamylase. Debranching enzymes such as pullulanase are gaining attention in the food industry due to its capability to modify the starch structure and its properties by selectively hydrolyzing branched chain of α-1,6-glycosidic bonds (Hong, Liu and Gu 2015; Li et al. 2017). Although glucoamylase could hydrolyze both the α-1,4- and -1,6-glycosidic bonds in starch, the strong affinity of pullulanase for the α-1,6 bonds distinguish this enzyme from other amylases. Hence, pullulanase has not yet been applied as a pretreatment method aiming at starch nanocrystal preparation. But, as a debranching enzyme, pullulanase may offer a new possibility and could be applied to starch modification alone or in combination with other enzymes to increase the efficiency of the SNC production process. If pullulanase and *exo*-amylases (i.e., β-amylase) are used concurrently during the hydrolysis of starch granules, pullulanase would preferentially hydrolyze the branching points in the amylopectin residues, while β-amylase will hydrolyze the linear α-1,4-glycosidic linkage. Currently, there is limited research on the use of debranching enzymes such as pullulanase, as a pretreatment protocol for nanocrystal production. Hence, in this study, a new efficient method for preparing SNCs with high yields was developed using pullulanase alone or in combination with β-amylase as enzymatic pretreatment followed by acid hydrolysis for SNCs fabrication from waxy corn starch. The produced SNCs were systematically studied with dynamic light scattering (DLS); transmission electron microscopy (TEM); differential scanning calorimetry (DSC); X-ray diffraction (XRD); and Fourier transform infrared spectroscopy (FTIR).

3.2. Materials and methods

3.2.1. Materials

Waxy corn starch (WSC) was purchased from (Sigma-Aldrich). Enzymes: β-amylase (EC 3.2.1.2) from barley and pullulanase from the microbial origin (EC2.4.1.2) were purchased from Sigma Aldrich. Sodium phosphate (Na_3PO_4), citric acid, and sodium hydroxide were purchased from Radchem Pty Ltd, South Africa. Ethanol (~97%).

3.2.2. Starch pretreatment with enzymes

The enzyme hydrolysis of native waxy corn starch was adapted from Hong, Liu and Gu (2015) with modifications. Pullulanase activity of 15 U/g starch was selected based on the preliminary experiment, which showed the maximum degree of oil absorption. Native waxy corn starch was dissolved in 250 ml sodium acetate buffer (0.01 M, pH 5.5). Then, the starch slurry (10.2% w/v) was agitated continuously under 150 rpm mechanical stirring at 55℃ using a silicon bath for 30 min, conditions known as the optimal (Hong, Liu and Gu 2015).

Pullulanase (15 U/g starch) was added to the mixture when the slurry temperature reached 55℃, and the hydrolysis process was maintained for 2 h. The enzyme reaction was ceased with ethanol (~97%). The formed precipitate was collected and washed with distilled water and then freeze-dried for further analysis. Native waxy corn starch was included for comparison, and starch was subjected to similar treatment conditions in the absence of enzyme and was used as control.

For compound enzyme treatment, starch hydrolysis was performed simultaneously with a mixture of pullulanase (15 U/g starch). and β-amylase. To obtain the higher adsorption capacity, for each compound enzyme mixtures; β-amylase activity was varied to 50 and 100 U/g starch. The hydrolysis process was performed under similar conditions as for the pullulanase enzyme described above. Immediately after the reaction, the solution was added with ethanol to inactive enzymes. The precipitates formed were washed with distilled water and then freeze-dried for further analysis.

3.2.3. Extent of hydrolysis

To evaluate the sensitivity of starch granules to enzyme hydrolysis, the extent of hydrolysis (EH) was determined by measuring the amount of glucose released using the 3,5-dinitrosalicylic acid (DNS) method (Miller 1959). A small aliquot was withdrawn from each sample of starch slurry after 2 h hydrolysis. Absorbance was measured at 504 nm by using a UV/visible spectrophotometer (UV/Vs SP-MUV8000T, OPTIZEN POP., Bengaluru, Delhi). Glucose was used as the standard. Each analysis was performed in duplicate. EH was calculated as follows:

$$EH = \frac{weight\ of\ reducing\ sugar\ expressed\ as\ glucose}{weight\ of\ dry\ initial\ starch} \times 100 \quad (1)$$

3.2.4. Degree of oil absorption (DOA)

The degree of oil absorption analysis was carried out to further assess the porous structure enzyme pretreated starches. The degree of oil absorption (DOA) was determined following a protocol described by LeCorre *et al.* (2012). Starch samples designated W were agitated (2000 rpm) with 2.5 ml sunflower oil in a 5 ml centrifuge tube for 5 min, followed by centrifugation at 4000 ×g for 15 min. The supernatant was then carefully removed. The remaining oil was decanted using filter paper. After the dripping of the oil had ceased, the amount of oil impregnated into the starch samples designated W_1 was weighed. The DOA was calculated as follows:

$$DOA(\%) = 100(W_1 - W)/W \quad (2)$$

3.2.5. Scanning electron microscopy

The morphological features of the samples were determined using a scanning electron microscope (SEM) (Zeiss Ultra Plus, Germany) instrument at a high voltage of 10 kV. A suspension of 0.002% was prepared for each sample and 2.5 µl of suspension was deposited onto a carbon grid. A thin layer of approximately 1 nm of Au-Pd conductive coating was deposited on top of the sample and they were viewed (Guo *et al.* 2020).

3.2.6. Preparation of starch nanocrystals.

Modified starches with a maximum degree of oil absorption and porosity were subject to sulfuric acid hydrolysis. The optimized method for nanocrystal production by Angellier *et al.* (2004) was adopted. Both native and enzyme pretreated waxy corn starches of 20 g were mixed with 140 ml of dilute sulfuric acid (3.16 M). The resulting suspensions were transferred to a shaking incubator at 100 rpm at 40℃ for 5 days. Samples were taken out after every 24 h interval period for 5 days. Each suspension was washed by successive centrifugation [15000 × g, 10 min.] with distilled water until reaching neutrality and re-dispersed using an ultrasonic machine for 5 min to break aggregates. The product samples were named: acid hydrolyzed starch without enzyme treatment (native), pullulanase and compound enzyme pretreated starches (PS, and PBS, respectively). The samples were then freeze-dried and weighed.

3.2.7. The Yield of SNC

The SNC yield was calculated as the percent ratio of hydrolysis residues (Y%) (after freeze-drying) based on the initial starch weight (LeCorre *et al.* 2012).

$$Y(\%) = \frac{weight\ of\ starch\ with\ a\ given\ hydrolysis\ (g)}{weight\ of\ initial\ starch\ (g)} \times 100 \quad (3)$$

3.2.8. Particle size distribution (PSD)

The particle size distribution of the SNCs was performed using Litersizer Nano ZS (Anton Paar, New Castle, Delaware) The samples at a concentration of 0.02% (w/v) were ultrasonically [360 W, 5 s] dispersed in distilled water and analyzed at 25℃ after reaching stable values (Mukurumbira *et al.* 2017). The refractive index for purified water was 1.33. The refractive index and absorption of particles were 1.53 and 0.01, respectively. The dispersions were expressed as changes in volume weight mean drawn from the representative measurement of 1–5 days hydrolysis. Samples were read six times per measurement.

3.2.9. SNC morphology

Transmission electron microscopy (TEM) was used to characterize the morphology of starch nanocrystals (JEOL 2100 HRTEM., Japan) at an accelerating voltage of 80 kV. A small droplet of the SNC suspension (0.005% w/v) was placed onto a carbon-coated copper grid and air-dried to record the TEM images (Mohammad Amini and Razavi 2016).

3.2.10. X-ray diffraction analysis

The crystalline features on powders from native waxy corn starch, hydrolyzed starches, and freeze-dried starch nanocrystals were conducted using an X-ray diffractometer (XRD) (Bruker AXS D8 Advance Rheinfelden., Germany). The operation conditions for the refractometer were: Cu-Kα radiation, angular range 5–45° (2θ), step size of 0.034°, counting time 92 s, and working voltage was 40kV. Relative crystallinity was calculated based on the method described by Nara, Sakakura and Komiya (1983).

3.2.11. Differential scanning calorimetry of SNCs

The thermal parameters for both native waxy corn starch and starch nanocrystals, such as melting temperatures and the enthalpy were estimated by differential scanning calorimetry (DSC) analyzer (TA Instrument DSC Q100.,New Castle, DE, USA) filled with a manual liquid nitrogen cooling

system. Freeze-dried SNC powder and dry native waxy corn starch were conditioned at 50% relative humidity and placed in a hermetically sealed T-zero pan. The samples were heated from 40℃ to 240℃ with a heat rate of 10℃/min (LeCorre, Bras and Dufresne 2012). The onset (T_o), peak (T_m), endset temperatures (T_e) and enthalpy (ΔH) were evaluated in the instrument software.

3.2.12. Fourier transform infrared (FT-IR) spectroscopy of SNCs

Fourier transform infrared spectra (ATR FTIR) of native waxy corn starch and starch nanocrystals was conducted to evaluate changes in the short-range ordered structure (i.e., double-helical order) in the external regions of the samples using an FTIR carry 630 ATR Diamond (Agilent Inc., USA). The resolution was 4 cm^{-1} and a total of 32 scans were performed. All spectra were baseline-corrected and then deconvolved in the range 1200 – 800 cm^{-1}. The intensity ratio of 1045 to 1018 cm^{-1} ($R_{1045/1018}$) was used to evaluate the short-range ordered structure of the native starch and SNC products.

3.2.13. Statistical analysis

Statistical analysis was performed on selected parameters using the IBM SPSS version 20.0 statistical software for Windows (Armonk, NY: IBM Corp.). Data were analyzed by one-way analysis of variance (ANOVA) and means were compared using the Fisher Least Significant Difference (LSD) test ($p < 0.05$). This determine if there were significant differences between the oil absorption capacities of starch samples and the amount of glucose release during enzyme treatment.

3.3. Results and discussion

3.3.1. Extent of hydrolysis

The extent of hydrolysis (EH) of starches was determined to evaluate the sensitivity of starch granules to enzymes hydrolysis. Compound enzymes pretreatment (pullulanase at 15 U/g starch and β-amylase at 100 U/g) starch had the highest EH value compared to single enzyme pretreatments (Figure 3.1E). High EH could indicate the effectiveness of the enzyme in hydrolyzing starch (i.e., more soluble sugars released per unit of time). Despite its effectiveness in hydrolyzing native starch, this treatment produced less porous starches (Figure 3.1C) when compared to starches modified with pullulanase alone and a compound enzyme system consisting of pullulanase 15 U/g starch and β-amylase (50 U/g starch). Presumably, β-amylase, in excess of

50 U/g starch, was mainly absorbed into the susceptible surface zones and degraded the external part of the granule by *exo*-corrosion instead of creating visible opened pores. Similar effects were observed by Dura, Blaszczak and Rosell (2014a) which indicated that the degree of porosity is greatly dependent on specific enzymes ratio. Overall, it is possible to observe that the combined enzymes pretreatment of pullulanase (15 U/g starch) and β-amylase (50 U/g starch) was more efficient in generating pores on starch granule surfaces. Pores, surface cracks, pitting and scratching provide a large specific surface which may be more beneficial for acid hydrolysis during SNC production.

3.3.2. Degree of oil absorption

DOA analysis was carried out to further assess the porous structure starches. Hydrolyzed starches with compound enzymes had the highest oil absorption capacity compared to either pullulanase or β-amylase alone (Figure 3.1E). DOA data corroborated the SEM images (Figure 1A-C), suggesting that more porous starches were obtained with the combination of pullulanase (15 U/g starch) and β-amylase (50 U/g starch). However, increasing the activity of β-amylase from 50 to 100 U/g starch in the combined enzyme system seemed to reduce the oil absorption capacity of the sample. This can be attributed to the creation of limited numbers of pores presence on starch granule surfaces, consequently the observed limited oil uptake ability.

3.3.3. Surface morphology of hydrolyzed starches

SEM analysis was used to evaluate the changes in the surface morphology of hydrolysed starches. Although the shape of the starch granules remained relatively unchanged, hydrolysed starch granules appeared porous (Figure 3.1A–C). The number and distribution of pores created on the surface of starch granules were dependent on type enzyme hydrolysis. As shown in Figure 3.1B, high-density surface pores were obtained from starch pretreated with compound enzymes compared with single enzyme pretreatment (Figure 3.1A). Increasing the activity of β-amylase from 50 to 100 U/g starch did not seem to produce any major effect on the surface structure of treated starches. Furthermore, hydrolyzed starched with pullulanase alone showed a less porous surface, which further demonstrates the effectively of using compound enzymes. The synergistic effect between these enzymes in native starch can explain the pronounced effect observed on the granular structure (Figure 3.1B). The tight packing of the crystalline amylopectin segments of the native waxy starch granules (mainly dominated by intermolecular α-(1→6) glycosidic cross-links)

makes its surface relatively impenetrable. However, the use of compound enzymes treatment such as pullulanase and β-amylase could have led to initial selective debranching of α-(1→6) linkages by pullulanase on granular surfaces to create a loosely organized region, which in turn enables the direct accessibility of β-amylase to hydrolyze α-(1→4) glycosidic bonds from the non-reducing end of the outer chains (Monnet *et al.* 2010).

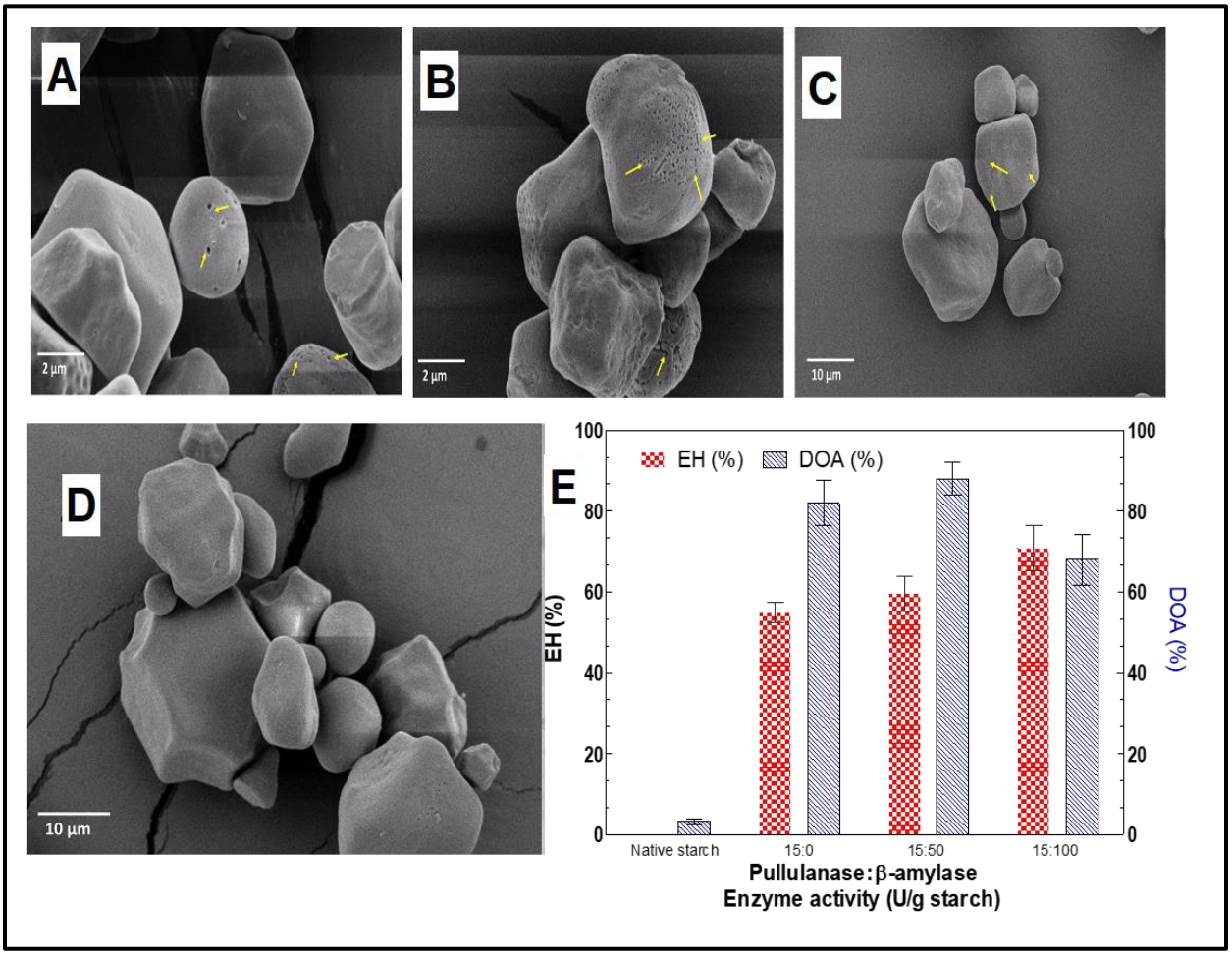

Figure 3.1: SEM images for enzymatic treated starches (A, B, and C; at 15:0, 15:50, and 15:100 U/g of starch, respectively) after 2 h of enzymatic hydrolysis, and native waxy corn starch (D). E: Degree of oil absorption (DOA), extent of hydrolysis (EH).

3.3.4. Recovery yield of SNCs

The progression of acid hydrolysis was monitored by measuring the residue recovered at days interval during nanocrystal preparation. In general, the yield of residue decreased with prolonged exposure to acid over the duration of hydrolysis (Figure 3.2). However, pullulanase treated starch (PS) displayed a sharp decrease in residual yield, reaching a plateau within 2 days with just a slight reduction observed at day 5. This sharp decrease in residual yield could be attributed to the severe fragmentation of starch chains in amorphous regions at the early stage of hydrolysis and could suggest a rapid achievement of nanocrystals. Unlike the pullulanase treated starch, combined pullulanase and β-amylase treated starch (PBS) showed a relatively similar and progressive yield of residue, with severe reduction observed from day 3 though day 5. The recovered residue at day 3 was approximately 19.8% for PS, lower than those of PBS (25.2%) and untreated starch (26.3%) for PS and PBS with an average particle of less than 5 nm. Harvested residues were subjected to TEM analysis to assess the formation of starch nanocrystals in enzymatic pretreated starches.

It is well established that the acid hydrolysis of starch granules exhibits two-stage hydrolysis kinetics (Le Corre-Bordes and Angellier-Coussy 2014). First-stage, the amorphous parts of starch are rapidly hydrolyzed until day 3, followed by the second hydrolysis stage corresponding to the disruption of the crystalline region on days 4 and 5, causing the complete disintegration of granules to nanocrystals. In this context, the first-stage of hydrolysis time for PS and PBS was minimized when compared to that of the untreated starch sample, possibly due to the presence of numerous surface pores (Figure 3.1A and B) on these enzymes pretreated starches allowed quick penetration of H_3O^+ resulting in rapid fragmentation of starch granule to nanoparticles, which likely affected the hydrolysis rate and the yield of SNCs (Liu *et al.* 2021b). Although PS appeared less porous from SEM, it seemed to favour rapid hydrolysis of the amorphous regions of starch. This was indicated by enhancement on quick penetration of H_3O^+ resulting in rapid fragmentation of starch granule, thus increasing the rate of SNCs formation. These observations may be explained by that the PS may resemble a few-larger pore size openings, which makes the amorphous starch more readily hydrolyzable within 2 days of acid hydrolysis. Whereas the lower yield of PS could be explained by the pullulanase pretreatment alone could also debranch the α-1→6 glycosidic linkages that are found in the crystalline regions of starch granules, hence debranching with pullulanase alone may be led to erosion and reduction in nanocrystals yield.

3.3.5. Particle size distribution and homogeneity of the SNCs

After 3 days, the acid hydrolysis of PS and PBS samples resulted in the fragmentation of starch granules into nanoscale particles (< 100 nm), whereas for native starch samples, it required 5 days (Figure 3.2). According to LeCorre, Bras and Dufresne (2011) native waxy corn starches (untreated starch sample) have sizes of 3–5 μm. Thus, the process applied to obtain the SNCs breaks the structures present in the starch granules, generating SNCs 100 times smaller than the original native starch. This might indicate that the enzymatic pretreatment of starch had a notable effect on the progression of acid hydrolysis. The presence of numerous pores on the PS and PBS samples enhanced the penetration of the acid solution into amorphous starch regions and consequently accelerate the hydrolysis and shortened the duration of SNC production. With the extension of acid hydrolysis time from day 3 to day 5, the mean diameter of the PS and PBS fragmented starches showed no significant decrease (~ 5 nm). Previous literature has reported the average crystalline size from 4 to 20 nm (Chavan *et al.* 2021). Similar trend was also observed in the values of PDI varied from 0.03 to 0.30, which might indicate a very narrow size distribution and homogeneity of the nanocrystals obtained. Furthermore, these smaller particles could be much easier to disperse in the nanocomposites with better homogeneity and reinforcement. Therefore, SNC can be obtained after 3 days of acid hydrolysis in both PS and PBS samples when compared with SNCs prepared by conventional acid hydrolysis (Angellier *et al.* 2004), due to a severe reduction in particle size of these enzymes pretreated starches (PS, and PBS) within 3 days of hydrolysis.

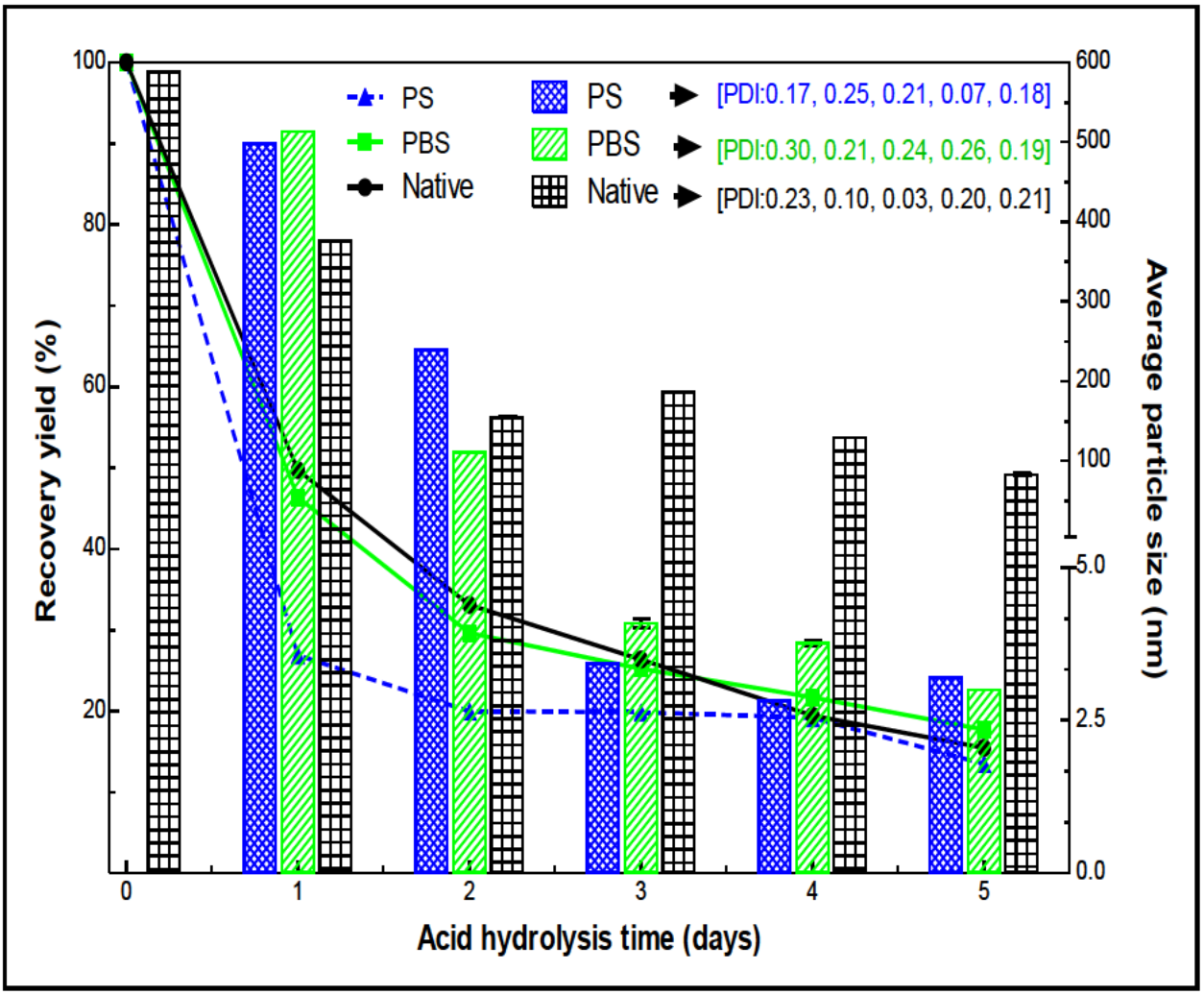

Figure 3.2: Recovery yields with average particle size and polydispersity index (PDI); in parentheses for enzymes modified starches with pullulanase (PS) and combined pullulanase and β-amylase (PBS) during acidic hydrolysis period (1–5 days).

3.3.6. Morphology of the SNCs

Figure 3.3 shows the TEM image of recovered residue each day of acid hydrolysis over a period of 5 days. Significant variation in microstructure was observed among recovered residues. Starch granules appeared in the residues after day 2, suggesting an incomplete hydrolysis and nanocrystals formation is still in progress. However, after 72 h of acid hydrolyses (day 3), TEM images revealed the formation of SNC, which appeared like platelet-like aggregates, or isolated round-edge particle shapes. These results suggest that the enzymes pretreated starch granules with

pullulanase or compound enzymes system of pullulanase and β-amylase (50 U/g starch) experienced severe fragmentation on starch granules into nanoscale particles during acid hydrolysis; consequently, shorten hydrolysis time to recover the acceptable SNC structure. Thus, a synergistic effect of pullulanase and β-amylase may improve the creation of a porous starch structure with increased surface pore density, thereby reducing the preparation time of SNCs. Compared to native waxy corn starch (untreated sample) it is possible to observed that the process of obtaining the nanocrystals changed the structure of the untreated starch; the granules initially had polygonal structures (Figure 3.1D) that were modified during the process.

Moreover, referring to the average particle size measurements in Figure 3.2, the mean particle size was rather smaller than that revealed by TEM data, indicating the existence of aggregates in the nanocrystals produced. Similar trend has been reported by other authors and can be attributed to the larger surface area of the platelets and their ability to interact through the formation of hydrogen bonds between hydroxyl groups, which are found in a substantial number of single areas of nanocrystals surfaces (Sanchez de la Concha *et al.* 2018; Liu *et al.* 2021a). However, the acid hydrolyzed PBS at day 3 was selected to further confirm whether its cohere with the characteristics of SNC, by analyzing the crystalline properties and chemical structure of the SNC produced from the newly developed method and compared with those obtained after 5 days of hydrolysis using XRD and FT-IR analysis.

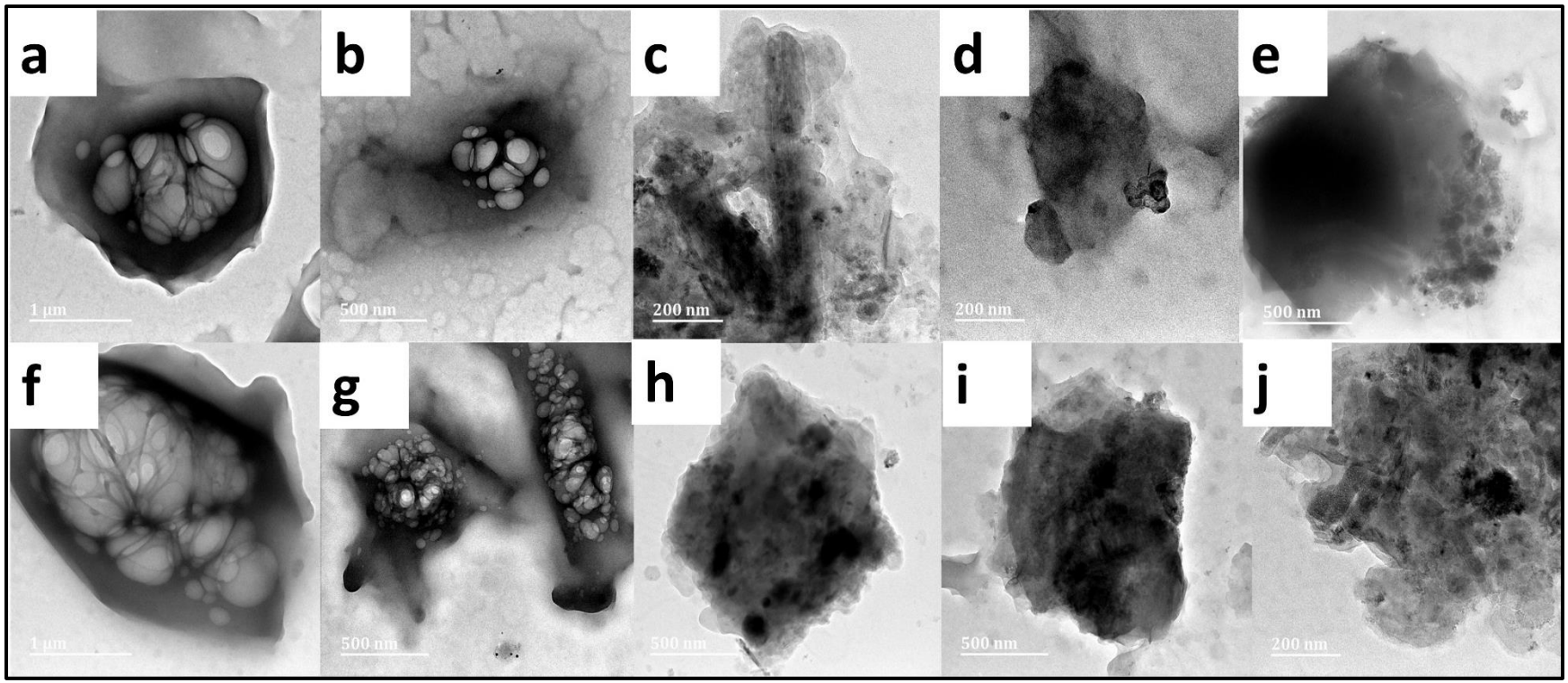

Figure 3.3: TEM images of recovered residue each day of acid hydrolysis over a period of 5 days for pullulanase (PS: a – e), and combined pullulanase and β-amylase (PBS: f – j) enzymes modified starches. Starch nanocrystals were observed on (c, e, h, and j assigned as PS-3d, PS-5d, PBS-3d, and PBS-5d, respectively).

3.3.7. Crystallinity of SNCs

XRD patterns of the SNC indicated the extensive hydrolysis of amorphous areas in the PBS sample (Figure 3.4B). This was evidenced by a significant increase in relative crystallinity in the PBS-3d (45.28%) and PBS-5d (47.7%) SNC products when compared to native starch. Starch nanocrystals exhibited A-type crystallinity, with significant diffraction peaks at $2\theta = 15°$, a doublet peak at 17–18°, and a third one at 23.1° (Figure 3.4), which was in agreement with the previous studies (LeCorre *et al.* 2012; Dai, Zhang and Cheng 2019; Velasquez-Castillo *et al.* 2020b). Neither enzymes pretreatment nor acid hydrolysis altered the original crystal structure of the native starch. These results suggest that the enzymatic pretreatment of native starch followed by sulfuric acid hydrolysis can effectively produce SNC products with preserved crystalline structure. Furthermore, high crystalline SNCs are suitable to be used as reinforcements in processing biocomposite films and coatings. (Martins, Latorres and Martins 2022). As shown in Figure 3.4A, the relative crystallinity of porous starch derived from PBS (32.90%) was similar to that of native starch (32.85%), whereas a slight decrease in relative crystallinity was observed from the PS (32.27%). A similar decreasing trend of crystallinity caused by pullulanase treatment was found in maize and potato granular starches (Li et *al*. 2017), and rice starch (Zhao et *al*. 2021). This may be attributed to the hydrolysis from pullulanase to both amorphous and crystalline regions of starch granules in the process of pullulanase debranching, which transforms the crystalline regions into an amorphous region (Ge et *al*. 2021). Thus, these results could further explain the significant reduction in nanocrystals yield recovered for the PS sample.

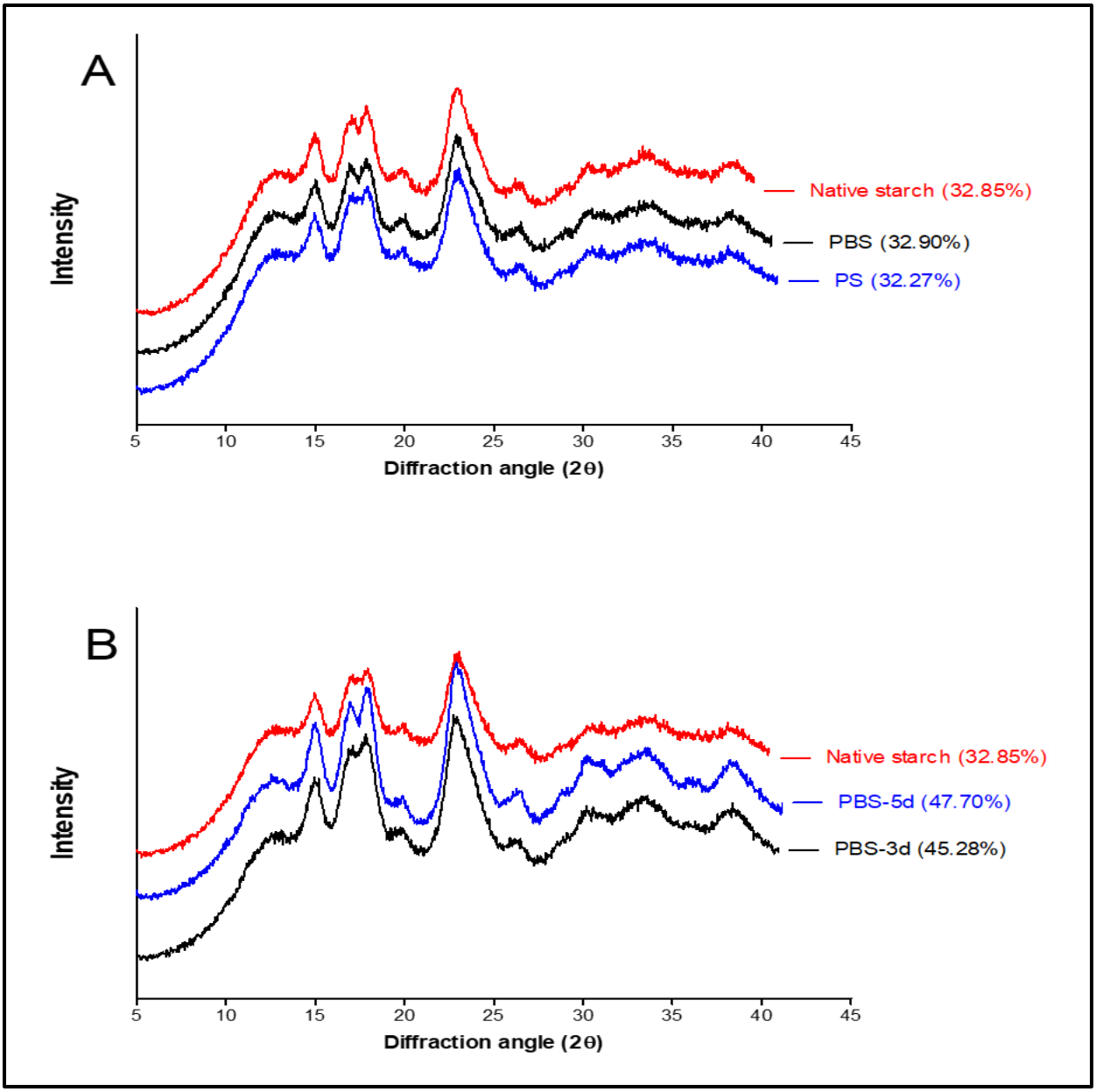

Figure 3.4: X-ray diffractograms of native waxy corn starch, enzymes modified starches, and starch nanocrystals. (A) native waxy corn starch, pullulanase (PS) and combined pullulanase and β-amylase (PBS) enzymes modified starches. (B) starch nanocrystals derived from compound enzyme system of pullulanase:β-amylase (15 : 50 U/g starch) modified starches at day 3 and 5 of acid hydrolysis (PBS-3d, and PBS-5d, respectively). The relative crystallinity is provided in parentheses.

3.3.8. FT-IR spectra

The structural characteristics and changes in the short-range molecular order of SNCs were investigated by FT-IR. As shown in Figure 3.5A, the FT-IR spectra of SNCs showed similar profiles to the native starch, suggesting that functional groups were retained after the acid hydrolysis. These results are similar to those noted in the literature for waxy corn starch nanocrystals (Velasquez-Castillo *et al.* 2020b). SNCs showed strong absorption peaks in the region of 3000–3500 cm^{-1}, 2800–3000 cm^{-1}, and the third peak at 1640 cm^{-1}, attributed to -OH and C–H stretching, and water bending vibrations, respectively (Mukurumbira *et al.* 2017), similarity to the native starch. In SNCs, the bending vibration 1640 cm^{-1} decrease in intensity with the increase of hydrolysis time, revealing the removal of tightly bound water in the starch structure (Kim *et al.* 2013a). The FT-IR spectra in the region of 800–1200 cm^{-1} are normally used to study changes in the short-range ordered structure (i.e., the crystalline structure) in the external regions of starch granules (Liu *et al.* 2021a). Particularly, the absorption bands at 995 and 1047 cm^{-1} are sensitive to the changes in order structure and crystallinity of starch polymers, whereas the absorption at 1018 and 1022 cm^{-1} are associated with the vibrational modes within the amorphous domains. The intensity ratio at 1045/1018 ($R_{1045/1018}$) could thus be used to quantify the relative amounts of crystalline structure or changes in the degree of order (Miskeen, Park and Kim 2019). The short-range ordered structure of the PBS-3d, and PBS-5d samples were more orderly than the native starch, confirmed by the highest ratio of $R_{1045/1018}$ (Figure 3.5B). The improvement in the short-range order of the SNC observed from PBS-3d and PBS-5d was possibly attributed to the preferential removal of starch amorphous chains as a consequence of acidic hydrolysis. In addition, the acid hydrolysis process gradually shifted the peaks at 1081 and 1156 cm^{-1} to lower wavenumber (around 1079, and 1151 cm^{-1}, respectively) indicating that the hydrogen bonds between starch molecular chains in the SNC became stronger. According to Ma *et al.* (2007), the lower the peak frequency was, the stronger the interaction between starch molecular chains. It is worth noting that the $R_{1045/1018}$ values for SNC were in accordance with its highly relative crystallinity (Figure 3.4B).

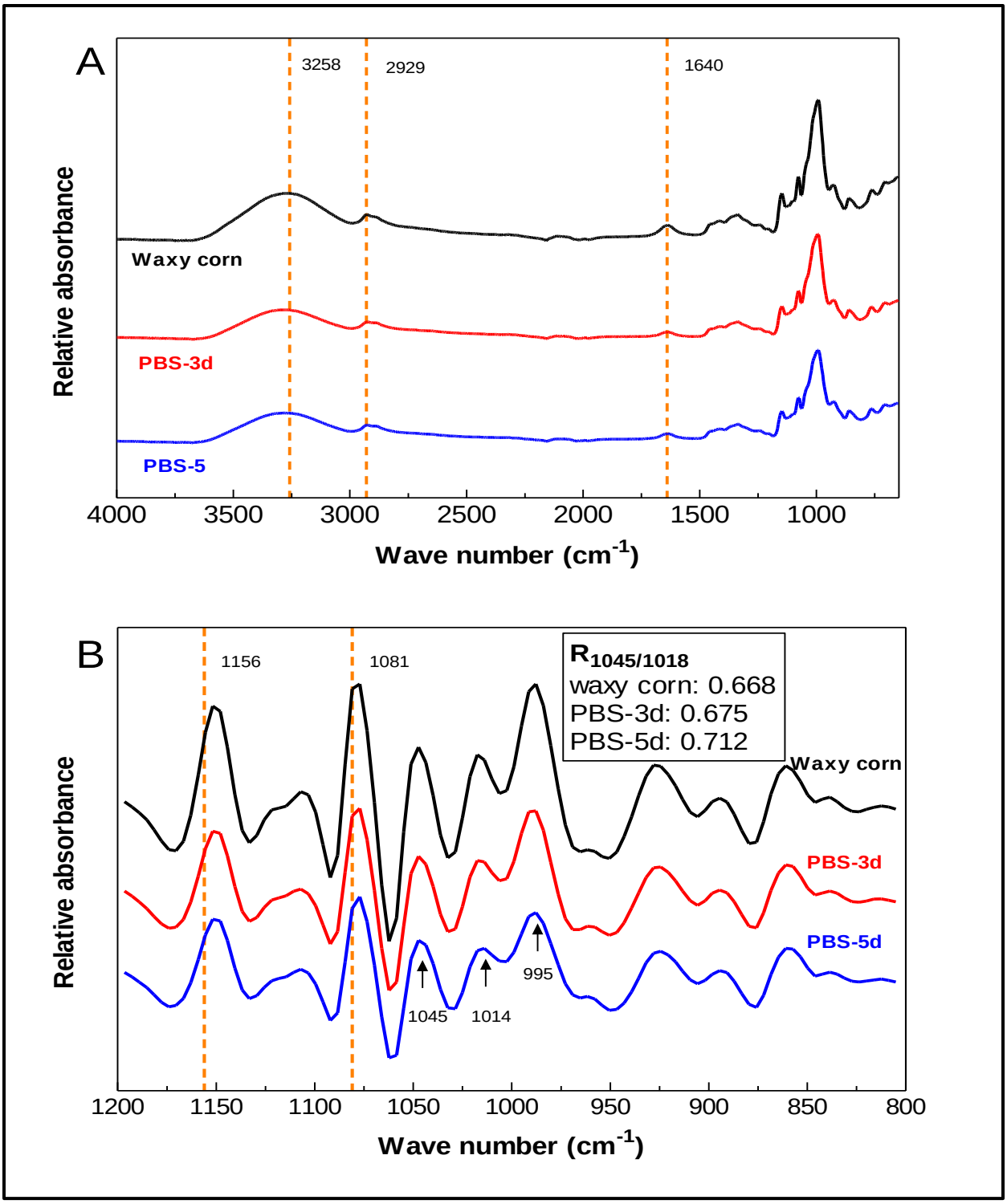

Figure 3.5: FTIR (A), and deconvoluted FTIR ranging from 1200 to 800 cm^{-1} (B) spectra of native waxy corn starch, starch nanocrystals from PBS-3d, and PBS-5d.

3.3.9. Thermal stability

DSC analysis was conducted to investigate the thermal properties of the SNCs, and the corresponding DSC curves are shown in Figure 3.6. For native waxy corn starch and SNCs, a single endothermic peak was observed. These results agreed with those reported by LeCorre, Bras and Dufresne (2012). In dry-state experiments, the single endothermic peak is attributed to the melting of crystallites with a direct transition from packed helices to unwinded helices (Kumari, Yadav and Yadav 2020). When comparing the melting peak temperatures of the SNCs with those of native starch, the SNCs showed a decrease in all temperatures related to melting. A similar result in the melting temperature of nanocrystals has been reported by other authors (Mukurumbira *et al.* 2017). The starch network is stabilized by strong hydrogen bonds, giving rise to high melting temperatures in a dry state. However, during SNCs production, the crystallinity of starch increases due to the selective removal of the amorphous regions. These crystalline residues of starch are mostly composed of a highly branched molecule with α-(1→6) glycosidic linkages. Previous studies confirmed the depressing effect of molecule branching on the glass transition (T_g) and consequently the melting temperatures. According to these authors, it was concluded that the native starch, because of its compact surface and the internal structure consisting of amylose and amylopectin more energy required to complete the T_g phase transition, even though there was lower crystallinity of native starch. It is worth noting that other scholars have observed a higher melting temperature for starch nanocrystals in comparison to native starch. Based on their findings and adopting a polymeric approach, a higher degree of molecular packing and a larger number of intramolecular bonds in SNCs require higher temperatures for their dissociation. However, the ΔH of fusion was in the order: PBS-3d > PBS-5D > native waxy corn, which was in accordance with the results of XRD analysis (Figure 3.4B).

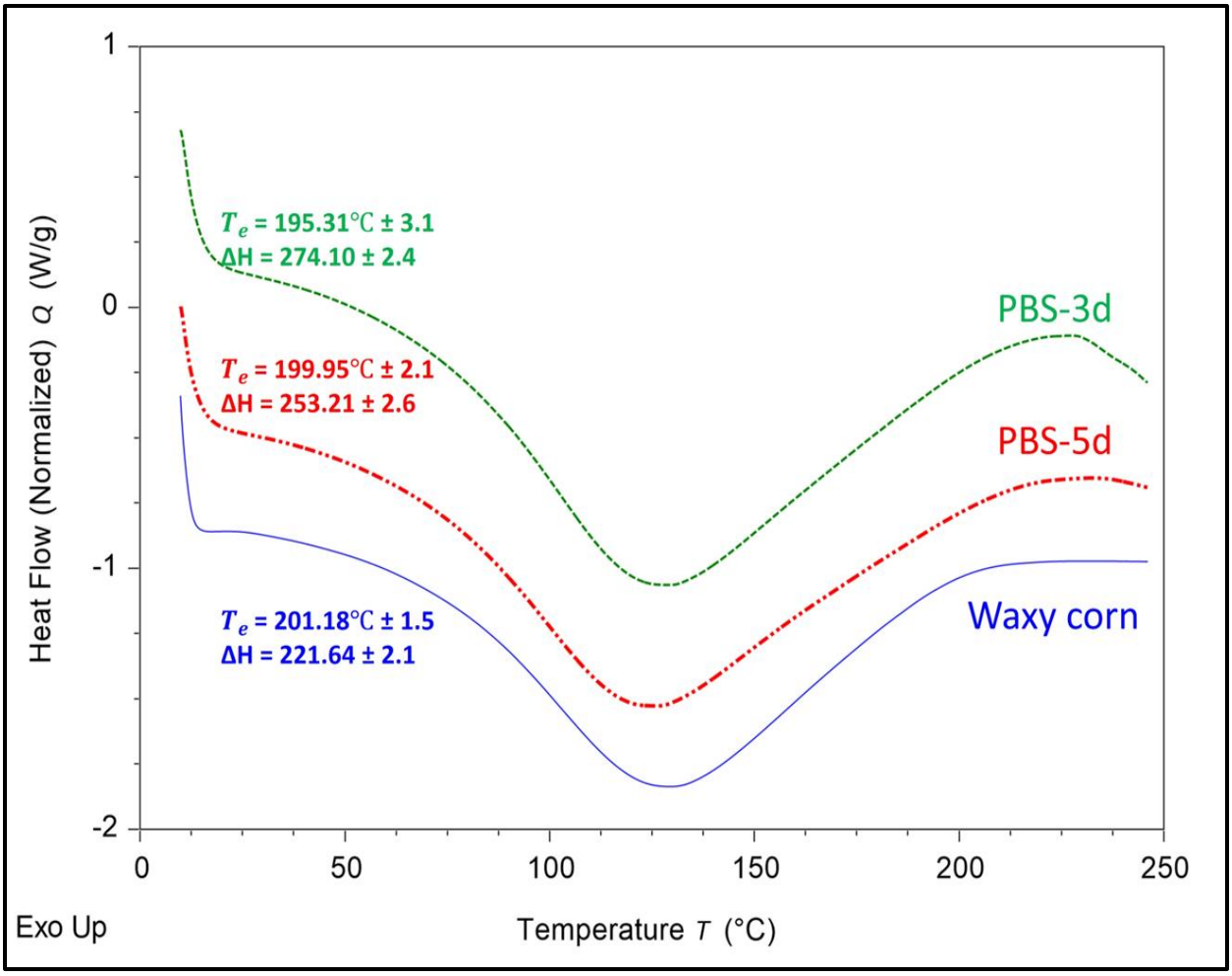

Figure 3.6: DSC curves for native waxy corn starch and SNCs prepared from compound enzyme system of Pullulanase:β-amylase (15 : 50 U/g starch) modified starches at day 3 and 5 of acid hydrolysis (PBS-3d, and PBS-5d, respectively) in the dry state (50% RH conditioning). ΔH (enthalpy of fusion, J/g), and T_e (endset temperature).

3.4. Conclusion

A compound enzyme system of pullulanase:β-amylase was proposed as an effective approach for SNC preparation compared to a single enzyme system (pullulanase). The presence of high-dense and more porous structures on starch surfaces created by the compound enzyme system led to the enhancement of sulfuric acid penetration thus improving the efficiency of the SNC preparation process with high yield. The duration of acid hydrolysis was significantly reduced from 5 to 3 days with a compound enzyme compared to the conventional acid hydrolysis process (5 days) and single

enzyme. The yield of SNC was approx. 25 wt.%, which is 3 times greater than that of the conventional SNC preparation method. Not only was the yield of SNC was improved, but its properties were also enhanced. Based on their morphological characteristics and particle size distribution, SNC appeared mostly as platelet and isolated round particle aggregates with a minimum size of less than 50 nm, which may expand its application as reinforcement in nanocomposite films. Nanocrystals from modified starches showed an A-type crystalline structure similar to the native starch, but with an increased degree of crystallinity from 32.85% to 45.28%. This study demonstrates that the compound enzymes consisting of pullulanase, and β-amylase hydrolysis seem to be the most effective and green approach to produce SNC in a shorter time with increased yield and enhanced properties.

CHAPTER FOUR

4.0 Enhancing the physicochemical, and mechanical properties of cassava starch films by synergistic interplay between starch nanocrystals and stearic acid

Abstract

The application of starch-based composite films in food packaging technology provides an opportunity to replace petroleum-based plastics. However, their application as food packaging materials has been restricted due to poor mechanical and barrier properties. This work aimed to apply starch nanocrystals (SNCs) with fatty acids to improve cassava starch-based nanocomposite film properties using a solution casting method. SNCs were incorporated in different concentrations (0, 5, 10, 15, and 20 wt.% starch). Nanocomposite films were analyzed for their mechanical strength, physicochemical and barrier properties. The addition of SNC from 5 to 15% combined with stearic acid into starch-based nanocomposite films presented better water resistance, water vapor permeability, and tensile strength than native cassava starch film. This could be linked to higher compactness in the polymer structure formed due to polymer matrix-SNC hydrogen bond interactions. Conversely, beyond 15% SNC content, nanocrystals seem to aggregate which impaired the tensile strength of the nanocomposite films. The surface of the nanocomposite films was relatively smooth and homogenous after addition of nanocrystals up to 15 wt.% concentration compared to native starch film as demonstrated by atomic force microscopy (AFM). The combined action of SNC and stearic acid promoted the polymer film with a high crystalline structure, resulting in a nanocomposite film with enhanced tensile strength and strong moisture resistance, all of which are significant properties in food packaging materials. These results indicate that the obtained nanocomposite films can be used in the development of films suitable for the packaging of high moisture foods and products.

Keywords: nanocomposite film, starch nanocrystals, stearic acids, tensile strength, and water vapor permeability.

4.1. Introduction

The application of starch-based composite films in food packaging technology provides an opportunity to replace petroleum-based plastics, which are detrimental to the environment (González et al. 2020). However, the adoption of starch-based film materials is faced with many challenges such as weak mechanical strength, poor barrier properties, and high moisture sensitivity, which limit their application in the food sector. Starch nanocrystals (SNCs) have attracted noteworthy attention as a new class of bionanomaterials, for the improvement of mechanical, thermal, and barrier properties of biopolymers films (Mukurumbira, Mellem and Amonsou 2017a; Condés *et al.* 2018).

The effect of SNC incorporation on the improvement of nanocomposite films has been investigated (González and Alvarez Igarzabal 2015; Condés *et al.* 2018; Dai, Zhang and Cheng 2020a). Martins, Latorres and Martins (2022) showed that the incorporation of the SNC up to 0.1% into rice starch-based films increased the mechanical strength and reduced water permeability and swelling through the formation of a filler-matrix interface. However, these authors observed degradation in the films' properties beyond 0.1% incorporation of the SNC. Other studies have reported the enhancement effect in films' properties with SNC addition at up to 10% in amadumbe starch films (Mukurumbira, Mellem and Amonsou 2017b), and 6% in amaranth protein films (Condés *et al.* 2018) thereafter, further increase resulted in the reduction in tensile strength. Films degradation at high concentrations of SNC was associated with the formation of agglomerations and unevenly dispersed of SNCs at higher concentrations in a polymer matrix (Martins, Latorres and Martins 2022). The effectiveness of the SNC as a reinforcement material has been found to depend on the homogeneity of the dispersion and the strength of interaction between the nanofiller and matrix (Jeevahan and Chandrasekaran 2019b; González *et al.* 2020). Further improvement on the mechanical and hydrophobic properties of biocomposite films using a single component like SNC is thus difficult due to the limited amount that can be incorporated into the matrix. Therefore, the inclusion of different modifiers such as fatty acid may be critical in fine-tuning the efficient dispersion of SNC even at higher concentration levels.

Fatty acids are recommended as a strategy to improve the water barrier properties of starch-based films. According to Schmidt et *al*. (2013) the improved moisture barrier properties of cassava starch film modified with stearic acid are due to the overall increase in the films' hydrophobicity.

Liu et *al*. (2018) demonstrated that the formation of inclusion complexes between lipids and amylose in starch also contributes to these improvements. However, there are some limitations associated with lipids application on biopolymer materials, which may impair the mechanical properties due to phase separation (Oyeyinka, Singh and Amonsou 2017). Hence, this study investigated the combined effect of fatty acids and SNC on the physicochemical properties of nanocomposite films using cassava starch. Cassava starch is considered the most promising raw material for producing edible food packaging films due to its odorless, tasteless, colorless, and non-toxic (Chiumarelli and Hubinger 2014; Piñeros-Hernandez et al. 2017). The goal of this research was to develop a starch-based nanocomposite film that allows for efficient dispersion of nanocrystals even at higher concentrations while also improving the physicochemical properties of bionanocomposite films.

4.2. Materials and methods

4.2.1. Materials

Cassava starch (CS) (amylose content ~18.3%) from (ChemLab supplies, South Africa), and stearic acid (SA) with reagent grade 98% (melting point 67–72°C) from Sigma Aldrich. Laboratory-grade glycerol (99.5% purity) from Merck Pty Ltd. Distilled water was used throughout this work.

4.2.2. Preparation of films

Cassava starch-based nanocomposite films were prepared using a method described by Liu et al. (2015) with some modifications. A 3% (w/v) dispersion of starch was mixed with 2% stearic acid (w/w dry starch) and distilled water in a 250 ml flask before heating. The dispersions were stirred (300 rpm) and heated concurrently at 95°C for 90 min. After heating, the plasticizer glycerol at a concentration of 33% (w/w dry starch) was added, and the mixture was homogenized with Ultra-Turrax (Germany) at 14,000 rpm for 4 min. The film dispersions were allowed to cool below 50°C and thereafter starch nanocrystals (SNCs) were added at concentrations: 0, 5, 10, 15, and 20% (w/w dry starch). The dispersions were homogenized using an ultrasonic processor [700 W, 5 min] to remove the air bubbles and improve the dispersion of SNCs. The film-forming suspension was dried at 30°C for 24 h using an oven with air circulation. Pure cassava starch-based film without

stearic acid and SNCs was considered the native sample. The cassava starch with stearic acid without SNCs was used as the control sample. All the film samples were equilibrated at 58% RH at 20℃ inside the desiccator for 48 h before being peeled for characterization.

4.2.3. Characterizations of nanocomposite films

4.2.3.1. Microscopy

Atomic force microscopy (AFM) was used to determine the morphological surface of the starch-based nanocomposite film samples. AFM measurements were performed on a Multimodal AFM (DI, Veeco, Instrumentation Group) with both tapping and conductive mode (C-AFM). The Multi130 tips were used for tapping and MESP for C-AFM.

4.2.3.2. Opacity

Opacity measurements of the starch-based nanocomposite films were determined using a UV-visible spectrophotometer at a selected wavelength of 600 nm. The opacity was calculated according to the following equation (Gao *et al.* 2021):

$$Opacity = \frac{A_{600}}{X} \quad (1)$$

Where A_{600} is the absorbance at 600 nm and X represents film thickness (mm).

4.2.3.3. Moisture content, swelling ratio, and solubility in water.

The moisture content of starch-based nanocomposite films was determined using AACC methods 44-15. Strips of the starch films were dried at 105℃ for 24 h and weight loss was determined.

The swelling ratio (SR) of starch-based nanocomposite films was determined by the method described by Cheng *et al.* (2022). The films were cut into pieces with dimensions of 3 cm × 5 cm, weighed W1 (g), added to the glass beakers with 40 ml of distilled water with sodium azide, and stored at room temperature for 24 h. The samples were then removed and W2 (g) was measured. The SR was calculated as follows:

$$SR\ (\%) = \frac{W2 - W1}{W1} \times 100 \quad (2)$$

The solubility of starch-based nanocomposite films in water (SW) was determined using the method described by Gao *et al.* (2021). Solubility was measured by immersion of film disks (2.0 cm in diameter) in water containing sodium azide, at 25℃ for a period of 24 h. The amount of dry

matter in the initial and final samples was determined by drying the samples at 105℃ for 24 h. All determinations were performed in triplicate.

4.2.3.4. Water vapor permeability (WVP)

Water vapor permeability values for the starch-based nanocomposite films were determined according to La Fuente *et al.* (2022) with some modifications. The test films (5 × 5 cm^2) were covered in a polypropylene centrifuge tube (50 ml) with silica desiccant beads (30 g). Then, the permeation tube was put into a desiccator containing saturated sodium chloride solution, followed by weighing once every 30 min until 8 h at 25℃. The WVP of films was obtained by Eq. (3)

$$WVP = \frac{C \times e}{A \times P(R_1 - R_2)} \quad (3)$$

where A is the effective area of the film (mm^2), C is the water vapor transmission rate that is the slope of the curve (g/s), e is the thickness of the film (mm), P is saturated water vapor pressure (Pa) at 25℃, R_1 and R_2 are relative humidity in the desiccator and the bottle, respectively.

4.2.3.5. Mechanical properties

The tensile properties of the starch-based nanocomposite film samples were obtained using a universal testing machine (EZ-SX, Shimadzu, Japan) according to the method described by Mukurumbira, Mellem and Amonsou (2017b). The film samples were cut into rectangular strips (6 × 1.5 cm). The initial distance of separation and velocity were adjusted to 40 mm and 1 mm/s respectively.

4.2.3.6. FTIR

Fourier transform infrared spectra (ATR FTIR) of the starch-based nanocomposite film samples using an FTIR carry 630 ATR Diamond (Agilent Inc., USA). The analyzing range of wavelength was 4000–400 cm^{-1} and a resolution of 4 cm^{-1} with a total of 32 scans were performed.

4.2.3.7. X-ray diffraction (XRD)

The crystalline structure of the starch-based nanocomposite film samples was measured using an X-ray diffractometer (Bruker Inc., Germany). The operation conditions for the refractometer were: Cu-Kα radiation, angular range 5–45° (2θ), step size of 0.034°, counting time 92 s, and working voltage was 40kV.

4.2.3.8. Thermal properties.

The thermal properties of starch films were measured using Differential Scanning Calorimeter, a TA Instrument DSC Q100 (New Castle, DE, USA) filled with a manual liquid nitrogen cooling system. Approximately 3 mg of starch, films were cut and placed into pans and thereafter hermetically sealed. The samples were heated from 25 to 250℃ with an interval heating rate of 10℃/min.

The TGA curves of the starch-based nanocomposite films (not more than 10 mg) were measured by the method described by Gao *et al.* (2021) using an STA 6000 simultaneous thermal analyzer (PerkinElmer) with a test temperature range profile of 25–450℃ and a heating rate of 25℃/min.

4.2.3.9. Statistical analysis.

The statistical analysis of the data was conducted using the IBM SPSS version 20.0 statistical software for Windows (Armonk, NY: IBM Corp.). All experiments were carried out in triplicate. Data were analyzed using analysis of variance (ANOVA) and means were compared using the Fisher Least Significant Difference (LSD) test ($p < 0.05$). This determine if there were significant differences between the moisture content (MC), swelling ratio (SR), solubility in water (SW), water vapor permeability (WVP), opacity, and tensile strength of SNC-filled nanocomposite films with native starch films.

4.3. Results and discussion

4.3.1. Surface morphology

Atomic force microscopy was employed to evaluate the surface morphology and roughness whose quantitative indexes included average roughness (Ra) and maximum roughness height (Rmax). Data and images of films are displayed in Figure 4.1. The surface roughness as indicated by Ra and Rmax was significantly different among the casted films. Specifically, Ra and Rmax decrease with the inclusion of SNC in the matrix, suggesting an enhancement in the properties of the films. The rough and more irregular surface structure (strong presence of voids in this case) displayed from native starch and starch with stearic acid films could be related to partial phase separation of starch–glycerol, and starch–fatty acids, as previously reported by other authors (Schmidt *et al.* 2013; Oyeyinka, Singh and Amonsou 2017; Gao *et al.* 2021). In addition, this might indicate that it was difficult to form a cohesion and continuous structure between starch chains. Liu *et al.*

(2021c) found that a smoother surface on the resultant film was observed after a 5% CMC addition. These findings might be due to the uniform distribution of SNC resulting in the homogeneous morphology of nanocomposite films. Furthermore, the formation of the V-type inclusion complex between amylose-lipid could improve the polymer film flatness (Liu *et al.* 2018). The surface roughness of film is an important property, especially in the preservation of fruits; starch-based nanocomposite coating may require having a smooth surface that can maintain cell membrane permeability. Therefore, in this study, SNC loading below 15% was considered acceptable content to achieve these smooth surface characteristics of nanocomposite films.

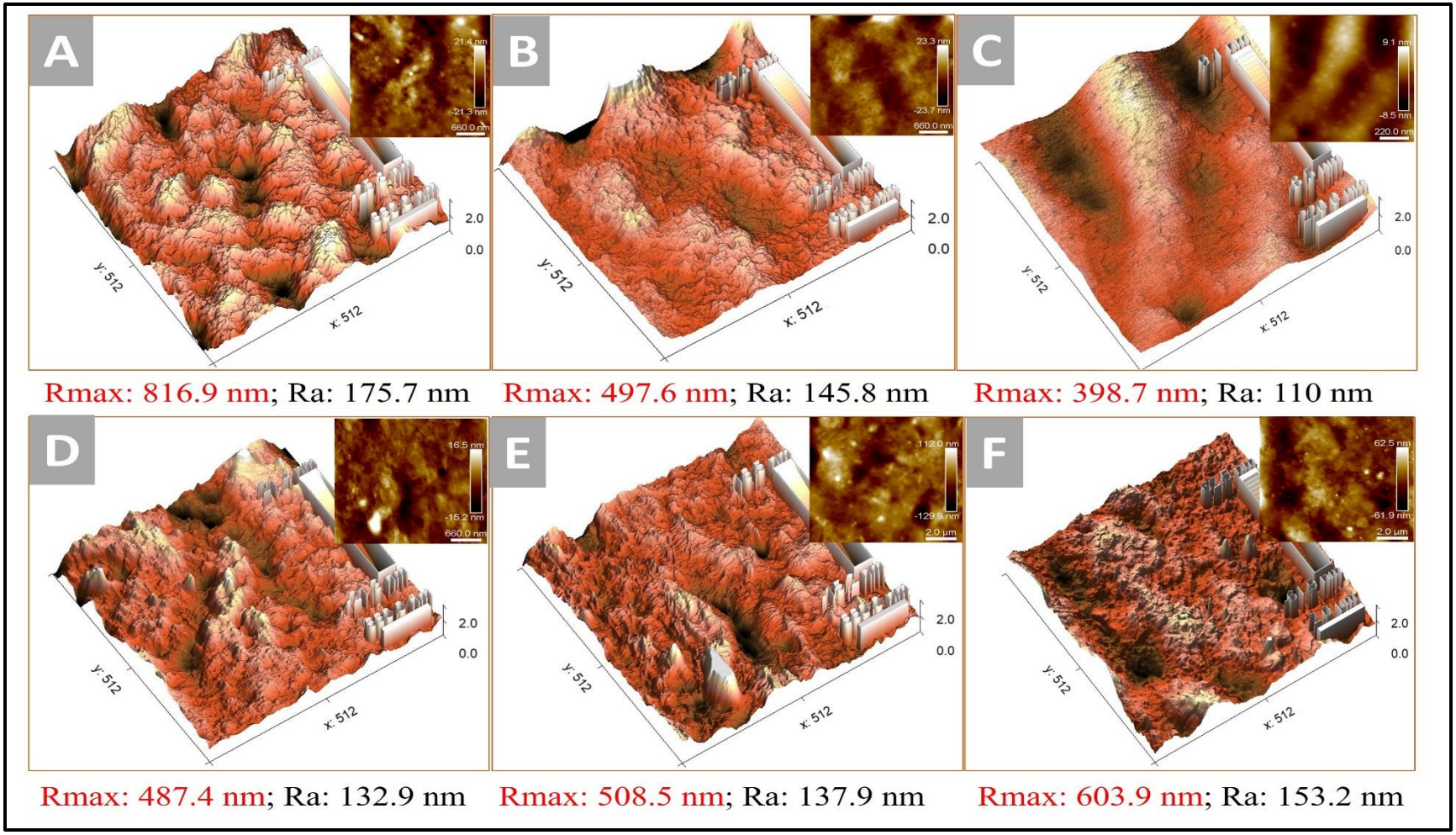

Figure 4.1: The surface morphology of starch-based nanocomposite films observed through atomic force microscopy (AFM). A – B; native starch and starch with stearic acid films, respectively. C – F; 5, 10, 15, and 20% SNC-filled nanocomposite films, respectively.

4.3.2. Opacity

Opacity is a critical parameter for biodegradable films, particularly when the films packaging photosensitive products (Gao *et al.* 2021). The opaqueness of the SNC-filled nanocomposite films progressively increased with the SNC content (Table 4.1). An increase in the opaqueness of the nanocomposite films could be caused by the presence of SNC which enabled the nanocomposite film to have a larger specific surface area and a higher refractive index (Oliveira *et al.* 2018). A similar phenomenon has been reported by other authors (Mukurumbira, Mellem and Amonsou 2017b; Martins, Latorres and Martins 2022). High opaqueness in the nanocomposite films suggests a uniform blending of stearic acid with nanocrystals in the polymer matrix creating a dense and close polymer network which contributed to the high opaqueness of the films (Oyeyinka, Singh and Amonsou 2017). Therefore, these films may be ideal food packaging materials; to prevent discoloration, nutrient loss, and off-flavor, as well as retard lipid oxidation in food systems.

Table 4.1: Effect of SNC concentration on the moisture content (MC), swelling ratio (SR), solubility in water (SW), water vapor permeability (WVP), and opacity of starch-based nanocomposite films.

Film samples	MC (%)	SR (%)	SW (%)	WVP (10^{-5}gPa^{-1}h^{-1}m^{-1})	Opacity (1/mm)
Native	22.06 ± 1.2^{a}	237 ± 3.2^{a}	28.58 ± 2.2^{b}	2.68 ± 0.2^{a}	1.48 ± 0.3^{c}
Control (SFA)	18.84 ± 1.3^{b}	114 ± 2.3^{b}	26.41 ± 3.0^{c}	2.4 ± 0.1^{b}	2.67 ± 0.1^{b}
SFA-5%SNC	16.52 ± 2.1^{c}	110.2 ± 2.1^{c}	21.51 ± 2.6^{f}	1.96 ± 0.2^{c}	2.71 ± 0.05^{ab}
SFA-10%SNC	13.48 ± 2.0^{d}	82.6 ± 3.5^{e}	16.62 ± 1.2^{d}	1.62 ± 0.1^{d}	2.75 ± 0.08^{a}
SFA-15%SNC	12.10 ± 3.4^{e}	74.54 ± 1.4^{f}	18.74 ± 2.3^{e}	1.44 ± 0.1^{e}	2.8 ± 0.04^{a}
SFA-20%SNC	17.45 ± 2.4^{c}	96.5 ± 2.8^{d}	38.47 ± 2.1^{a}	2.38 ± 0.3^{b}	2.98 ± 0.1^{a}

Mean ± SD is reported. Means with different superscript columns are significantly different ($p < 0.05$).

4.3.3. Water susceptibility

Most food products are susceptible to moisture and require higher moisture resistant packaging (Jeevahan and Chandrasekaran 2019b). Thus, the addition of hydrophobic components (i.e., stearic acid) and nanofillers such as SNC can synergistically reduce the number of hydroxyl groups on starch by modifying macromolecules' interfacial properties to reduce water-macromolecules interactions (Giteru, Ali and Oey 2021). Moisture content (MC), swelling ratio (SR), solubility in water (SW), and water vapor permeability (WVP) of starch-based nanocomposite films are presented in Table 4.1. In general, the MC, SR, and SW of the nanocomposite films significantly decreased with increasing SNC content up to 15% in the film matrix in comparison with the native and starch with stearic acid films. Martins, Latorres and Martins (2022) also reported a reduction in solubility for starch-based nanocomposite film compared to pure starch film, suggesting that the addition of SNC to starch matrix formed strong hydrogen bond interactions between the nanofiller and the matrix which positively affected the barrier properties of nanocomposite film. This could also be attributed to the development of inclusion complexes between amylose-lipid, which are considered to serve as an insoluble layer on the film surface, limiting water absorption by the starch matrix. Further increasing the SNC to 20% did not improve the MC, SR, and SW of films. Increasing SNC concentration above 15% possibly creates excess availability of these nanofillers for interaction with water (Martins, Latorres and Martins 2022).

The WVP of nanocomposite films decreased significantly with increasing SNC concentration from 5 to 15% (Table 4.1). In comparison to native starch film, a 46% reduction in WVP was observed for nanocomposite film loaded with 15% SNC (Table 4.1). Two possible explanations can be used for such a reduction in WVP; firstly, the inclusion of stearic acid may cover the cassava starch granular surfaces and increase its hydrophobicity, thus restricting the water vapor transfer through the starch-based films (Liu *et al.* 2016; Kang *et al.* 2020). Secondly, incorporating SNC in the starch film matrix created a tortuosity structure that increases migration pathways of the water molecules and consequently limits permeability (Mukurumbira, Mellem and Amonsou 2017a). Furthermore, the platelet-like morphology of SNC may cause a decrease in diffusion of water molecules by filling the porosities (Li *et al.* 2015; Mukurumbira, Mellem and Amonsou 2017a); hence, lower WVP values are obtained. However, a further increase in SNC content to 20% caused a significant increase in WVP. An increase in the WVP of nanocomposite film at higher concentrations (20% SNC) could be explained by the agglomeration effect of the nanocrystals

which causes the formation of larger pores in the film matrix and facilitate the passage of gases through the film. Similar behaviour of WVP has been reported by several authors (González and Alvarez Igarzabal 2015; Mukurumbira, Mellem and Amonsou 2017a). The permeability of the films is controlled by the diffusion of water within the film matrix (Diaz-Montes and Castro-Munoz 2021). Therefore, nanometric materials such as SNC can be used to develop new tightly connected three-dimensional networks that can prevent the migration of water in foods.

4.3.4. Mechanical properties

The mechanical properties of nanocomposite films were significantly influenced by their SNC contents (Figure 4.2). The tensile strength (TS) of nanocomposite films significantly increased with SNC content, showing the highest value of 12.8 MPa at 15% SNC content (Figure 4.2A). In comparison to native starch films, an increase of 71.6% in TS was successfully achieved for nanocomposite film at 15% SNC content. This was expected since the high crystallinity of SNCs makes it difficult to dissolve in water and rigid particles acted as reinforcement agents (Li *et al.* 2015). The tensile strength values observed in this study were greater than those reported from the literature (Costa *et al.* 2017; Mukurumbira, Mellem and Amonsou 2017b; Dai, Zhang and Cheng 2020a). This could suggest that the mechanical strength of the films can further be improved by adjusting the quantity and uniform distribution of the nanocrystals used. Moreover, a strong filler-matrix interaction may influence the enhancements in strength properties (Piyada, Waranyou and Thawien 2013). However, increasing the concentration of SNC beyond 15% in the film structure seemed to impair the TS of the nanocomposite film. Previous literature studies have confirmed that addition of SNC at a certain higher concentration cause agglomeration of the nanocrystals within the starch matrix which reduces their active surface area for interacting with the matrix; in turns weakens their adhesion on the surface of the composite matrix interface (Dai *et al.* 2018; Martins, Latorres and Martins 2022). Similar pattern was also reported by Piyada, Waranyou and Thawien (2013) and Mukurumbira, Mellem and Amonsou (2017a) loaded with rice, and amadumbe starch nanocrystals, respectively.

Increasing nanocrystals content resulted in a decrease in the E (%) from 127.3% (native starch film) to 65.4% (nanocomposite film) as shown in Figure 4.2B. The reduction in E (%) can be attributed to the uniform dispersion of nanocrystals in the starch matrix that prevents the mobility of macromolecules (Condés *et al.* 2018).

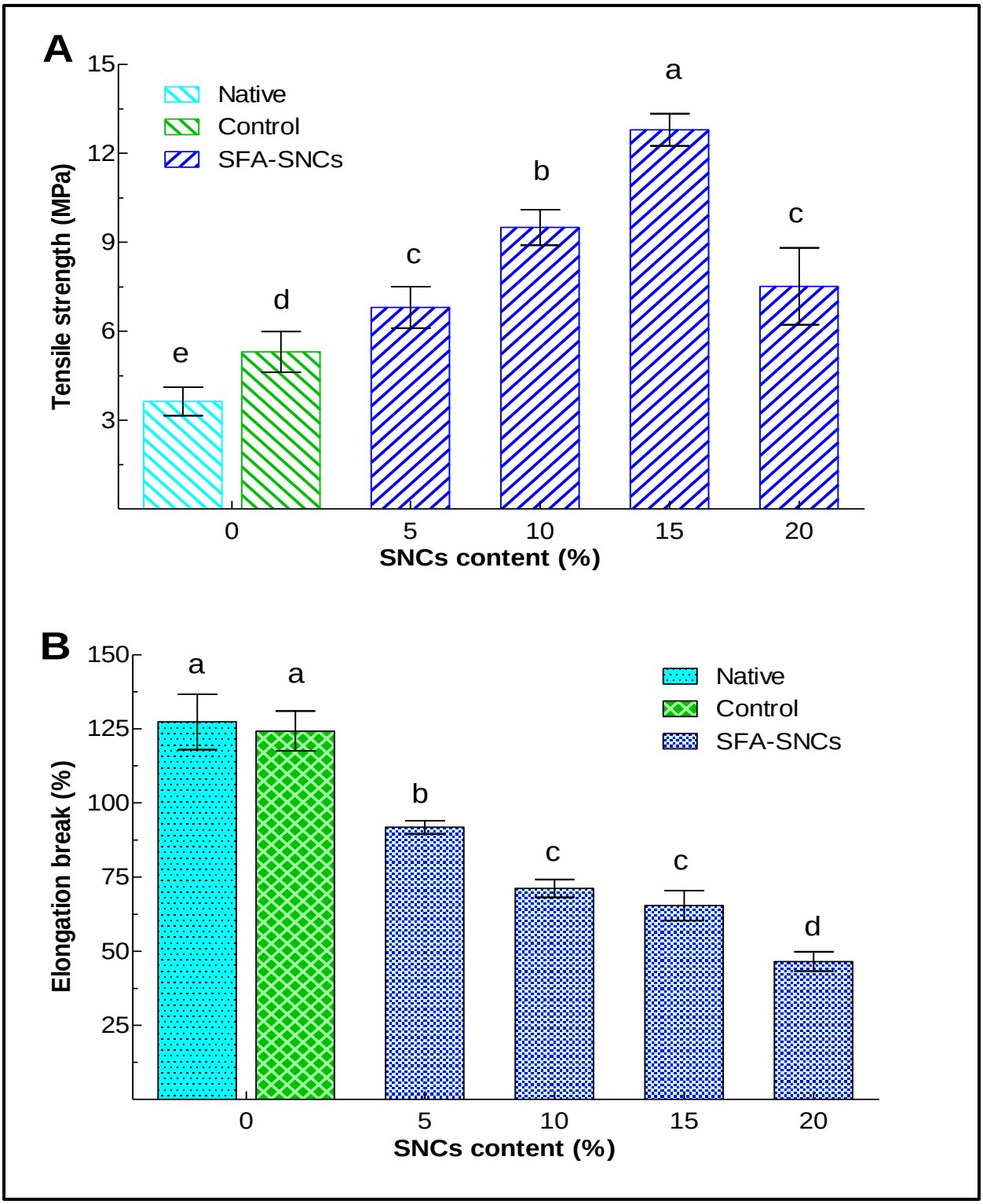

Figure 4.2: Effect of SNCs concentration on the mechanical properties of SNC-filled nanocomposite films at different concentrations. Values represent mean ± standard deviation. Values in column with different letters are significantly different ($p < 0.05$).

4.3.5. Chemical structures by FT-IR spectra

All film samples had similar spectra (Figure 4.3A), characterized by bands of 800–1500 cm^{-1}, 2800–3000 cm^{-1}, 3000–3600 cm^{-1} which represent the fingerprint region (crystalline and amorphous fractions), the C-H stretched region, and the O-H stretched regions, respectively (Guo *et al.* 2018). The main functional groups existing in starch are the hydroxyl groups (3000–3600 cm^{-1}) that act as a hydrophilic character. When both SNC and hydrophobic agent were incorporated in the starch polymer matrix, the absorption peak in this region (3000–3600 cm^{-1}) shifted to lower wavelengths. This shift may indicate that the intermolecular interactions were enhanced between the polymer matrix and SNC, by replacing O-H groups with hydrophobic interactions. Furthermore, after addition of stearic acid and SNC, the nanocomposite films had a new peak at 1736.1, 2322, and 2922 cm^{-1} in the FT-IR spectrum, indicating some small aggregate of uncomplexed SA, amylose-lipid complex, and C-H stretch, respectively. Furthermore, the spectral region 1200–800 cm^{-1} of FT-IR can be used for the detection and quantification of crystallization (at 1047 cm^{-1}) and amorphous (at 1022 cm^{-1}) fractions, owing to their sensitivity to starch short-range structure (Tang *et al.* 2022). With addition of nanocrystals, crystalline intensity bands increased while the amorphous region (1022 cm^{-1}) decreased (Figure 4.3B). These results suggested that both the addition of stearic acid and SNC changed the crystallinity and conformation properties of nanocomposite films, forming strong interactions with hydrogen bonds, which is consistence with the increase TS results (section 4.3.4).

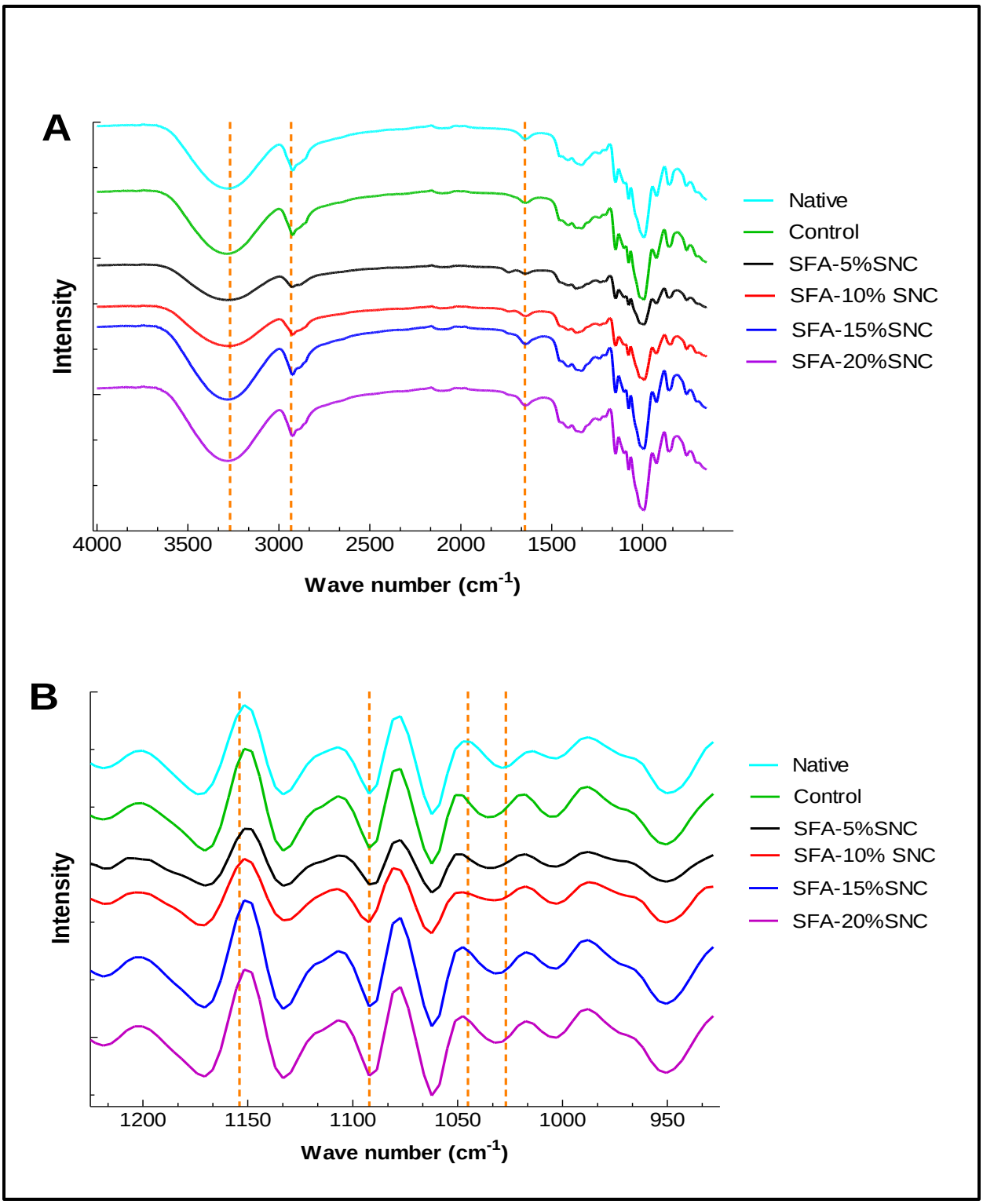

Figure 4.3: FTIR (A), and deconvoluted FTIR ranging from 1200 to 800 cm^{-1} (B) spectra of native starch, starch with stearic acid, and SNC-filled nanocomposite films at different concentrations.

4.3.6. Crystalline structures

The XRD patterns for starch-based films were affected by the addition of both stearic acid and SNC (Figure 4.4). The broad bump peak centered around 2θ = 17.9° for native starch film, indicated the presence of amorphous material. In the case of the control (starch film with stearic acid) film, the appearance of sharp peaks at approximately 2θ of 13.5° and 20.3° are characteristics of a typical V-type crystalline pattern and were attributed to the complexation of stearic acid with amylose (Guo *et al.* 2018). The incorporation of SNC slightly enhanced the intensity peak at 2θ = 15° and 23.1° which represent the A-type crystalline pattern. However, no clear effect was confirmed by the present study with a variety of peaks when SNC content increased on the nanocomposite films.

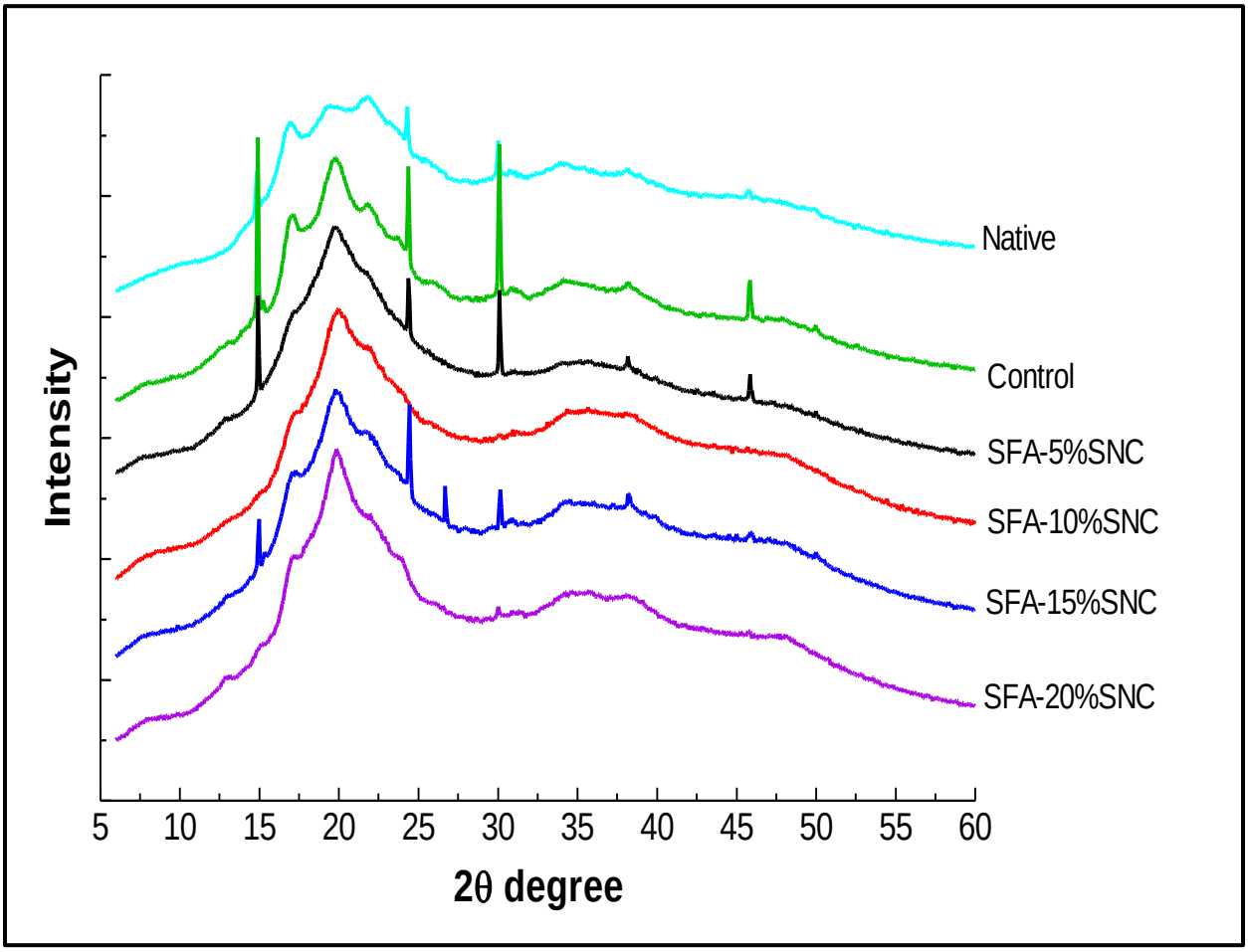

Figure 4.4: X-ray diffraction patterns of native starch, starch with stearic acid and SNC-filled nanocomposite films at varying concentration of SNCs.

4.3.7. Thermal stability

The TGA and differential TGA (DTG) studies of films containing SNC, and stearic acid were performed to further understand the structure and interaction between polymer matrix and SNC with a stearic acid blend. These thermal curves for native starch, starch with stearic acid, and nanocomposite films are shown in Figure 4.5. All films underwent three main stages of thermal decomposition. The initial stage occurred at low temperatures (60 – 120°C) and is associated with the loss of water (La Fuente *et al.* 2022). The second stage corresponded to the decomposition of the free glycerol-rich phase and occurred in the range (120 – 290°C). The third stage occurred at 290 – 335°C, with a severe weight loss of 58.2–68.4% (Table 4.2). Furthermore, as shown in Figure 4.4B, degradation of the nanocomposite films began at a higher temperature than native starch film in all cases. Peaks at similar temperatures were observed in normal maize starch (González *et al.* 2020), and cassava starch studies (Teodoro *et al.* 2015). These results suggest that nanocomposite films filled with SNC have better thermal stability than those without SNC.

The thermal behaviour of starch-based films with stearic acid and SNC addition was also determined using DSC. Glass transition temperatures (T_g) and melting temperature (T_m) of nanocomposite films with their corresponding enthalpy changes (ΔH_m) were significantly affected by SNC content (Table 4.2). These thermal parameters of nanocomposite films with different SNC content displayed almost the same trends as WVP and TS. Other scholars have confirmed that when SNCs are well dispersed in the polymer matrix, the thermal properties of the resulting composite film can be enhanced (Li *et al.* 2015). The increment in the T_g values was impaired by a high concentration of SNC loaded in the nanocomposite films. The result is related to the different interactions and efficient dispersion of nanofillers in the corresponding nanocomposite film (Zhang *et al.* 2021).

Table 4.2: Thermal properties of starch-based nanocomposite films.

Film samples	T_g (°C)	T_m (°C)	ΔH_m (J/g)	DTG Max (°C)	Mass loss (%)
Native	53.3	72.2 ± 1.14^{f}	34.6 ± 0.98^{f}	317	58.2
Control (SFA)	59.52	89.56 ± 4.32^{e}	129.13 ± 1.18^{d}	324	68.4
SFA-5%SNC	62.98	96.46 ± 5.23^{d}	118.01 ± 0.84^{e}	320	62.1
SFA-10%SNC	68.27	112.16 ± 1.26^{c}	167.07 ± 1.84^{c}	323	59.0
SFA-15%SNC	78.61	143.58 ± 1.24^{a}	227.34 ± 2.42^{a}	324	64.7
SFA-20%SNC	70.73	122.41 ± 3.34^{b}	197.15 ± 1.58^{b}	324	63.2

Mean ± SD is reported. Means with different superscript columns are significantly different ($p < 0.05$).

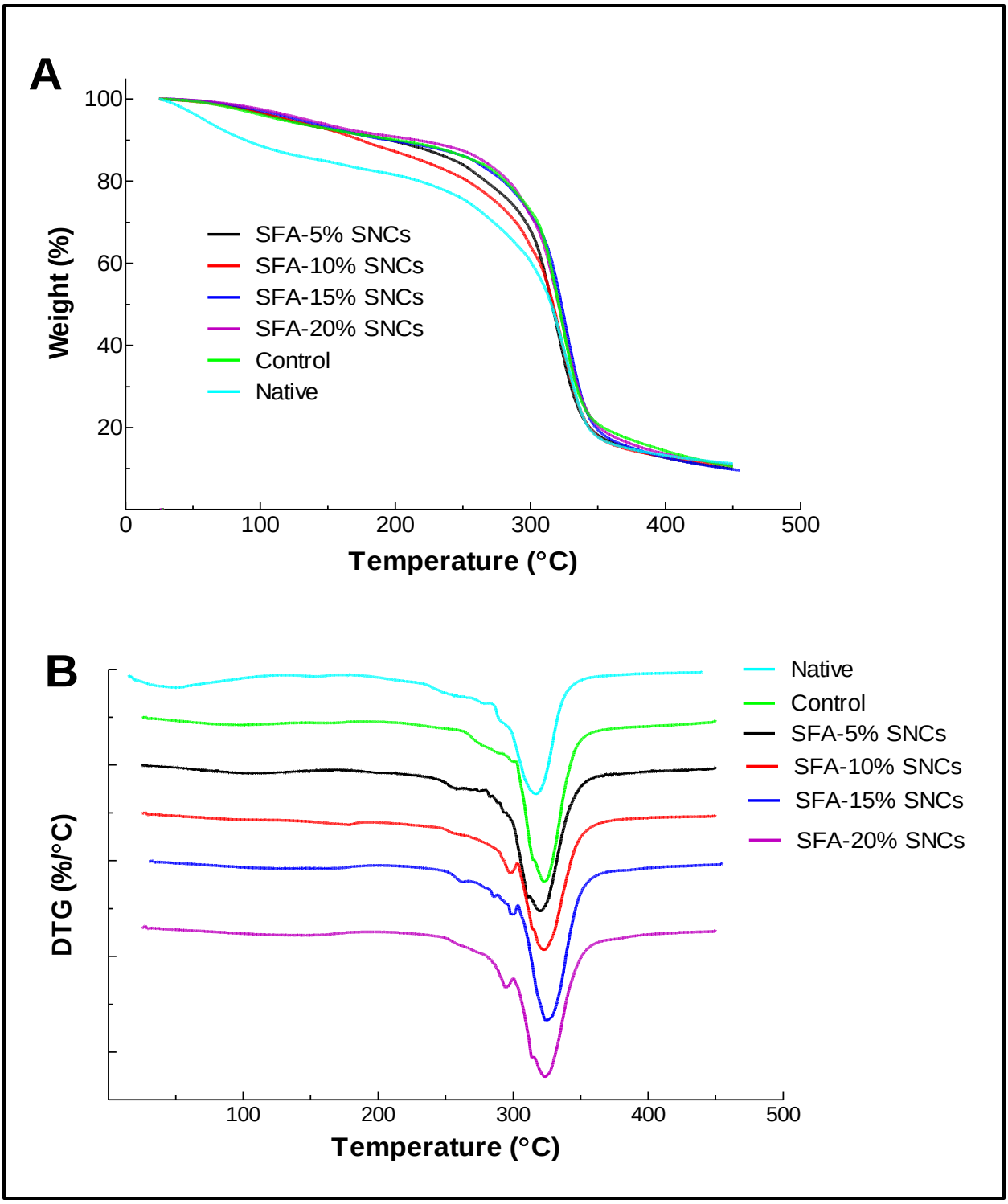

Figure 4. 5: Curves of TGA (A) and DTG (B) for native starch, starch with stearic acid, and SNC-filled nanocomposite films at varying concentration of SNCs.

4.4. Conclusion

The addition of SNCs from 5 to 15% combined with stearic acid into starch-based nanocomposite films presented better water resistance, water vapor permeability, and tensile strength than the native cassava starch film. The surface smoothness of the nanocomposite films was enhanced with SNC addition. These manifestations may indicate the formation of a stronger network structure, which is possibly caused by the efficient dispersion of SNC within the starch matrix. However, higher loadings of SNC beyond 15% seem to induce nanocrystals aggregation and interfere with hydrogen bonds in starch polymer chains, which impair the tensile strength of the nanocomposite film. Furthermore, SNC incorporation was able to decrease WVP values in starch films and appeared more opaque, which might be beneficial in the packaging of foods that are easily degraded when exposed to high moisture and light. The combined effect of SNCs at different concentrations and stearic acid into cassava starch-based film was a successful approach to further improve the mechanical reinforcement and barrier properties of nanocomposite films. Moreover, findings of this study offers intriguing possibilities of expanding the use of starch nanocomposite films reinforced by SNCs to in-package high-moisture products and preservation of fruit quality. However, further studies are needed to investigate potential performance improvement for industrialized used of the nanocomposite films for food products.

CHAPTER FIVE

5.0 General discussion

The purpose of this research was to develop a new and efficient method for starch nanocrystals (SNCs) production using pullulanase alone or in combine with β-amylase to modify the starch before acid hydrolysis. Thereafter, SNCs were applied as reinforcement agents together with stearic acid to improve cassava starch-based nanocomposite film properties using a solution casting method. The first part of this section discusses the production and characterization of SNCs whilst the second part focuses on the application of SNCs in the nanocomposite.

5.1. Effect of compound enzymatic pretreatment on starch nanocrystals production process and physicochemical properties

The enzymatic pretreated starch granules appeared porous. The number and distribution of pores created on the surface of starch granules were dependent on enzyme type and activity (Benavent-Gil and Rosell 2017c). According to DOA and SEM data, pullulanase (15 U/g starch), and compound enzymes of pullulanase:β-amylase (15:50 U/g starch) pretreated starches (assigned as PS, and PBS, respectively) were selected for SNCs preparation using sulfuric acid hydrolysis method. The progression of acid hydrolysis measured at day intervals revealed a sharp decrease in the residual yield of PS and PBS samples. This sharp decrease in residual yield could be attributed to the severe fragmentation of starch chains in amorphous regions at the early stage of hydrolysis and could suggest a rapid achievement of nanocrystals. After 3 days of acid hydrolysis, the recovered residue was approximately 19.8 wt.% for PS, slightly lower than that of PBS (25.2 wt.%) with both having an average particle of less than 5 nm. Unlike the untreated starch, starch nanometric size (< 100 nm) with residue yield of 15.4 wt.% was only achieved after 5 days of acid hydrolysis. According to a two-staged of the acid hydrolysis kinetics of starch granules (Le Corre-Bordes and Angellier-Coussy 2014), the first-stage of hydrolysis for PS and PBS was minimized when compared to that of the untreated starch sample, possibly due to the presence of numerous surface pores on these enzymes pretreated starches allowed quick penetration of H_3O^+ resulting in rapid fragmentation of starch granule to nanoparticles, which likely affected the hydrolysis rate and the yield of SNCs (Liu *et al.* 2021b). TEM images confirmed that the formation of SNC in both PS and PBS samples was achieved after 3 days of acid hydrolysis, which appeared like

platelet-like aggregates or isolated round-edge particle shapes. However, the majority of nanocrystals appeared as aggregates with sizes ranging from 200 to 500 nm. Similar trend has been reported by other authors and can be attributed to the larger surface area of the platelets and their ability to interact through the formation of hydrogen bonds between hydroxyl groups, which are found in a substantial number of single areas of nanocrystals surfaces (Sanchez de la Concha *et al.* 2018; Liu *et al.* 2021a). SNCs obtained from PBS sample after 3 days of hydrolysis (PBS-3d) was selected to further confirm whether they are congruent with the characteristics of conventional SNCs, by analyzing crystalline properties and chemical structure of the SNCs produced from the newly developed method and compared with those obtained after 5 days of hydrolysis (PBS-5d) using XRD and FT-IR analysis.

There was a significant increase in the relative crystallinity of the PBS-3d (45.28%) and PBS-5d (47.7%) SNC products when compared to native starch. This was expected due to the extensive removal of the amorphous regions during the hydrolysis process which results in a higher proportion of the crystalline regions. In accordance with the present results, an increase in relative crystallinity after acid hydrolysis has been reported by others (LeCorre, Bras and Dufresne 2011; Mukurumbira *et al.* 2017; Liu *et al.* 2021b). Starch nanocrystals exhibited A-type crystallinity, with significant diffraction peaks at $2\theta = 15°$, a doublet peak at 17 - 18°, and a third one at 23.1° which was in agreement with the previous studies (LeCorre *et al.* 2012; Dai, Zhang and Cheng 2019; Velasquez-Castillo *et al.* 2020b). Therefore, neither enzyme pretreatment nor acid hydrolysis altered the original crystal structure of the native starch. The structural characteristics and changes in the short-range molecular order of SNCs were investigated by FT-IR. SNCs showed strong absorption peaks in the region of 3000–3500 cm^{-1}, 2800–3000 cm^{-1}, and the third peak at 1640 cm^{-1}, attributed to -OH and C–H stretching, and water bending vibrations, respectively (Mukurumbira *et al.* 2017), similarity to the native starch. These results suggest that functional groups were retained after the acid hydrolysis. Similar observations have been reported for waxy corn starch nanocrystals (Velasquez-Castillo *et al.* 2020b). The short-range ordered structure of the SNC products was more orderly than the native starch, confirmed by the highest ratio of $R_{1045/1018.}$ The improvement in the short-range order of the SNCs observed from PBS-3d and PBS-5d was possibly attributed to the preferential removal of starch amorphous chains as a consequence of acidic hydrolysis (Liu *et al.* 2021a).

DSC analysis was conducted to investigate the thermal properties of the SNCs in dry-state experiments. For native waxy corn starch and SNCs, a single endothermic peak was observed. These results agreed with those reported by LeCorre, Bras and Dufresne (2012). When comparing the melting peak temperatures of the SNCs with those of native starch, the SNCs showed a decrease in all temperatures related to melting. A similar result in the melting temperature of nanocrystals has been reported by other authors (Mukurumbira *et al.* 2017). The starch network is stabilized by strong hydrogen bonds, giving rise to high melting temperatures in a dry state. However, during SNCs production, the crystallinity of starch increases due to the selective removal of the amorphous regions. These crystalline residues of starch are mostly composed of a highly branched molecule with α-(1→6) glycosidic linkages. Previous studies confirmed the depressing effect of molecule branching on the glass transition (T_g) and consequently the melting temperatures. According to these authors, it was concluded that the native starch, because of its compact surface and internal structure consisting of amylose and amylopectin more energy was required to complete the T_g phase transition, even though there was lower crystallinity of native starch. It is worth noting that other scholars have observed a higher melting temperature for starch nanocrystals in comparison to native starch. Based on their findings and adopting a polymeric approach, a higher degree of molecular packing and a larger number of intramolecular bonds in SNCs require higher temperatures for their dissociation.

5.2. Effect of starch nanocrystals addition combined with stearic acid on the microstructure, physicochemical, and mechanical properties of cassava starch films

The combined effect of starch nanocrystals (SNCs) with stearic acid to improve cassava starch-based nanocomposite film properties were investigated using a solution casting method. The influence of SNCs was studied at varying concentrations (0, 5, 10, 15, and 20 wt.%). The surface morphology of the nanocomposite films was affected by the presence of SNCs. Specifically, the surface roughness (Ra and Rmax) decreases with the inclusion of SNCs in the matrix, suggesting an enhancement in the properties of the films. The addition of SNCs in the nanocomposite films increased the opaqueness, which is beneficial when prevention of discoloration, nutrient loss, and off-flavor is intended from a food packaging product. It can be suggested that the increase in the opaqueness of the nanocomposite films could be caused by the presence of SNCs which enabled the nanocomposite film to have a larger specific surface area and a higher refractive index. Similar phenomenon has been reported by other authors (Mukurumbira, Mellem and Amonsou 2017b;

Martins, Latorres and Martins 2022). The water resistance properties (solubility and swelling behaviour) of the nanocomposite films were enhanced with the addition of SNC fillers. These results were explained in terms of the formation of the strong hydrogen bond interactions between the nanofiller and the starch matrix, which provide physical barriers to the permeation of water into the film matrix (Martins, Latorres and Martins 2022). This could also be attributed to the development of inclusion complexes between amylose-lipid, which are considered to serve as an insoluble layer on the film surface, limiting water absorption by the starch matrix.

The addition of SNCs from 5 to 15% combined with stearic acid proved to be effective in decreasing the water vapor permeability of the starch-based nanocomposite films. Jeevahan and Chandrasekaran (2019a) mentioned that the efficiency dispersion of nanocrystals within the polymer matrix creates a strong interaction between starch polymer and nanofillers, which results in the formation of a rigid network structure and tortuosity pathways of water molecules to enter the starch matrix. The other explanation could be that the inclusion of stearic acid may cover the cassava starch granular surfaces and increase its hydrophobicity, thus restricting the water vapor transfer through the starch-based films (Liu *et al.* 2016; Kang *et al.* 2020). However, a further increase in SNC content by up to 20% caused a significant increase in WVP. An increase in the WVP of nanocomposite film at higher concentrations (20% SNC) could be explained by the agglomeration effect of the nanocrystals which causes the formation of larger pores in the film matrix and facilitate the passage of gases through the film. Similar behaviour of WVP has been reported by several authors (González and Alvarez Igarzabal 2015; Mukurumbira, Mellem and Amonsou 2017a). The permeability of the films is controlled by the diffusion of water within the film matrix (Diaz-Montes and Castro-Munoz 2021). Therefore, nanometric materials such as SNCs can be used to develop new tightly connected three-dimensional networks that can prevent the migration of water in foods.

In comparison to the films made from native starch and starch with stearic acid films, the nanocomposite films showed a higher tensile strength. The maximum tensile strength was observed at 15% SNC concentration. This was expected since the high crystallinity of SNCs makes it difficult to dissolve in water and rigid particles acted as reinforcement agents. Similar observations were confirmed from previous literature studies (Mukurumbira, Mellem and Amonsou 2017a; Martins, Latorres and Martins 2022). These values for tensile strength (TS)

showed a significant improvement when compared with a previous study on cassava starch composite film reinforced by SNCs, whereby a maximum TS value of 9.17 MPa was only achieved at 6% SNC content (Dai, Zhang and Cheng 2020a). These results might suggest the possibility of dispersing nanocrystals homogeneously even at higher concentrations > 10% can be achieved. FT-IR and XRD analysis suggested that the presence of SNCs with stearic acid suppressed the hydrophilic nature of cassava starch films while improving its hydrophobicity, which is consistent with the increased water vapor permeability and mechanical properties of the nanocomposite films.

The TGA and differential TGA (DTG) studies of films containing SNCs, and stearic acid were performed to further understand the structure and interaction between polymer matrix and SNC with a stearic acid blend. All films underwent three main stages of thermal decomposition. Furthermore, as shown in Figure 4.4B, degradation of the nanocomposite films began at a higher temperature than native starch film in all cases. Peaks at similar temperatures were observed in normal maize starch (González et *al*. 2020), and cassava starch studies (Teodoro et *al*. 2015). These results suggest that nanocomposite films filled with SNCs have better thermal stability than those without SNC. Thermal behaviour of starch-based films with stearic acid and SNC addition was also determined using DSC. Glass transition temperatures (T_g) and melting temperature (T_m) of nanocomposite films with their corresponding enthalpy changes (ΔH_m) were significantly improved with the addition of SNCs compared to native starch film. According to Zheng et *al*. (2009), efficient dispersion of nanofillers into a polymer matrix increases compactness in the polymer structure which leads to high melting temperatures of nanocomposite film. Furthermore, the incorporation of SNCs into polymers increases the crystallinity which could result in high enthalpy of melting. The increment in the T_g values was impaired by a high concentration of SNC loaded in the nanocomposite films. The result is related to the different interactions and efficient dispersion of nanofillers in the corresponding nanocomposite film (Zhang et *al*. 2021). In general, the findings of this study extend the application of nanocomposite films reinforced by SNCs to in-package of high-moisture products and preservation of fruits. However, further studies are needed to investigate potential performance improvement for industrialized used of the nanocomposite films for food products.

5.3. Conclusion and recommendations

The production process of starch nanocrystals was successfully improved by enzymatic pretreatment with pullulanase (PS) or a compound enzyme system consisting of pullulanase and β-amylase (PBS) before acid hydrolysis. Nanocrystals were produced after 3 days with modified starches instead of 5 days. These results indicated that the high-density surface pores generated by enzyme pretreatment on the native starch affected the hydrolysis rate and yield of SNCs. Compared with the SNCs prepared by conventional acid hydrolysis methods (4 wt.%), the SNCs yield recovered from the PBS after 3 days (25.2 wt.%) was relatively higher. TEM revealed that SNCs appeared like platelet-like aggregates or isolated round-edge particle shapes. X-ray diffraction confirmed the increase of crystallinity (from 32.85% to 45.28%) with a preserved A-type crystalline structure for nanocrystals recovered on day 3. The combined action of SNCs and stearic acid promoted the polymer film with a high crystalline structure, resulting in a nanocomposite film with enhanced tensile strength and strong moisture resistance compared to the native starch film. This could suggest that the mechanical strength and barrier properties of the nanocomposite films can further be improved by adjusting the quantity and degree of dispersion of the nanocrystals used. However, higher loadings of SNCs beyond 15% seem to induce nanocrystals aggregation and interfere with hydrogen bonds in starch polymer chains, which impair the tensile strength of the nanocomposite film. These results indicate that the obtained nanocomposite films can be used in the development of films suitable for the packaging of high moisture foods and products.

The findings of this research provide contributions to ongoing efforts in the process of improvement of starch nanocrystals for food applications. Despite some prominent improvements in the SNC yield and hydrolysis duration, further research is required to enhance yield and shorten the acid hydrolysis time. Introduction of alternative methodologies, such as an enzymatic trimming that could selectively remove the amorphous starch chains after the shortest time exposure to mild acid hydrolysis (within 48 h). This may further improve the SNC yield whilst also shortening the preparation process time. Further work should be performed to evaluate the synergistic mechanism between SNCs and fatty acids on nanofiller dispersion and interaction with the starch matrix.

REFERENCES

Abdalla, A. A., Ahmed, U. M., Ahmed, A. R., El Tinay, A. and Ibrahim, K. A. 2009. Physicochemical characterization of traditionally extracted pearl millet starch (Jir). *Journal of Applied Sciences Research*, 5 (11): 2016-2027.

Abral, H., Basri, A., Muhammad, F., Fernando, Y., Hafizulhaq, F., Mahardika, M., Sugiarti, E., Sapuan, S. M., Ilyas, R. A. and Stephane, I. 2019. A simple method for improving the properties of the sago starch films prepared by using ultrasonication treatment. *Food Hydrocolloids*, 93: 276-283.

Abreu, A. S. L. M., de Moura, I. G., de Sá, A. V. and Machado, A. V. A. 2017. Biodegradable polymer nanocomposites for packaging applications. In: *Food packaging*. Elsevier, 329-363.

Ahmad, M., Gani, A., Masoodi, F. A. and Rizvi, S. H. 2020. Influence of ball milling on the production of starch nanoparticles and its effect on structural, thermal and functional properties. *International Journal of Biological Macromolecules*, 151: 85-91.

Ahmed, J. 2020. Thermomechanical and surface morphology of biopolymer–nanoparticle composite films. In: *Biopolymer-Based Formulations*. Elsevier, 463-512.

Ahmed, T., Shahid, M., Azeem, F., Rasul, I., Shah, A. A., Noman, M., Hameed, A., Manzoor, N., Manzoor, I. and Muhammad, S. 2018. Biodegradation of plastics: current scenario and future prospects for environmental safety. *Environmental Science and Pollution Research*, 25 (8): 7287-7298.

Albert, C., Beladjine, M., Tsapis, N., Fattal, E., Agnely, F. and Huang, N. 2019. Pickering emulsions: Preparation processes, key parameters governing their properties and potential for pharmaceutical applications. *Journal of Control Release*, 309: 302-332.

Angellier-Coussy, H., Putaux, J. L., Molina-Boisseau, S., Dufresne, A., Bertoft, E. and Perez, S. 2009. The molecular structure of waxy maize starch nanocrystals. *Carbohydrate Research*, 344 (12): 1558-1566.

Angellier, H., Choisnard, L., Molina-Boisseau, S., Ozil, P. and Dufresne, A. 2004. Optimization of the preparation of aqueous suspensions of waxy maize starch nanocrystals using a response surface methodology. *Biomacromolecules*, 5 (4): 1545-1551.

Arcan, İ., Boyacı, D. and Yemenicioğlu, A. 2017. The Use of Zein and Its Edible Films for the Development of Food Packaging Materials. In: *Reference Module in Food Science*.

Arora, A. and Padua, G. 2010. Review: Nanocomposites in food packaging. *Journal of food science,* 75 1: R43-49.

Aswathanarayan, J. B. and Vittal, R. R. 2019. Nanoemulsions and their potential applications in food industry. *Frontiers in Sustainable Food Systems,* 95 (3): 1622-1643.

Azfaralariff, A., Fazial, F. F., Sontanosamy, R. S., Nazar, M. F. and Lazim, A. M. 2020. Food-grade particle stabilized pickering emulsion using modified sago (*Metroxylon sagu*) starch nanocrystal. *Journal of Food Engineering,* 280

Bel Haaj, S., Magnin, A., Petrier, C. and Boufi, S. 2013a. Starch nanoparticles formation via high power ultrasonication. *Carbohydrate Polymers,* 92 (2): 1625-1632.

Bel Haaj, S., Magnin, A., Pétrier, C. and Boufi, S. 2013b. Starch nanoparticles formation via high power ultrasonication. *Carbohydrate Polymers,* 92 (2): 1625-1632.

Benavent-Gil, Y. and Rosell, C. M. 2017a. Comparison of porous starches obtained from different enzyme types and levels. *Carbohydrate Polymers,* 157: 533-540.

Benavent-Gil, Y. and Rosell, C. M. 2017b. Morphological and physicochemical characterization of porous starches obtained from different botanical sources and amylolytic enzymes. *International Journal of Biological Macromolecules,* 103: 587-595.

Benavent-Gil, Y. and Rosell, C. M. 2017c. Performance of granular starch with controlled pore size during hydrolysis with digestive enzymes. *Plant Foods and Human Nutrition,* 72 (4): 353-359.

Bertoft, E. 2017. Understanding starch structure: Recent progress. *Agronomy,* 7 (3)

Bertoldo, C. and Antranikian, G. 2002a. Starch-hydrolyzing enzymes from thermophilic archaea and bacteria. *Current Opinion Chemical Biology,* 6 (2): 151-160.

Bertoldo, C. and Antranikian, G. 2002b. Starch-hydrolyzing enzymes from thermophilic archaea and bacteria. *Current Opinions in Chemical Biology* 6(2): 151-160.

Chavan, P., Sinhmar, A., Nehra, M., Thory, R., Pathera, A. K., Sundarraj, A. A. and Nain, V. 2021. Impact on various properties of native starch after synthesis of starch nanoparticles: A review. *Food Chemistry*, 364: 130416.

Chellaram, C., Murugaboopathi, G., John, A. A., Sivakumar, R., Ganesan, S., Krithika, S. and Priya, G. 2014. Significance of nanotechnology in food industry. *APCBEE Procedia*, 8: 109-113.

Chen, H., Wang, J., Cheng, Y., Wang, C., Liu, H., Bian, H., Pan, Y., Sun, J. and Han, W. 2019. Application of protein-based films and coatings for food packaging: A review. *Polymers (Basel)*, 11 (12)

Chen, J., Wang, Y., Liu, J. and Xu, X. 2020. Preparation, characterization, physicochemical property and potential application of porous starch: A review. *International Journal of Biological Macromolecules*, 148: 1169-1181.

Chen, P., Xie, F., Zhao, L., Qiao, Q. and Liu, X. 2017. Effect of acid hydrolysis on the multi-scale structure change of starch with different amylose content. *Food Hydrocolloids*, 69: 359-368.

Chen, Y., Huang, S., Tang, Z., Chen, X. and Zhang, Z. 2011. Structural changes of cassava starch granules hydrolyzed by a mixture of α-amylase and glucoamylase. *Carbohydrate Polymers*, 85 (1): 272-275.

Cheng, M., Cui, Y., Yan, X., Zhang, R., Wang, J. and Wang, X. 2022. Effect of dual-modified cassava starches on intelligent packaging films containing red cabbage extracts. *Food Hydrocolloids*, 124

Chiumarelli, M. and Hubinger, M. D. 2014. Evaluation of edible films and coatings formulated with cassava starch, glycerol, carnauba wax and stearic acid. *Food Hydrocolloids*, 38: 20-27.

Cho, S. Y., Lee, S. Y. and Rhee, C. 2010. Edible oxygen barrier bilayer film pouches from corn zein and soy protein isolate for olive oil packaging. *LWT - Food Science and Technology*, 43 (8): 1234-1239.

Choi, H. D., Hong, J. S., Pyo, S. M., Ko, E., Shin, H. Y. and Kim, J. Y. 2020. Starch nanoparticles produced via acidic dry heat treatment as a stabilizer for a Pickering emulsion: Influence of the physical properties of particles. *Carbohydrate Polymers*, 239: 116241.

Condés, M. C., Añón, M. C., Dufresne, A. and Mauri, A. N. 2018. Composite and nanocomposite films based on amaranth biopolymers. *Food Hydrocolloids*, 74: 159-167.

Condés, M. C., Añón, M. C., Mauri, A. N. and Dufresne, A. 2015. Amaranth protein films reinforced with maize starch nanocrystals. *Food Hydrocolloids*, 47: 146-157.

Copeland, L., Blazek, J., Salman, H. and Tang, M. C. 2009. Form and functionality of starch. *Food Hydrocolloids*, 23 (6): 1527-1534.

Cornejo-Ramírez, Y. I., Martínez-Cruz, O., Del Toro-Sánchez, C. L., Wong-Corral, F. J., Borboa-Flores, J. and Cinco-Moroyoqui, F. J. 2018. The structural characteristics of starches and their functional properties. *CyTA - Journal of Food*, 16 (1): 1003-1017.

Costa, É. K. d. C., de Souza, C. O., da Silva, J. B. A. and Druzian, J. I. 2017. Hydrolysis of part of cassava starch into nanocrystals leads to increased reinforcement of nanocomposite films. *Journal of Applied Polymer Science*, 134 (41)

Dai, L., Li, C., Zhang, J. and Cheng, F. 2018. Preparation and characterization of starch nanocrystals combining ball milling with acid hydrolysis. *Carbohydrate Polymers*, 180: 122-127.

Dai, L., Qiu, C., Xiong, L. and Sun, Q. 2015. Characterisation of corn starch-based films reinforced with taro starch nanoparticles. *Food Chemistry*, 174: 82-88.

Dai, L., Zhang, J. and Cheng, F. 2019. Succeeded starch nanocrystals preparation combining heat-moisture treatment with acid hydrolysis. *Food Chemistry*, 278: 350-356.

Dai, L., Zhang, J. and Cheng, F. 2020a. Cross-linked starch-based edible coating reinforced by starch nanocrystals and its preservation effect on graded Huangguan pears. *Food Chem*, 311: 125891.

Dai, L., Zhang, J. and Cheng, F. 2020b. Cross-linked starch-based edible coating reinforced by starch nanocrystals and its preservation effect on graded Huangguan pears. *Food Chemistry*, 311: 125891.

Diaz-Montes, E. and Castro-Munoz, R. 2021. Edible Films and Coatings as Food-Quality Preservers: An Overview. *Foods*, 10 (2)

Dufresne, A. 2013. Nanocellulose: a new ageless bionanomaterial. *Materials today*, 16 (6): 220-227.

Duncan, T. V. 2011. Applications of nanotechnology in food packaging and food safety: barrier materials, antimicrobials and sensors. *Journal of colloid and interface science*, 363 (1): 1-24.

Dura, A., Blaszczak, W. and Rosell, C. M. 2014a. Functionality of porous starch obtained by amylase or amyloglucosidase treatments. *Carbohydr Polym*, 101: 837-845.

Dura, A., Blaszczak, W. and Rosell, C. M. 2014b. Functionality of porous starch obtained by amylase or amyloglucosidase treatments. *Carbohydrate Polymers*, 101: 837-845.

Echeverría, I., Eisenberg, P. and Mauri, A. N. 2014. Nanocomposites films based on soy proteins and montmorillonite processed by casting. *Journal of Membrane Science*, 449: 15-26.

Espino-Pérez, E., Gilbert, R. G., Domenek, S., Brochier-Salon, M., Belgacem, M. and Bras, J. 2016. Nanocomposites with functionalised polysaccharide nanocrystals through aqueous free radical polymerisation promoted by ozonolysis. *Carbohydrate Polymers*, 135: 256-266.

Fakhouri, F. M., Fontes, L. C. B., Innocentini-Mei, L. H. and Collares-Queiroz, F. P. 2009. Effect of Fatty Acid Addition on the Properties of Biopolymer Films Based on Lipophilic Maize Starch and Gelatin. *Starch - Stärke*, 61 (9): 528-536.

Galus, S. and Kadzińska, J. 2015. Food applications of emulsion-based edible films and coatings. *Trends in Food Science & Technology*, 45 (2): 273-283.

Gao, W., Zhu, J., Kang, X., Wang, B., Liu, P., Cui, B. and Abd El-Aty, A. M. 2021. Development and characterization of starch films prepared by extrusion blowing: The synergistic plasticizing effect of water and glycerol. *LWT - Food Science and Technology*, 148

Ge, X., Shen, H., Su, C., Zhang, B., Zhang, Q., Jiang, H., Yuan, L., Yu, X. and Li, W. 2021. Pullulanase modification of granular sweet potato starch: Assistant effect of dielectric barrier discharge plasma on multi-scale structure, physicochemical properties. *Carbohydrate Polymers*, 272: 118481.

Giteru, S. G., Ali, A. and Oey, I. 2021. Understanding the relationship between rheological characteristics of pulsed electric fields treated chitosan-zein-poly(vinyl alcohol)-polyethylene glycol composite dispersions and the structure-function of their resulting thin-films. *Food Hydrocolloids*, 113

González, A. and Alvarez Igarzabal, C. I. 2015. Nanocrystal-reinforced soy protein films and their application as active packaging. *Food Hydrocolloids*, 43: 777-784.

González, A., Barrera, G. N., Galimberti, P. I., Ribotta, P. D. and Alvarez Igarzabal, C. I. 2019a. Development of edible films prepared by soy protein and the galactomannan fraction extracted from Gleditsia triacanthos (Fabaceae) seed. *Food Hydrocolloids*, 97

González, A., Gastelú, G., Barrera, G. N., Ribotta, P. D. and Álvarez Igarzabal, C. I. 2019b. Preparation and characterization of soy protein films reinforced with cellulose nanofibers obtained from soybean by-products. *Food Hydrocolloids*, 89: 758-764.

González, K., Iturriaga, L., González, A., Eceiza, A. and Gabilondo, N. 2020. Improving mechanical and barrier properties of thermoplastic starch and polysaccharide nanocrystals nanocomposites. *European Polymer Journal*, 123

Grumezescu, A. 2017. *Nanotechnology in the Agri-Food Industry Food Packaging*.

Guo, L., Li, J., Gui, Y., Zhu, Y., Yu, B., Tan, C., Fang, Y. and Cui, B. 2020. Porous starches modified with double enzymes: Structure and adsorption properties. *International Journal of Biological Macromolecules*, 164: 1758-1765.

Guo, Z., Jia, X., Miao, S., Chen, B., Lu, X. and Zheng, B. 2018. Structural and thermal properties of amylose-fatty acid complexes prepared via high hydrostatic pressure. *Food Chemistry*, 264: 172-179.

Haaj, S. B., Thielemans, W., Magnin, A. and Boufi, S. 2014. Starch nanocrystal stabilized Pickering emulsion polymerization for nanocomposites with improved performance. *ACS Applied Material Interfaces*, 6 (11): 8263-8273.

Hamad, A. F., Han, J. H., Kim, B. C. and Rather, I. A. 2018. The intertwine of nanotechnology with the food industry. *Saudi Journal of Biological Science*, 25 (1): 27-30.

Han, J. H. 2014. Innovations in Food Packaging In. second edn. USA: Elsevier.

Hao, Y., Chen, Y., Li, Q. and Gao, Q. 2018a. Preparation of starch nanocrystals through enzymatic pretreatment from waxy potato starch. *Carbohydr Polym*, 184: 171-177.

Hao, Y., Chen, Y., Li, Q. and Gao, Q. 2018b. Preparation of starch nanocrystals through enzymatic pretreatment from waxy potato starch. *Carbohydrate Polymers*, 184: 171-177.

He, X. and Hwang, H. M. 2016. Nanotechnology in food science: Functionality, applicability, and safety assessment. *Journal of Food Drug Analysis*, 24 (4): 671-681.

Hedayati, S., Niakousari, M. and Mohsenpour, Z. 2020. Production of tapioca starch nanoparticles by nanoprecipitation-sonication treatment. *International Journal of Biological Macromolecules*, 143: 136-142.

Hii, S. L., Tan, J. S., Ling, T. C. and Ariff, A. B. 2012. Pullulanase: role in starch hydrolysis and potential industrial applications. *Enzyme Research*, 2012: 921362.

Hong, Y., Liu, G. and Gu, Z. 2015. RETRACTED: Preparation and characterization of hydrophilic debranched starch modified by pullulanase on swollen granule starch. *Food Research International*, 67: 212-218.

Javidi, F., Razavi, S. M. A. and Mohammad Amini, A. 2019. Cornstarch nanocrystals as a potential fat replacer in reduced fat O/W emulsions: A rheological and physical study. *Food Hydrocolloids*, 90: 172-181.

Jeevahan, J. and Chandrasekaran, D. M. 2019a. Nanoedible films for food packaging: a review. *Journal of Materials Science*, 54: 1-29.

Jeevahan, J. and Chandrasekaran, M. 2019b. Nanoedible films for food packaging: a review. *Journal of Materials Science*, 54 (19): 12290-12318.

Jiang, S., Liu, C., Han, Z., Xiong, L. and Sun, Q. 2016. Evaluation of rheological behavior of starch nanocrystals by acid hydrolysis and starch nanoparticles by self-assembly: A comparative study. *Food Hydrocolloids*, 52: 914-922.

Jiménez, A., Fabra, M. J., Talens, P. and Chiralt, A. 2012. Edible and Biodegradable Starch Films: A Review. *Food and Bioprocess Technology*, 5 (6): 2058-2076.

Kang, X., Liu, P., Gao, W., Wu, Z., Yu, B., Wang, R., Cui, B., Qiu, L. and Sun, C. 2020. Preparation of starch-lipid complex by ultrasonication and its film forming capacity. *Food Hydrocolloids*, 99

Kaptso, K. G., Njintang, Y. N., Nguemtchouin, M. M. G., Scher, J., Hounhouigan, J. and Mbofung, C. M. 2015. Physicochemical and micro-structural properties of flours, starch and proteins from two varieties of legumes: bambara groundnut (Vigna subterranea). *Journal of food science and technology*, 52 (8): 4915-4924.

Kaur, J., Kaur, G., Sharma, S. and Jeet, K. 2018. Cereal starch nanoparticles-A prospective food additive: A review. *Critical Reviews in Food Science and Nutrition*, 58 (7): 1097-1107.

Keeratiburana, T., Hansen, A. R., Soontaranon, S., Blennow, A. and Tongta, S. 2020. Pre-treatment of granular rice starch to enhance branching enzyme catalysis. *Carbohydrate Polymers*, 247: 116741.

Kim, H. Y., Han, J. A., Kweon, D. K., Park, J. D. and Lim, S. T. 2013a. Effect of ultrasonic treatments on nanoparticle preparation of acid-hydrolyzed waxy maize starch. *Carbohydrate Polymers*, 93 (2): 582-588.

Kim, H. Y., Park, D. J., Kim, J. Y. and Lim, S. T. 2013b. Preparation of crystalline starch nanoparticles using cold acid hydrolysis and ultrasonication. *Carbohydrate Polymers*, 98 (1): 295-301.

Kim, H. Y., Park, S. S. and Lim, S. T. 2015. Preparation, characterization and utilization of starch nanoparticles. *Colloids and Surfaces B: Biointerfaces*, 126: 607-620.

Kim, J.-Y., Park, D. and Lim, S.-T. 2008. Fragmentation of Waxy Rice Starch Granules by Enzymatic Hydrolysis. *Cereal Chemistry*, 85: 182-187.

Kumari, S., Yadav, B. S. and Yadav, R. B. 2020. Synthesis and modification approaches for starch nanoparticles for their emerging food industrial applications: A review. *Food Research International*, 128: 108765.

La Fuente, C. I. A., do Val Siqueira, L., Augusto, P. E. D. and Tadini, C. C. 2022. Casting and extrusion processes to produce bio-based plastics using cassava starch modified by the dry heat treatment (DHT). *Innovative Food Science & Emerging Technologies*, 75

Lacerda, L. D., Leite, D. C. and da Silveira, N. P. 2019. Relationships between enzymatic hydrolysis conditions and properties of rice porous starches. *Journal of Cereal Science*, 89

Le Corre-Bordes, D. and Angellier-Coussy, H. 2014. Preparation and Application of starch nanoparticles for nanocomposites: A review. *Reactive and Functional Polymers*, 85

Le Corre, D. and Dufresne, A. 2013. Preparation of starch nanoparticles. *Biopolymer Nanocomposites: Processing, Properties, and Applications*: 153-180.

LeCorre, D., Bras, J. and Dufresne, A. 2011. Influence of botanic origin and amylose content on the morphology of starch nanocrystals. *Journal of Nanoparticle Research*, 13 (12): 7193-7208.

LeCorre, D., Bras, J. and Dufresne, A. 2012. Influence of native starch's properties on starch nanocrystals thermal properties. *Carbohydrate Polymers*, 87 (1): 658-666.

LeCorre, D., Vahanian, E., Dufresne, A. and Bras, J. 2012. Enzymatic pretreatment for preparing starch nanocrystals. *Biomacromolecules*, 13 (1): 132-137.

Li, H., Yan, S., Mao, H., Ji, J., Xu, M., Zhang, S., Wang, J., Liu, Y. and Sun, B. 2020. Insights into maize starch degradation by sulfuric acid from molecular structure changes. *Carbohydrate Polymers*, 229: 115542.

Li, P., He, X., Dhital, S., Zhang, B. and Huang, Q. 2017. Structural and physicochemical properties of granular starches after treatment with debranching enzyme. *Carbohydrate Polymers*, 169: 351-356.

Li, X., Qiu, C., Ji, N., Sun, C., Xiong, L. and Sun, Q. 2015. Mechanical, barrier and morphological properties of starch nanocrystals-reinforced pea starch films. *Carbohydrate Polymers*, 121: 155-162.

Li, Z., Kong, X., Zhou, X., Zhong, K., Zhou, S. and Liu, X. 2016. Characterization of multi-scale structure and thermal properties of Indica rice starch with different amylose contents. *Royal Society of Chemistry Advances*, 6 (109): 107491-107497.

Lin, N., Jin, H., Chang, P., Anderson, D. and Yu, J. 2011. Preparation, Modification, and Application of Starch Nanocrystals in Nanomaterials: A Review. *Journal of Nanomaterials*, 2011

Lindeboom, N., Chang, P. R. and Tyler, R. T. 2004. Analytical, biochemical and physicochemical aspects of starch granule size, with emphasis on small granule starches: a review. *Starch-Stärke*, 56 (3-4): 89-99.

Liu, C., Li, K., Li, X., Zhang, M. and Li, J. 2021a. Formation and structural evolution of starch nanocrystals from waxy maize starch and waxy potato starch. *Int J Biol Macromol*, 180: 625-632.

Liu, C., Li, K., Li, X., Zhang, M. and Li, J. 2021b. Formation and structural evolution of starch nanocrystals from waxy maize starch and waxy potato starch. *International Journal Biological Macromolecules*, 180: 625-632.

Liu, G., Gu, Z., Hong, Y., Cheng, L. and Li, C. 2017. Structure, functionality and applications of debranched starch: A review. *Trends in Food Science & Technology*, 63: 70-79.

Liu, P., Gao, W., Zhang, X., Wang, B., Zou, F., Yu, B., Lu, L., Fang, Y., Wu, Z., Yuan, C. and Cui, B. 2021c. Effects of ultrasonication on the properties of maize starch/stearic acid/ sodium carboxymethyl cellulose composite film. *Ultrasonics Sonochemistry*, 72: 105447.

Liu, P., Sun, S., Hou, H. and Dong, H. 2016. Effects of fatty acids with different degree of unsaturation on properties of sweet potato starch-based films. *Food Hydrocolloids*, 61: 351-357.

Liu, P., Sun, S., Hou, H., Wang, W. and Dong, H. 2015. Effect of five saturated fatty acids on the properties of sweet-potato-starch-based films. *Journal of Applied Polymer Science*, 132 (5): n/a-n/a.

Liu, P., Wang, R., Kang, X., Cui, B. and Yu, B. 2018. Effects of ultrasonic treatment on amylose-lipid complex formation and properties of sweet potato starch-based films. *Ultrasonics Sonochemistry*, 44: 215-222.

Liu, W., Zhang, M. and Bhandari, B. 2020. Nanotechnology - A shelf life extension strategy for fruits and vegetables. *Critical Reviews in Food Science and Nutrition*, 60 (10): 1706-1721.

Ma, X., Yu, J., He, K. and Wang, N. 2007. The Effects of Different Plasticizers on the Properties of Thermoplastic Starch as Solid Polymer Electrolytes. *Macromolecular Materials and Engineering*, 292: 503-510.

Mangaraj, S., Yadav, A., Bal, L. M., Dash, S. K. and Mahanti, N. K. 2018. Application of Biodegradable Polymers in Food Packaging Industry: A Comprehensive Review. *Journal of Packaging Technology and Research*, 3 (1): 77-96.

Martins, P. C., Latorres, J. M. and Martins, V. G. 2022. Impact of starch nanocrystals on the physicochemical, thermal and structural characteristics of starch-based films. *LWT - Food Science and Technology*, 156

Miller, G. L. 1959. Use of dinitrosalicylic acid reagent for determination of reducing sugar. *Analytical chemistry*, 31 (3): 426-428.

Miskeen, S., Park, E. Y. and Kim, J. Y. 2019. Controlled fragmentation of starch into nanoparticles using a dry heating treatment under mildly acidic conditions. *International Journal of Biological Macromolecules*, 123: 810-816.

Mohammad Amini, A. and Razavi, S. M. A. 2016. A fast and efficient approach to prepare starch nanocrystals from normal corn starch. *Food Hydrocolloids*, 57: 132-138.

Monnet, D., Joly, C., Dole, P. and Bliard, C. 2010. Enhanced mechanical properties of partially beta-amylase trimmed starch for material applications. *Carbohydrate Polymers*, 80 (3): 747-752.

Mujtaba, M., Koc, B., Salaberria, A. M., Ilk, S., Cansaran-Duman, D., Akyuz, L., Cakmak, Y. S., Kaya, M., Khawar, K. M., Labidi, J. and Boufi, S. 2019. Production of novel chia-mucilage nanocomposite films with starch nanocrystals; An inclusive biological and physicochemical perspective. *International Journal of Biological Macromolecules*, 133: 663-673.

Mukurumbira, A., Mariano, M., Dufresne, A., Mellem, J. J. and Amonsou, E. O. 2017. Microstructure, thermal properties and crystallinity of amadumbe starch nanocrystals. *International Journal of Biological Macromolecules*, 102: 241-247.

Mukurumbira, A. R., Mellem, J. J. and Amonsou, E. O. 2017a. Effects of amadumbe starch nanocrystals on the physicochemical properties of starch biocomposite films. *Carbohydrates Polymers*, 165: 142-148.

Mukurumbira, A. R., Mellem, J. J. and Amonsou, E. O. 2017b. Effects of amadumbe starch nanocrystals on the physicochemical properties of starch biocomposite films. *Carbohydr Polym*, 165: 142-148.

Nakamura, Y. 2015. *Starch*. Springer.

Nara, S., Sakakura, M. and Komiya, T. 1983. On the Acid Resistance of Starch Granules. *Starch - Stärke*, 35 (8): 266-270.

Noda, T., Takigawa, S., Matsuura-Endo, C., Kim, S.-J., Hashimoto, N., Yamauchi, H., Hanashiro, I. and Takeda, Y. 2005. Physicochemical properties and amylopectin structures of large, small, and extremely small potato starch granules. *Carbohydrate Polymers*, 60 (2): 245-251.

Oates, C. G. 1997. Towards an understanding of starch granule structure and hydrolysis. *Trends in Food Science & Technology*, 8 (11): 375-382.

Odeniyi, M. A., Omoteso, O. A., Adepoju, A. O. and Jaiyeoba, K. T. 2018. Starch nanoparticles in drug delivery: A review. *Polymers in Medicine*, 48: 41-45.

Oliveira, A. V., da Silva, A. P. M., Barros, M. O., de sá M. Souza Filho, M., Rosa, M. F. and Azeredo, H. M. C. 2018. Nanocomposite Films from Mango Kernel or Corn Starch with Starch Nanocrystals. *Starch - Stärke*, 70 (11-12)

Oyeyinka, S. A., Singh, S. and Amonsou, E. O. 2017. Physicochemical and Mechanical Properties of Bambara Groundnut Starch Films Modified with Stearic Acid. *Journal of food science*, 82 (1): 118-123.

Park, S. H., Na, Y., Kim, J., Kang, S. D. and Park, K. H. 2018. Properties and applications of starch modifying enzymes for use in the baking industry. *Food Science and Biotechnology*, 27 (2): 299-312.

Park, W., Li, J., Song, R., Messing, J. and Chen, X. 2002. CARPEL FACTORY, a Dicer homolog, and HEN1, a novel protein, act in microRNA metabolism in Arabidopsis thaliana. *Current Biology*, 12 (17): 1484-1495.

Pérez, S. and Bertoft, E. 2010. The molecular structures of starch components and their contribution to the architecture of starch granules: A comprehensive review. *Starch - Stärke*, 62 (8): 389-420.

Perez, S. and Imberty, A. 2002. Structure and Morphology of Starch. *An Internet Review Article*: 00-00.

Piñeros-Hernandez, D., Medina-Jaramillo, C., López-Córdoba, A. and Goyanes, S. 2017. Edible cassava starch films carrying rosemary antioxidant extracts for potential use as active food packaging. *Food Hydrocolloids*, 63: 488-495.

Piyada, K., Waranyou, S. and Thawien, W. 2013. Mechanical, thermal and structural properties of rice starch films reinforced with rice starch nanocrystals. *International Food Research Journal*, 20 (1): 439.

Punia Bangar, S., Ashogbon, A. O., Singh, A., Chaudhary, V. and Whiteside, W. S. 2022. Enzymatic modification of starch: A green approach for starch applications. *Carbohydrate Polymers*, 287: 119265.

Putaux, J.-L., Molina-Boisseau, S., Momaur, T. and Dufresne, A. 2003. Platelet nanocrystals resulting from the disruption of waxy maize starch granules by acid hydrolysis. *Biomacromolecules*, 4 (5): 1198-1202.

Rhim, J.-W. and Kim, Y.-T. 2014. Biopolymer-based composite packaging materials with nanoparticles. In: *Innovations in food packaging*. Elsevier, 413-442.

Samal, D. 2017. Use of nanotechnology in food industry: A review. *International Journal of Environment, Agriculture and Biotechnology*, 2 (4): 2270-2278.

Sanchez de la Concha, B. B., Agama-Acevedo, E., Nuñez-Santiago, M. C., Bello-Perez, L. A., Garcia, H. S. and Alvarez-Ramirez, J. 2018. Acid hydrolysis of waxy starches with different granule size for nanocrystal production. *Journal of Cereal Science*, 79: 193-200.

Santana, Á. and Meireles, M. A. 2014. New starches are the trend for industry applications: A review. *Food and Public Health*, 5: 229.

Schirmer, M., Höchstötter, A., Jekle, M., Arendt, E. and Becker, T. 2013. Physicochemical and morphological characterization of different starches with variable amylose/amylopectin ratio. *Food Hydrocolloids*, 32 (1): 52-63.

Schmidt, V. C. R., Porto, L. M., Laurindo, J. B. and Menegalli, F. C. 2013. Water vapor barrier and mechanical properties of starch films containing stearic acid. *Industrial Crops and Products*, 41: 227-234.

Shao, P., Zhang, H., Niu, B. and Jin, W. 2018. Physical stabilities of taro starch nanoparticles stabilized Pickering emulsions and the potential application of encapsulated tea polyphenols. *International Journal of Biological Macromolecules*, 118 (Pt B): 2032-2039.

Silva, A. P. M., Oliveira, A. V., Pontes, S. M. A., Pereira, A. L. S., Souza Filho, M. S. M., Rosa, M. F. and Azeredo, H. M. C. 2019. Mango kernel starch films as affected by starch nanocrystals and cellulose nanocrystals. *Carbohydrate Polymers*, 211: 209-216.

Silva, N. M. C. D., Lima, F. F. d., Fialho, R. L. L., Albuquerque, E. C. d. M. C., Velasco, J. I. and Fakhouri, F. M. 2018. Production and characterization of starch nanoparticles. In: *Applications of Modified Starches*.

Singh, J. and Singh, N. 2003. Studies on the morphological and rheological properties of granular cold water soluble corn and potato starches. *Food Hydrocolloids*, 17 (1): 63-72.

Singh, T., Shukla, S., Kumar, P., Wahla, V. and Bajpai, V. K. 2017. Application of nanotechnology in food science: Perception and overview. *Frontiers in Microbiology*, 8: 1501.

Siracusa, V. 2012. Food packaging permeability behaviour: A report. *International Journal of Polymer Science*, 2012

Song, H., Li, B., Lin, Q.-B., Wu, H.-J. and Chen, Y. 2011. Migration of silver from nanosilver–polyethylene composite packaging into food simulants. *Food Additives & Contaminants: Part A*, 28 (12): 1758-1762.

Sun, Q., Gong, M., Li, Y. and Xiong, L. 2014. Effect of retrogradation time on preparation and characterization of proso millet starch nanoparticles. *Carbohydrate Polymers*, 111: 133–138.

Swain, S. K., Sarkar, N., Patra, B. and Sahoo, G. 2018. Polymer-based bionanocomposites for future packaging materials. In: *Bionanocomposites for packaging applications*. Springer, 33-48.

Tang, J., Liang, Q., Ren, X., Raza, H. and Ma, H. 2022. Insights into ultrasound-induced starch-lipid complexes to understand physicochemical and nutritional interventions. *International Journal of Biological Macromolecules*, 222: 950-960.

Tao, S., Jiang, H., Gong, S., Yin, S., Li, Y. and Ngai, T. 2021. Pickering emulsions simultaneously stabilized by starch nanocrystals and zein nanoparticles: Fabrication, characterization, and application. *Langmuir*, 37 (28): 8577-8584.

Teodoro, A. P., Mali, S., Romero, N. and de Carvalho, G. M. 2015. Cassava starch films containing acetylated starch nanoparticles as reinforcement: Physical and mechanical characterization. *Carbohydrate Polymers*, 126: 9-16.

Tester, R., Karkalas, J. and Qi, X. 2004a. Starch—Composition, fine structure and architecture. *Journal of Cereal Science*, 39: 151-165.

Tester, R. F., Karkalas, J. and Qi, X. 2004b. Starch—composition, fine structure and architecture. *Journal of Cereal Science*, 39 (2): 151-165.

Tihminlioglu, F., Atik, İ. D. and Özen, B. 2010. Water vapor and oxygen-barrier performance of corn–zein coated polypropylene films. *Journal of Food Engineering*, 96 (3): 342-347.

Trajkovska Petkoska, A., Daniloski, D., D'Cunha, N. M., Naumovski, N. and Broach, A. T. 2021. Edible packaging: Sustainable solutions and novel trends in food packaging. *Food Research International*, 140

Velasquez-Castillo, L. E., Leite, M. A., Ditchfield, C., Sobral, P. and Moraes, I. C. F. 2020a. Quinoa starch nanocrystals production by acid hydrolysis: Kinetics and properties. *International Journal of Biological Macromolecules*, 143: 93-101.

Velasquez-Castillo, L. E., Leite, M. A., Ditchfield, C., Sobral, P. and Moraes, I. C. F. 2020b. Quinoa starch nanocrystals production by acid hydrolysis: Kinetics and properties. *Int J Biol Macromol*, 143: 93-101.

Vilpoux, O. F. and Santos Silveira Junior, J. F. 2023. Chapter 3 - Global production and use of starch. In: Pascoli Cereda, M. and François Vilpoux, O. eds. *Starchy Crops Morphology, Extraction, Properties and Applications*. Academic Press, 43-66. Available: https://www.sciencedirect.com/science/article/pii/B9780323900584000141 (Accessed

Wei, B., Xu, X., Jin, Z. and Tian, Y. 2014. Surface chemical compositions and dispersity of starch nanocrystals formed by sulfuric and hydrochloric acid hydrolysis. *PloS one*, 9 (2): e86024-e86024.

Wittaya, T. 2012. Protein-based edible films: Characteristics and improvement of properties. *Structure and function of food engineering*: 43-70.

Wolff, A. G. 2018. *Starch in Food, Structure, Function and Applications*. second ed. Woodhead.

Xiong, X., Huang, M., Zhou, X., Zhou, H., Zeng, C., Zhao, Z. and Xiao, Q. 2021. Physicochemical studies of nanocrystals of starches from two rice (Oryza sativa L.) types and their characteristics using various modern instrument techniques. *Journal of Science Food Agriculture*, 101 (3): 1038-1046.

Xu, Y. X., Sismour, E. N., Grizzard, C., Thomas, M., Pestov, D., Huba, Z., Wang, T. W. and Bhardwaj, H. L. 2014. Morphological, structural, and thermal properties of starch nanocrystals affected by different botanic origins. *Cereal Chemistry*, 91 (4): 383-388.

Yadav, M. and Chiu, F. C. 2019. Cellulose nanocrystals reinforced kappa-carrageenan based UV resistant transparent bionanocomposite films for sustainable packaging applications. *Carbohydrate Polymers*, 211: 181-194.

Yang, Z., Xu, X., Singh, R., de Campo, L., Gilbert, E. P., Wu, Z. and Hemar, Y. 2019. Effect of amyloglucosidase hydrolysis on the multi-scale supramolecular structure of corn starch. *Carbohydrate Polymers*, 212: 40-50.

Zambrano-Zaragoza, M. L., Gonzalez-Reza, R., Mendoza-Munoz, N., Miranda-Linares, V., Bernal-Couoh, T. F., Mendoza-Elvira, S. and Quintanar-Guerrero, D. 2018. Nanosystems in edible coatings: A novel strategy for food preservation. *International Journal of Molecular Sciences*, 19 (3)

Zan, K., Wang, J., Ren, F., Yu, J., Wang, S., Xie, F. and Wang, S. 2021. Structural disorganization of cereal, tuber and bean starches in aqueous ionic liquid at room temperature: Role of starch granule surface structure. *Carbohydrate Polymers*, 258: 117677.

Zhang, L., Zhao, J., Zhang, Y., Li, F., Jiao, X. and Li, Q. 2021. The effects of cellulose nanocrystal and cellulose nanofiber on the properties of pumpkin starch-based composite films. *International Journal of Biological Macromolecules*, 192: 444-451.

Zhao, A.-Q., Yu, L., Yang, M., Wang, C.-J., Wang, M.-M. and Bai, X. 2018. Effects of the combination of freeze-thawing and enzymatic hydrolysis on the microstructure and physicochemical properties of porous corn starch. *Food Hydrocolloids*, 83: 465-472.

Zhao, X., Xu, Z., Xu, H., Lin, N. and Ma, J. 2021. Surface-charged starch nanocrystals from glutinous rice: Preparation, crystalline properties and cytotoxicity. *International Journal of Biological Macromolecules*, 192: 557-563.

Zheng, H., Ai, F., Chang, P., Huang, J. and Dufresne, A. 2009. Structure and properties of starch nanocrystal-reinforced soy protein plastics. *Polymer Composites*, 30: 474-480.

Zhou, L., Fang, D., Wang, M., Li, M., Li, Y., Ji, N., Dai, L., Lu, H., Xiong, L. and Sun, Q. 2020. Preparation and characterization of waxy maize starch nanocrystals with a high yield via dry-heated oxalic acid hydrolysis. *Food Chemistry*, 318: 126479.